INTERNATIONAL ATOMIC ENERGY AGENCY
UNITED NATIONS EDUCATIONAL, SCIENTIFIC AND CULTURAL ORGANIZATION
INTERNATIONAL CENTRE FOR THEORETICAL PHYSICS
I.C.T.P., P.O. BOX 586, 34100 TRIESTE, ITALY, CABLE: CENTRATOM TRIESTE

UNITED NATIONS INDUSTRIAL DEVELOPMENT ORGANIZATION

INTERNATIONAL CENTRE FOR SCIENCE AND HIGH TECHNOLOGY
c/o INTERNATIONAL CENTRE FOR THEORETICAL PHYSICS 34100 TRIESTE (ITALY) VIA GRIGNANO, 9 (ADRIATICO PALACE) P.O. BOX 586 TELEPHONE 040-224572 TELEFAX 040-224575 TELEX 460449 APH I

H4.SMR/540-20

Second Training College on Physics and Technology of Lasers and Optical Fibres

21 January - 15 February 1991

Dye Lasers (25 years)

B. Nikolaus
Lambda Physik
Lasertechnik
Göttingen, Germany

Dye Lasers (25 years)

Dr. B. Nikolaus
Lambda Physik

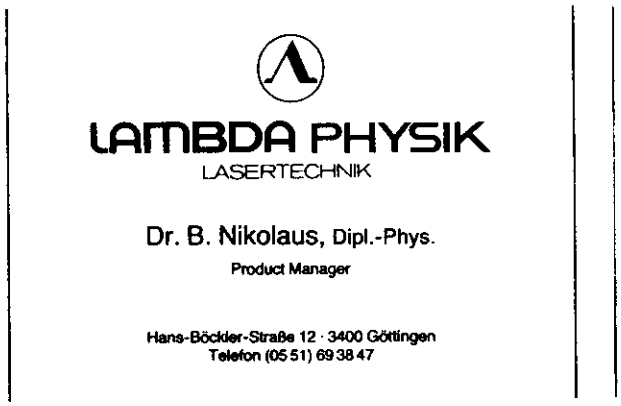

Basic Literature

1.) Dye Laser; edited by F.P. Schäfer
Topics in Applied Physics (Volume I) /Springer Verlag

2) Dye Laser Principles, edited by F.J. Duarte
and Lloyd Wittellmann / Academy Press, Inc.

3) Lambda Chrome Laser Dyes, U. Brackmann / Lambda Physik

4) Tunable Dye Lasers; T.F. Johnston, Jr.
Encyclopedia of Phys. Science & Tech., Vol. 14
Academic Press, Inc.

Outline

I) Introduction

- brief history of dye lasers
- power range of commercial dye lasers
- principle of laser dye operations
- pump sources for dye lasers
- current versions of Dye Lasers

II) Pulsed Dye Laser

- Oscillator design (comparison)
- grating equation
- key specification
- features and engineering of commercial dye lasers

III) Methods of ultrashort pulse generation

- modelocking technique
- distributed feedback dye laser (DFDL)
- short cavity transients
- photochemical quenching

1) Dye Lasers – Introduction

Discovered in 1966 by:

1. F. P. Schäfer (D)
2. P. Sorokin, J. Lankard (USA)
3. Stephanov (USSR)

- Dyes were used for Q-switching of Ruby laser at that time

- Discovery of the dye laser started a revolution in atomic and molecular Spectroscopy; dye lasers have been the most important type of laser in scientific research!

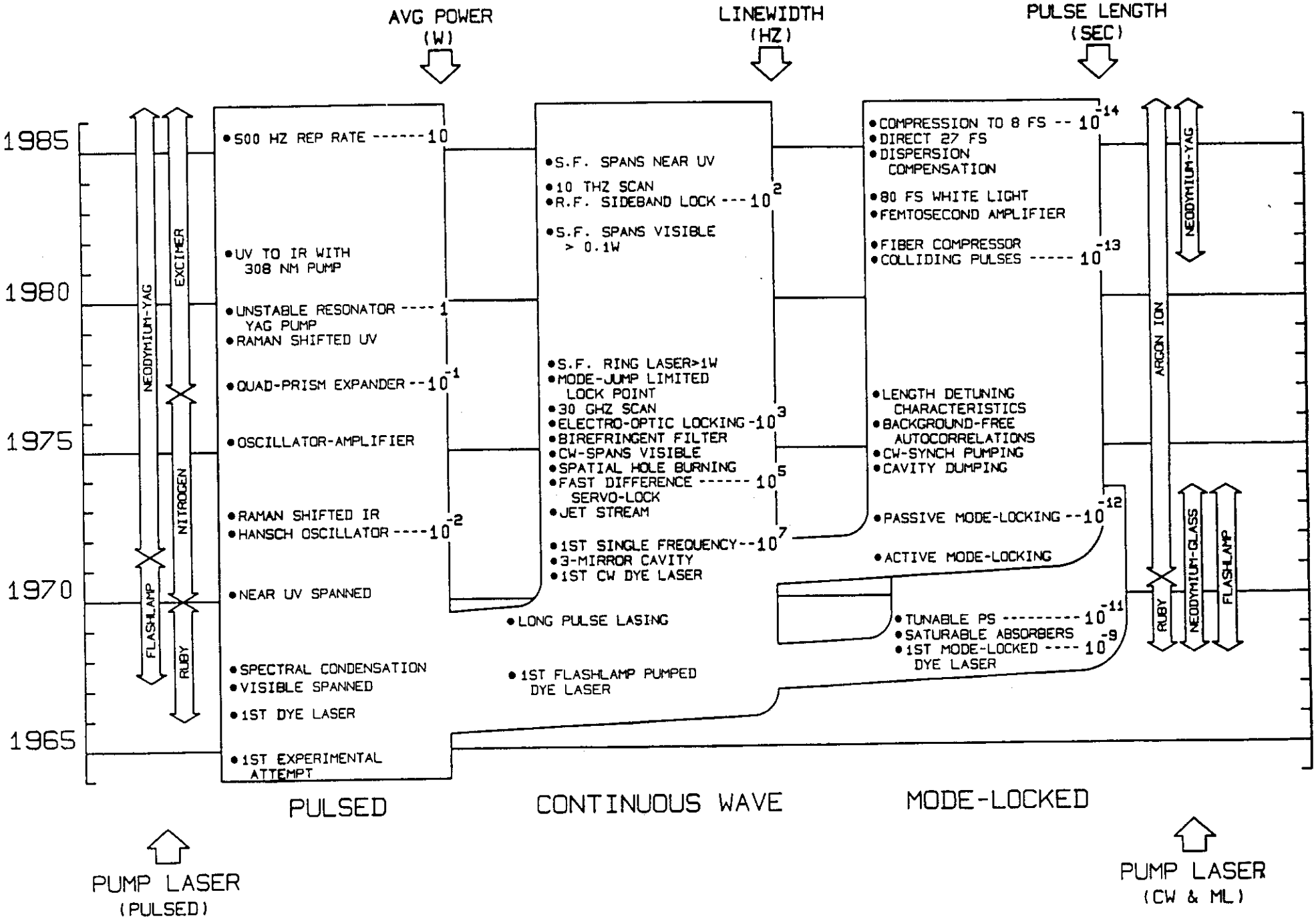
AVG POWER (W)
LINEWIDTH (HZ)
PULSE LENGTH (SEC)
1985
1980
1975
1970
1965
NEODYMIUM-YAG
EXCIMER
NITROGEN
FLASHLAMP
RUBY
ARGON ION
NEODYMIUM-YAG
NEODYMIUM-GLASS
FLASHLAMP
RUBY
• 500 HZ REP RATE ------ 10
• UV TO IR WITH 308 NM PUMP
• UNSTABLE RESONATOR ---- 1
YAG PUMP
• RAMAN SHIFTED UV
• QUAD-PRISM EXPANDER -- 10^{-1}
• OSCILLATOR-AMPLIFIER
• RAMAN SHIFTED IR
• HANSCH OSCILLATOR ---- 10^{-2}
• NEAR UV SPANNED
• SPECTRAL CONDENSATION
• VISIBLE SPANNED
• 1ST DYE LASER
• 1ST EXPERIMENTAL ATTEMPT
• S.F. SPANS NEAR UV
• 10 THZ SCAN
• R.F. SIDEBAND LOCK --- 10^{2}
• S.F. SPANS VISIBLE > 0.1W
• S.F. RING LASER>1W
• MODE-JUMP LIMITED LOCK POINT
• 30 GHZ SCAN
• ELECTRO-OPTIC LOCKING - 10^{3}
• BIREFRINGENT FILTER
• CW-SPANS VISIBLE
• SPATIAL HOLE BURNING
• FAST DIFFERENCE ------ 10^{5}
SERVO-LOCK
• JET STREAM
• 1ST SINGLE FREQUENCY -- 10^{7}
• 3-MIRROR CAVITY
• 1ST CW DYE LASER
• LONG PULSE LASING
• 1ST FLASHLAMP PUMPED DYE LASER
• COMPRESSION TO 8 FS -- 10^{-14}
• DIRECT 27 FS
• DISPERSION COMPENSATION
• 80 FS WHITE LIGHT
• FEMTOSECOND AMPLIFIER
• FIBER COMPRESSOR
• COLLIDING PULSES ----- 10^{-13}
• LENGTH DETUNING CHARACTERISTICS
• BACKGROUND-FREE AUTOCORRELATIONS
• CW-SYNCH PUMPING
• CAVITY DUMPING
• PASSIVE MODE-LOCKING -- 10^{-12}
• ACTIVE MODE-LOCKING
• TUNABLE PS --------- 10^{-11}
• SATURABLE ABSORBERS
• 1ST MODE-LOCKED ---- 10^{-9}
DYE LASER
PULSED
CONTINUOUS WAVE
MODE-LOCKED
PUMP LASER (PULSED)
PUMP LASER (CW & ML)

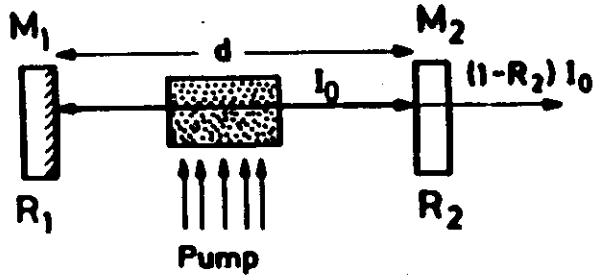
M1
d
M2
I0
(1-R2) I0
R1
R2
Pump

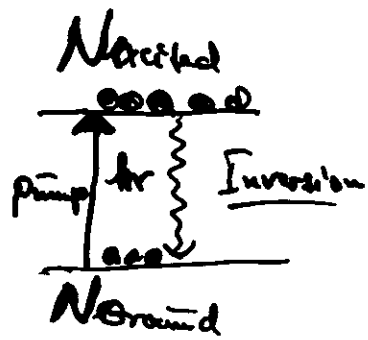
Nexcited
pump
hν
Inversion
Nground

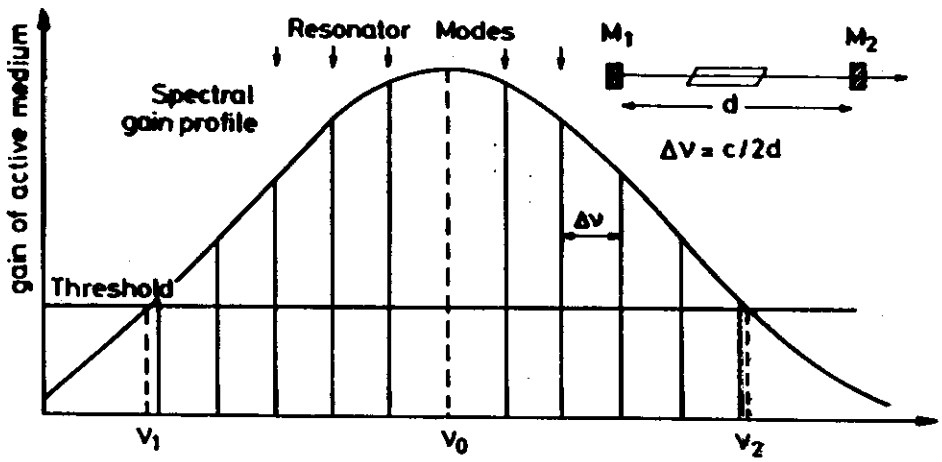
gain of active medium
Resonator Modes
Spectral gain profile
M1
M2
d
Δν = c/2d
Δν
Threshold
ν1
ν0
ν2

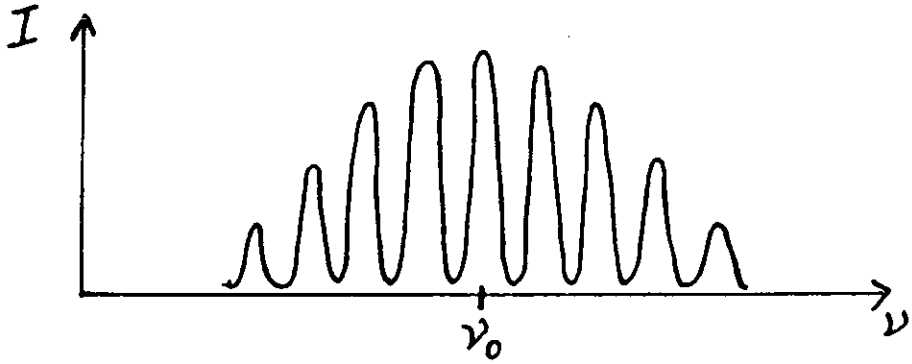
I
ν0
ν

RHODAMINE 6G WAVE FUNCTIONS

$$\psi_g = \frac{1}{\sqrt{2}}(\phi_1 + \phi_2)$$
$$\psi_e = \frac{1}{\sqrt{2}}(\phi_1 - \phi_2)$$

(a) where ϕ_1 = (b) and ϕ_2 =

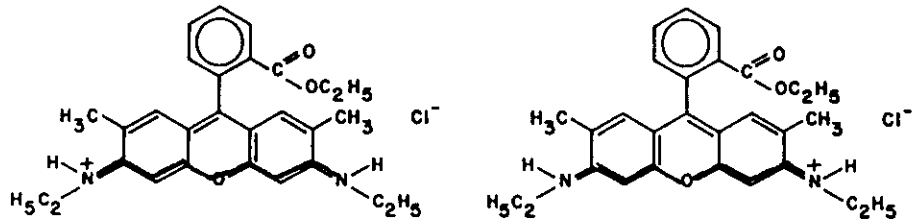

FIG. 2. Chemical symbols for two "resonant" forms of the structure of the rhodamine 6G dye molecule and the wave functions to which this resonance gives rise.

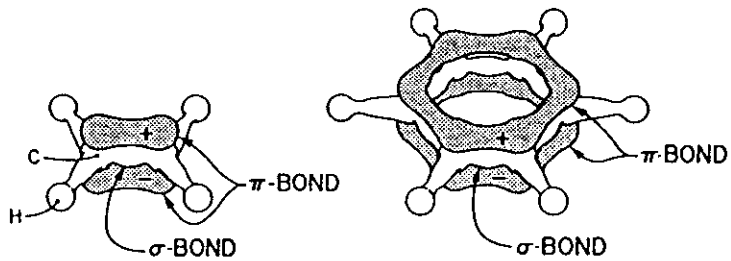

(a) ETHYLENE $H_2C{=}CH_2$ (b) BENZENE C_6H_6 or ⬡

FIG. 3. Chemical symbols and schematic three-dimensional representations of the electron density distributions, for (a) a double bond system, ethylene, and (b) a conjugated double bond system, benzene. The shapes show the surfaces of constant electron density except for distortions necessary for clarity in depicting the overlapping σ-bond and π-bond electron clouds.

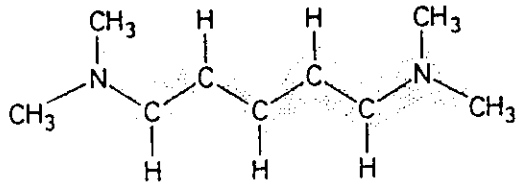

a

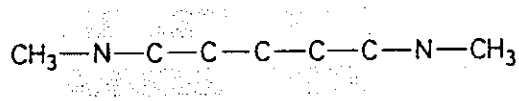

b

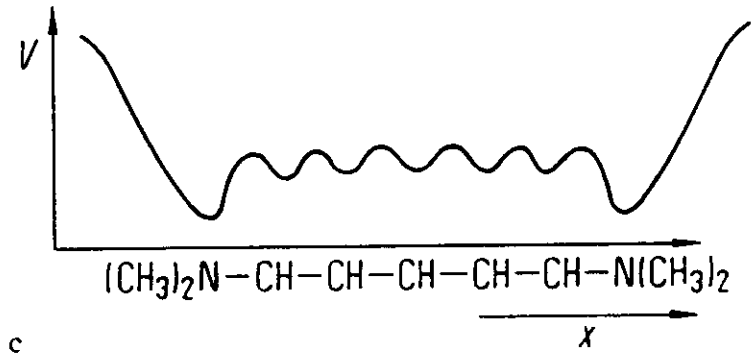

c

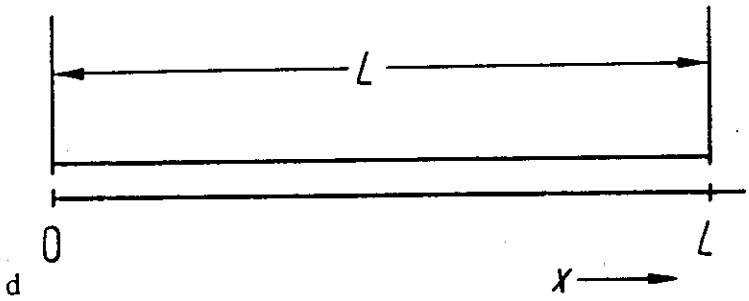

d

$$\Delta E_{\min} = \frac{h^2}{8mL^2}(N+1) \quad \text{or} \quad \lambda_{\max} = \frac{8mc_0}{h}\,\frac{L^2}{N+1}.$$

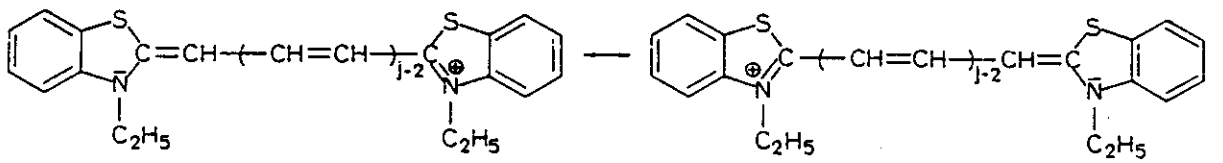

Wavelength (in nm) of absorption maximum for thiacyanines

	Number of conjugated double bonds j =			
	2	3	4	5
Calculated	395	521	649	776
Experimental	422	556	652	760

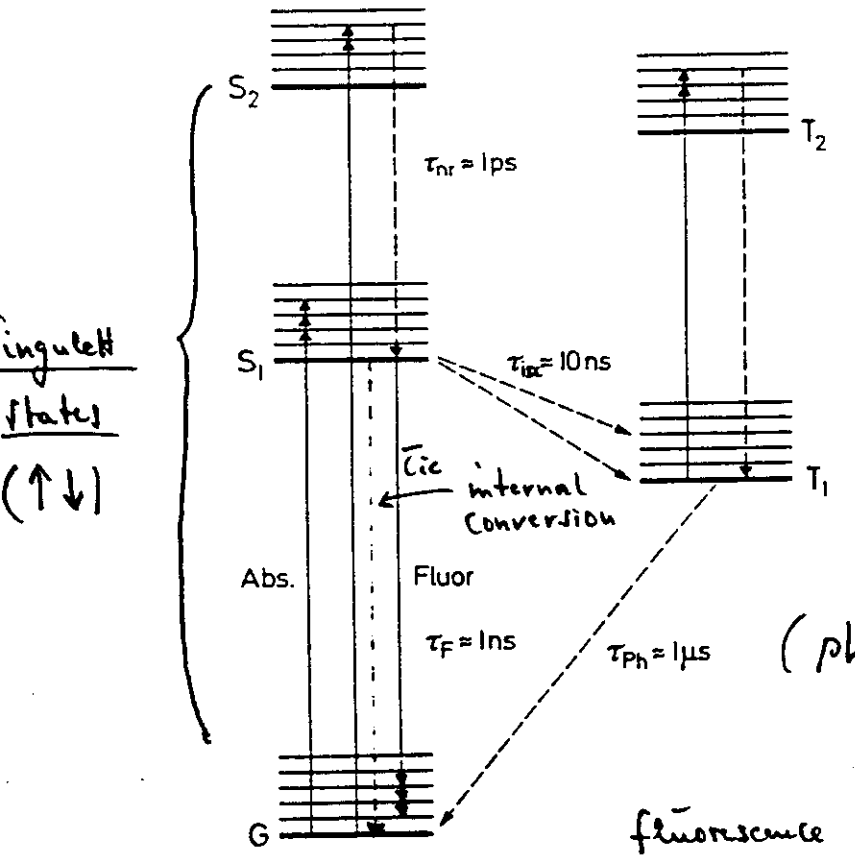

Fig. 1.15. Eigenstates of a typical dye molecule with radiative (*solid lines*) and nonradiative (*broken lines*) transitions

fluorescence yield $\Phi = \frac{1/\tau_F}{1/\tau_F + 1/\tau_{isc} + 1/\tau_{ic}}$

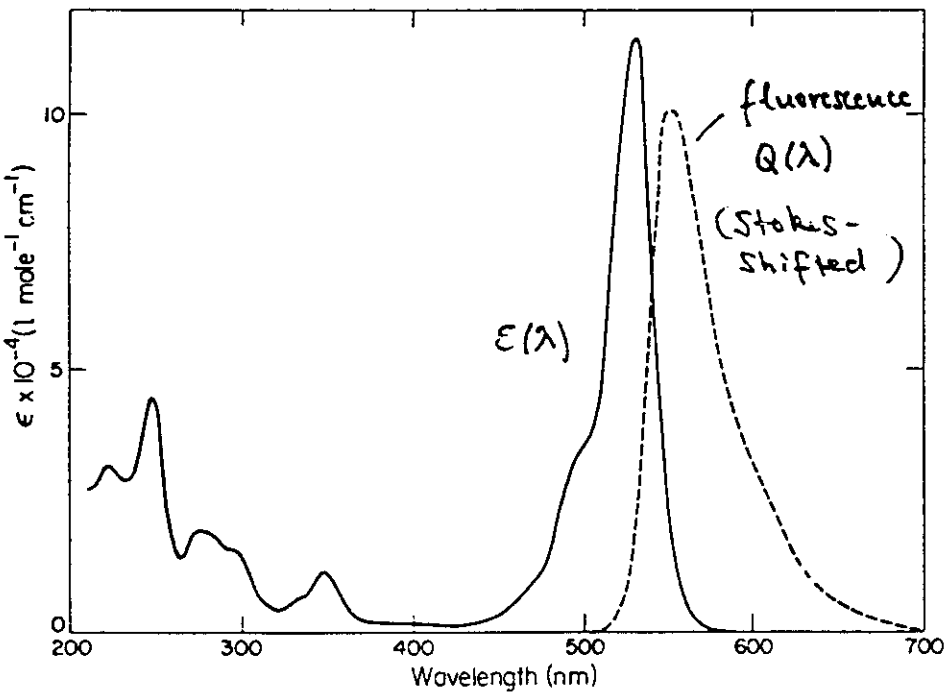

Lambert-Beer's law:

$$I_{\omega,l} = I_{\omega,0}\, e^{-\sigma_{abs}(\omega)\, N_0\, l} = I_{\omega,0}\, 10^{-\varepsilon_\omega c l}$$

Absorption cross-section

$\sigma_{abs}(max) \approx 2\text{-}3 \cdot 10^{-16}$ cm² (typically)

Fig. 5.4. Rhodamine 6G in ethanol. (———) Absorption spectrum (ε molar decadic extinction coefficient); (– – –) quantum spectrum of fluorescence (arbitrary units)

AND

PHOTONS

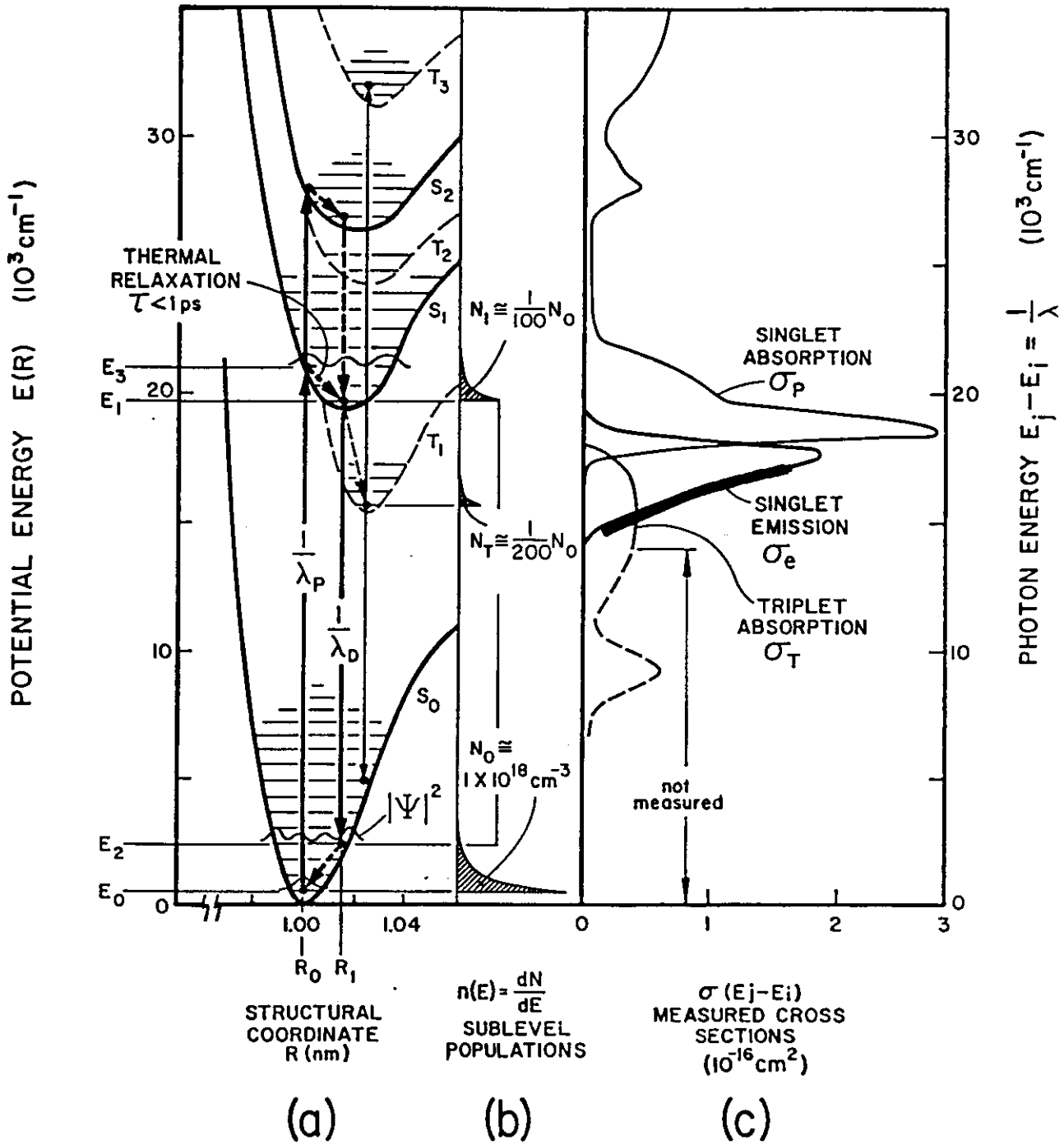

Figure 4. Schematic potential energy wells constructed to be consistent with the measured spectra for the rhodamine 6G dye molecule. (a) The potential energy versus generalized structural coordinate (nuclear separation) for the first three singlet, and first three triplet energy bands. Laser light absorption and emission (at pump and dye laser wavelengths) are indicated by heavy arrows, non-radiative (collision) processes by light arrows. (b) Thermal equilibrium sublevel population distributions in these six bands (only the lowest three are appreciably populated). (c) Absorption and emission cross sections measured for this dye (except that the triplet absorption between 5 k to 14 k cm^{-1} is inferred from spectra on similar dyes).

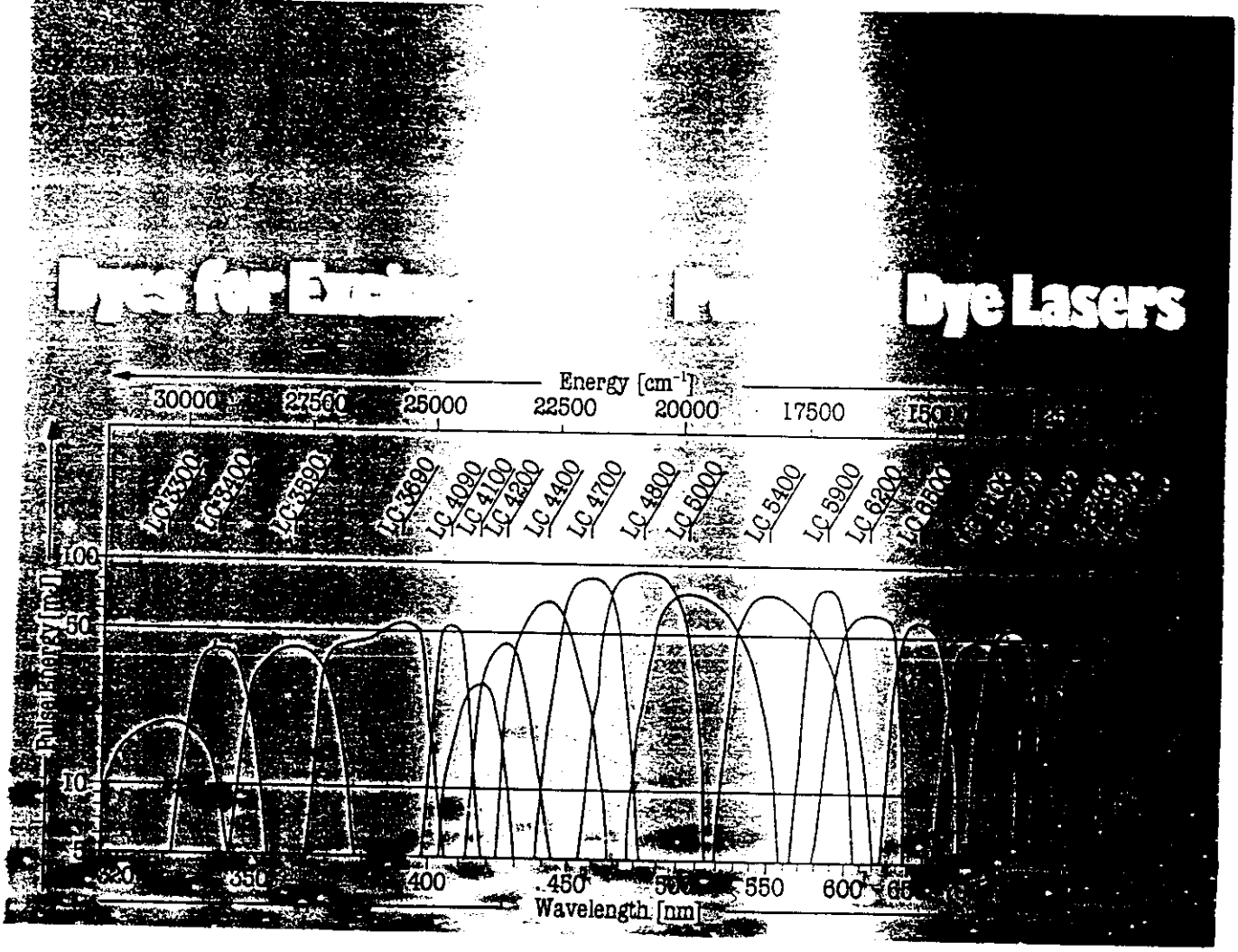

899 RING LASER TUNING CURVES

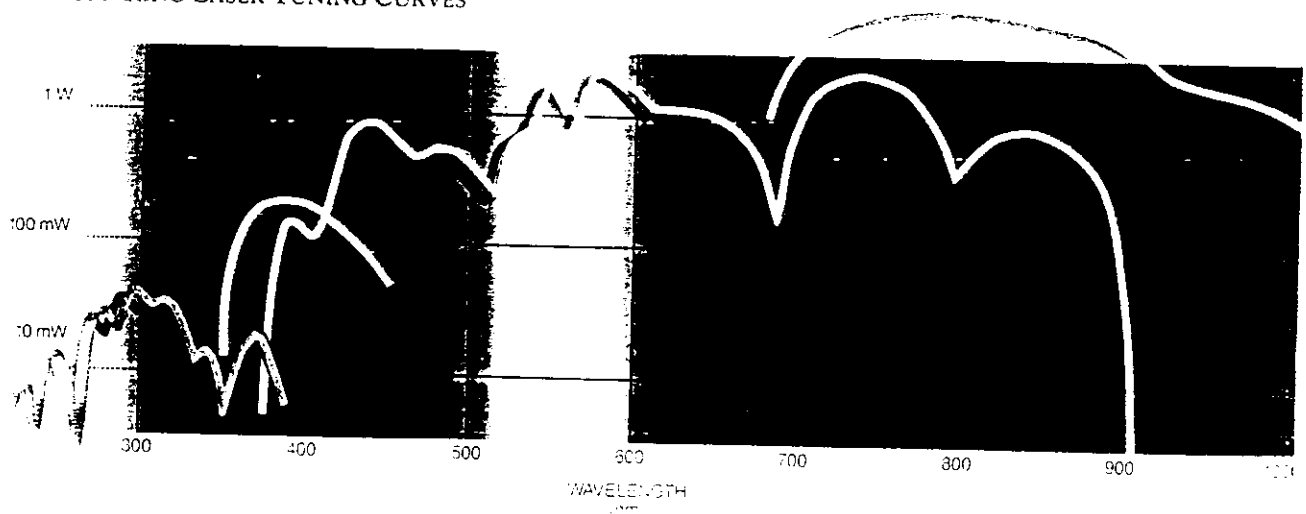

Important properties of Laser Dyes

1) Good solubility in many liquids (H_2O, EOH...)
   ↳ flexible control of gain, pump volume, and beam crossection by changing the concentration

2) High fluorescence quantum yield (≈ 1)
   ↳ High laser efficiency for $S_0 \rightarrow S_1$ pumping

3) Broad and smooth fluorescence spectrum (1000 cm^{-1})
   ↳ makes tunable & narrow bandwidth laser operation possible

4) Laser dyes for the whole spectral range
   UV (320 nm) $\longleftrightarrow$ IR (1,1 µm) available
   ↳ Most important spectral range for spectroscopy

5) No permanent damage of active volume when using liquid dye solution
   ↳ Liquids provide large heat capacity, in addition, pumps can ensure a fast exchange of pumped volume

KINETIK (KINETICS)

Pumpe (Pump) — stim. Em. — spont.

Phot. $\frac{\partial I}{\partial z} + \frac{n}{c}\frac{\partial I}{\partial t} = + \sigma_e I N_1$

e.g. Moleküle (excited molecules): $\frac{\partial N_1}{\partial t} = +\sigma_p I_p N_0 - \sigma_e I N_1 - \frac{1}{\tau} N_1$

$$N_0 = N - N_1$$

$$W = \sigma_p I_p \quad [s^{-1}]$$

▶ INVERSION

$$\frac{\partial N_1}{\partial t} = W \cdot (N - N_1) - \sigma_e I N_1 - \frac{1}{\tau} N_1$$

Stationarität (stationary solution) ↓

$$\boxed{N_1 = \frac{W}{W + \frac{1}{\tau} + \sigma_e I}}$$

$\frac{\partial N_1}{\partial t} \to 0$

● VERSTÄRKUNG VON I

(Amplification of Intensity I)

Stationär (stationary): $\frac{\partial I}{\partial z} = +\sigma_e I N_1$

$$N_1 = \frac{W}{W + \frac{1}{\tau} + \sigma_e I}$$

▶ DIFFERENTIAL GLEICHUNG (equation)

$$\boxed{\frac{\partial I}{\partial z} = \frac{g_0}{(1 + I/I_s)} \cdot I}$$

KLEINSIGNAL-VERSTÄRKUNGS KOEFFIZIENT (Small signal gain)

$$g_0 = \sigma_e \frac{W}{W + \frac{1}{\tau}} N$$

"SÄTTIGUNGS-PHOTONENFLUSS (FLÄCHEN) DICHTE (Saturation Intensity)

$$I_s = \frac{W + \frac{1}{\tau}}{\sigma_e}$$

LÖSUNG DER DIFF. VERSTÄRKUNGS-GLEICHUNG

(Solution of diff. equation)

$$\frac{\partial I}{\partial z} = \frac{g_0}{(1 + I/I_S)} \cdot I = I_S \cdot \frac{(1+I/I_S)-1}{(1+I/I_S)} \cdot g_0$$

$$= I_S \left[g_0 - \frac{g_0}{(1+I/I_S)} \right]$$

$$\frac{\frac{\partial I}{\partial z}}{I_S} - g_0 = - \frac{g_0}{(1+I/I_S)} = - \frac{\partial \ln I}{\partial z}$$

Integriert von $z=0$ bis $z=\ell$: (after integration $\int_0^\ell$)

$$\frac{I_\ell - I_0}{I_S} - g_0 \cdot \ell = - \ln\left(\frac{I_\ell}{I_0}\right)$$

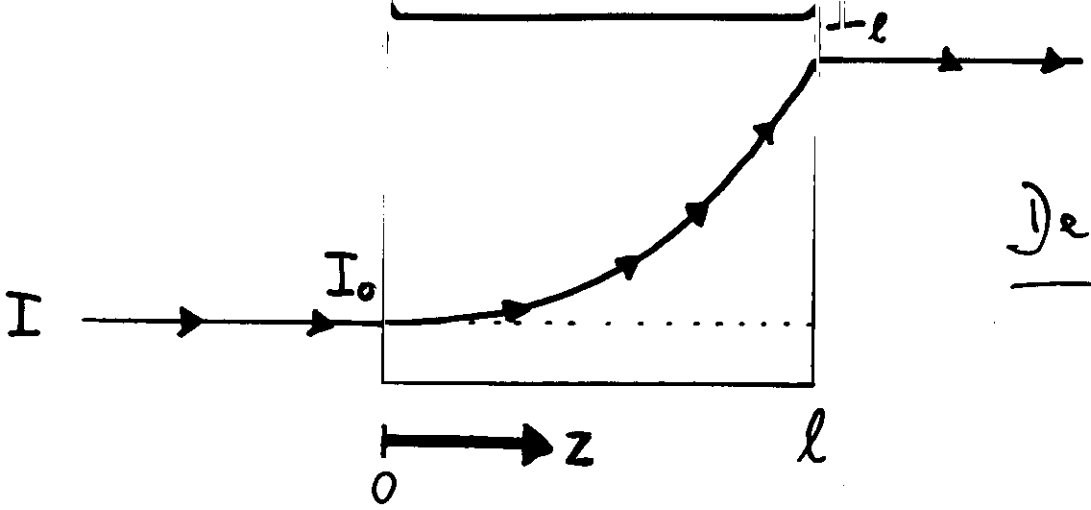

Dependency of I_0

VERSTÄRKUNG $\quad G = \dfrac{I_l}{I_0}$

KLEINSIGNAL VERSTÄRKUNG $\quad G_0 = \lim_{I_0 \to 0} \left(\dfrac{I_l}{I_0} \right)$

$$\frac{\ln\left(\frac{G}{G_0}\right)}{(1-G)} = \frac{I_0}{I_S}$$

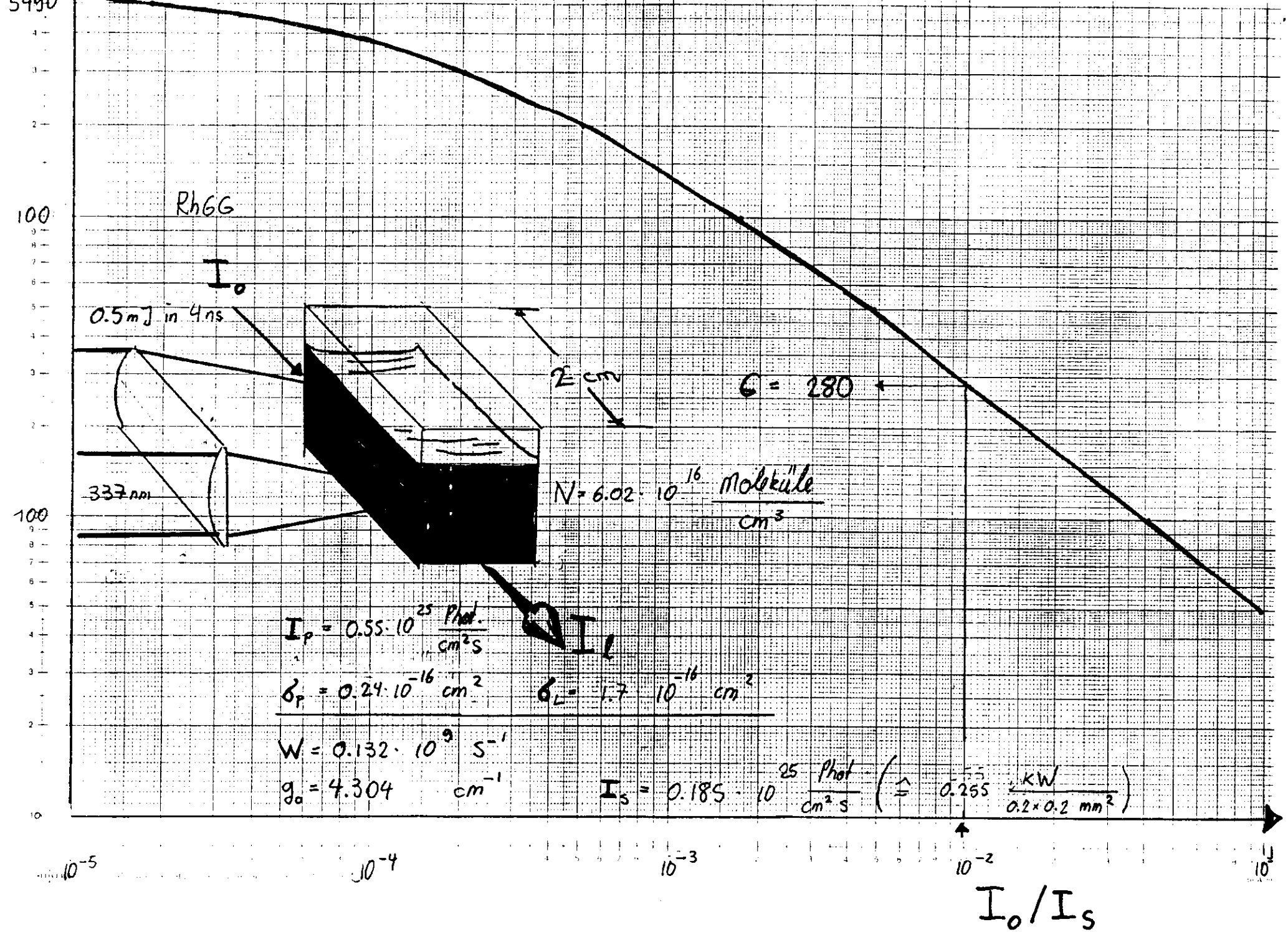
RhGG
I_0
0.5 mJ in 4 ns
337 nm
2 cm
C = 280
$N = 6.02 \cdot 10^{16}$ Moleküle / cm³
$I_P = 0.55 \cdot 10^{25}$ Phot. / cm²s
$\sigma_P = 0.24 \cdot 10^{-16}$ cm²
I_L
$\sigma_L = 1.7 \cdot 10^{-16}$ cm²
$W = 0.132 \cdot 10^9$ s⁻¹
$g_a = 4.304$ cm⁻¹
$I_S = 0.185 \cdot 10^{25}$ Phot. / cm²s (≙ 0.255 kW / 0.2 × 0.2 mm²)
5490
100
100
10^{-5}
10^{-4}
10^{-3}
10^{-2}
I_0 / I_S

ABHANGIGKEIT DES I VON DEM WEG z

(Dependency of I versus path length z)

$$\frac{I_z - I_0}{I_s} + \ln\left(\frac{I_z}{I_0}\right) = g_0 \cdot z$$

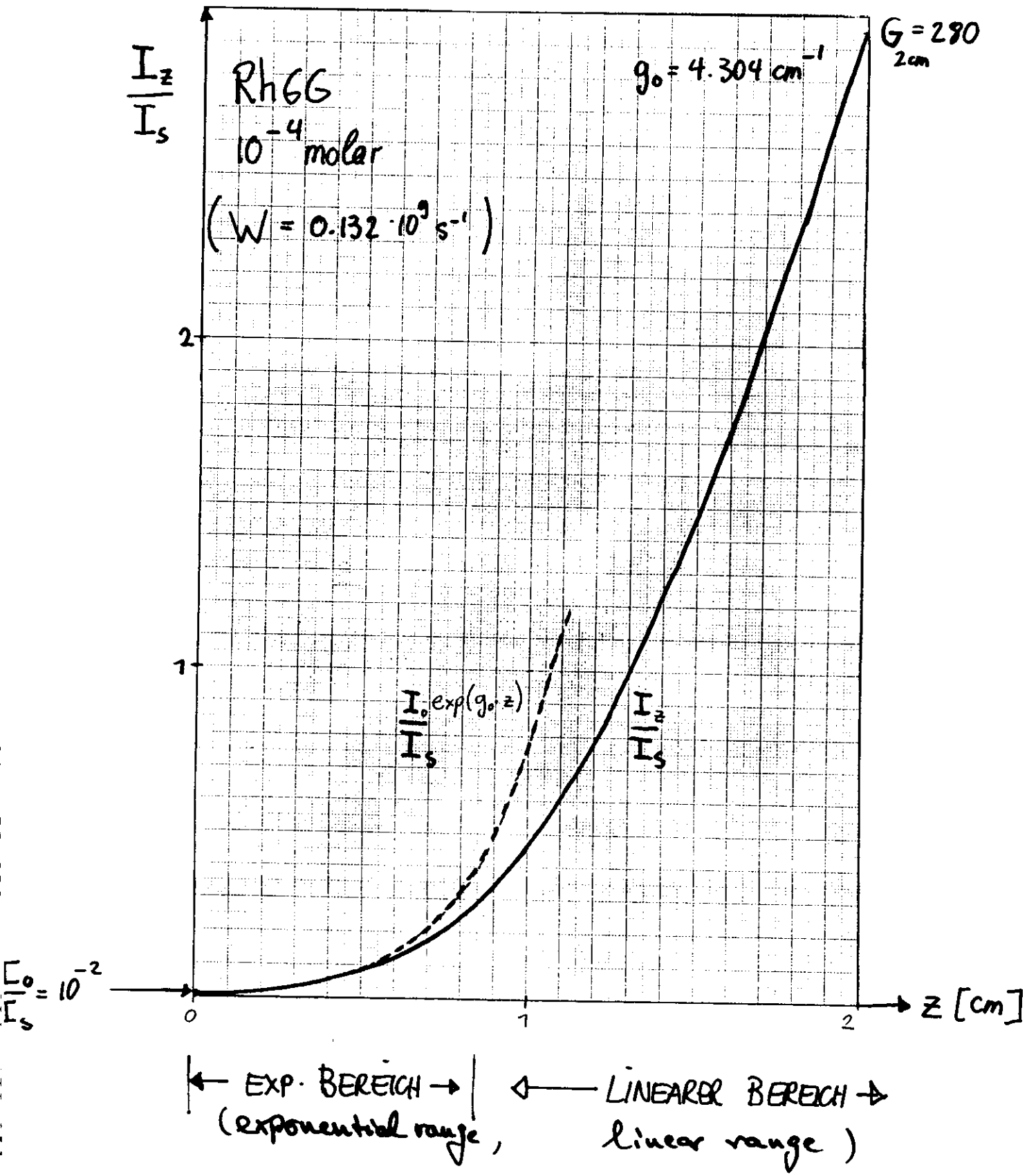

← EXP. BEREICH → | ← LINEARER BEREICH →

(exponential range, linear range)

Dye Laser

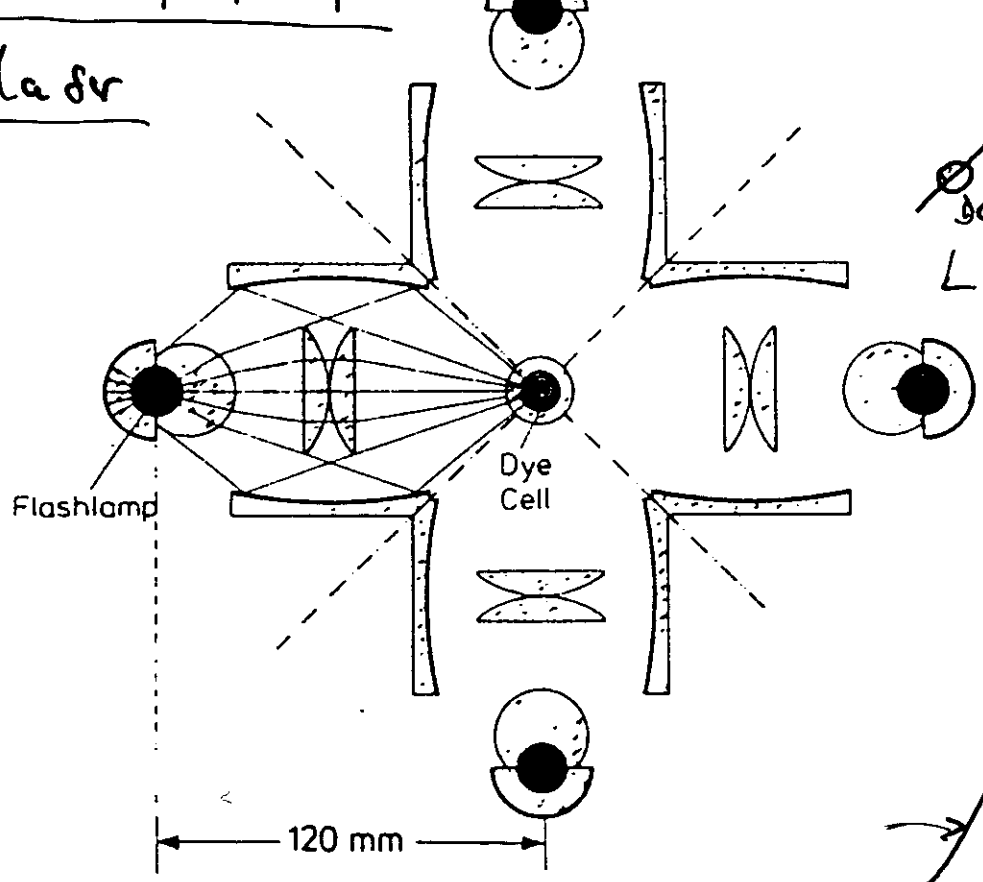

$\varnothing_{DC}$ = 10mm

L = 150mm

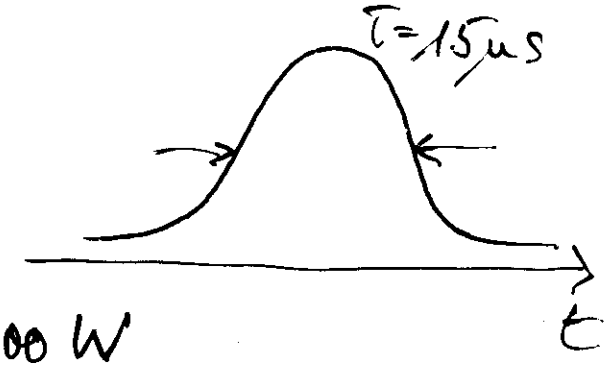

Fig. 1. Pumping cavity.

Average power at 50 Hz : 100 W

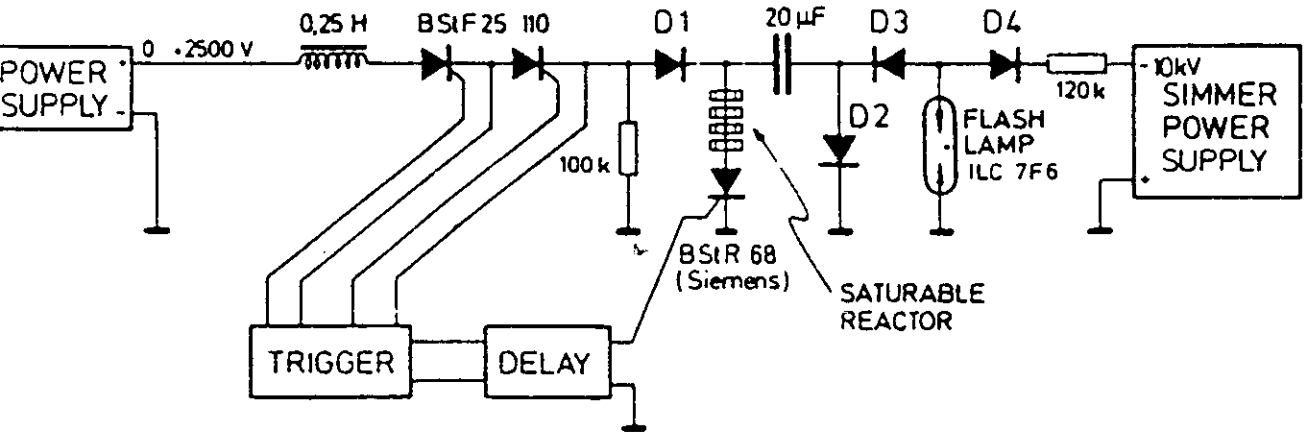

Jethwa et al., IEEE J. Quant. Electr. QE-14 (1978), 119

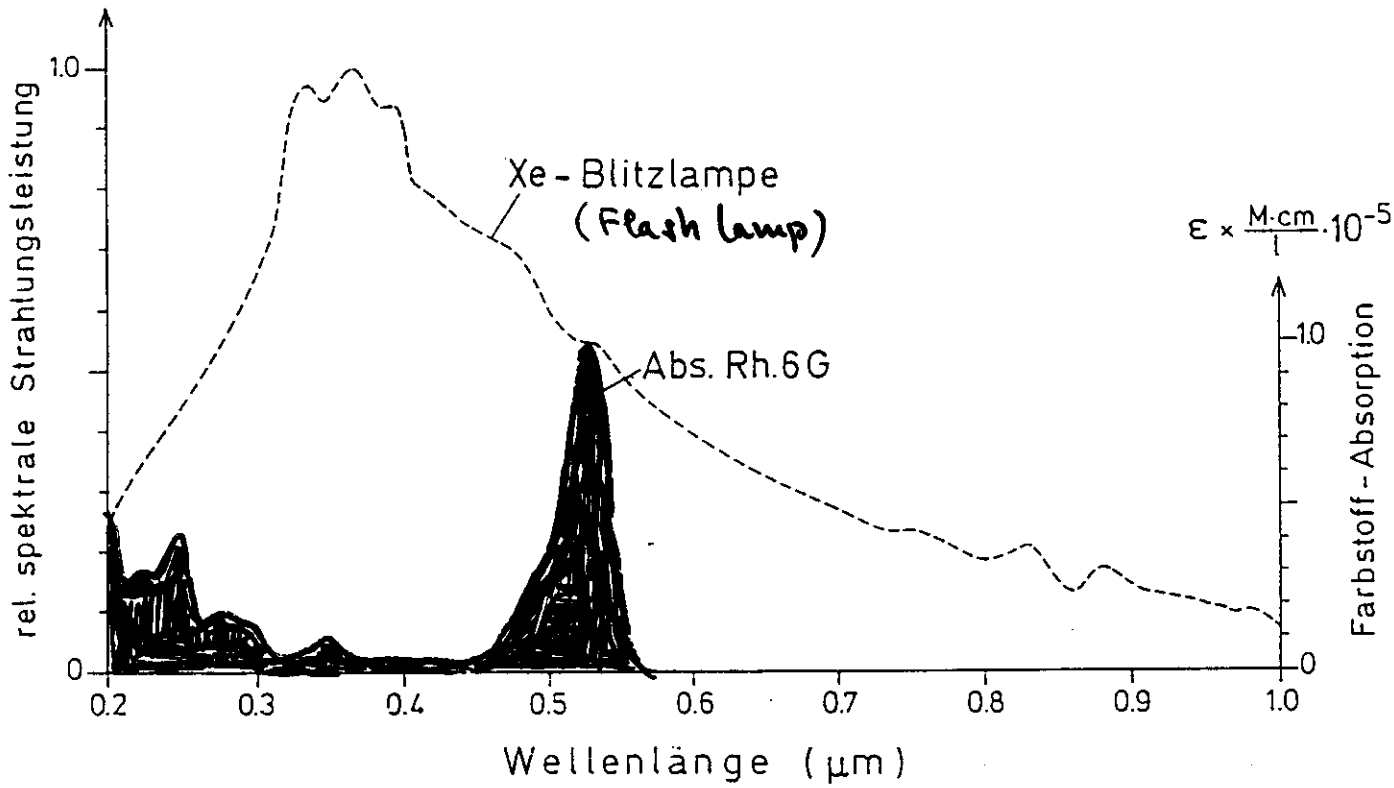

Strahlungslose Energieübertragung nach dem Förster–Mechanismus

$$k_{\substack{\text{Transfer} \\ \text{Donator} \rightarrow \text{Akzeptor}}} \sim \frac{1}{r^6} \cdot \int F_D(\nu) \cdot \varepsilon_A(\nu) \cdot d\nu$$

Abstands-Bedingung — Überlappungs-Bedingung

Dipol-Dipol interaction

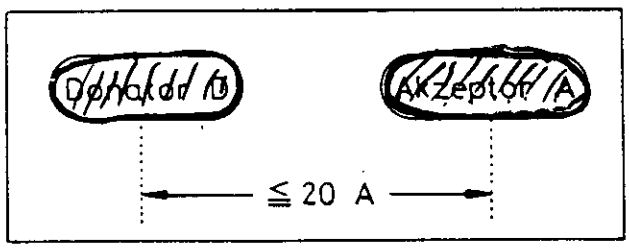

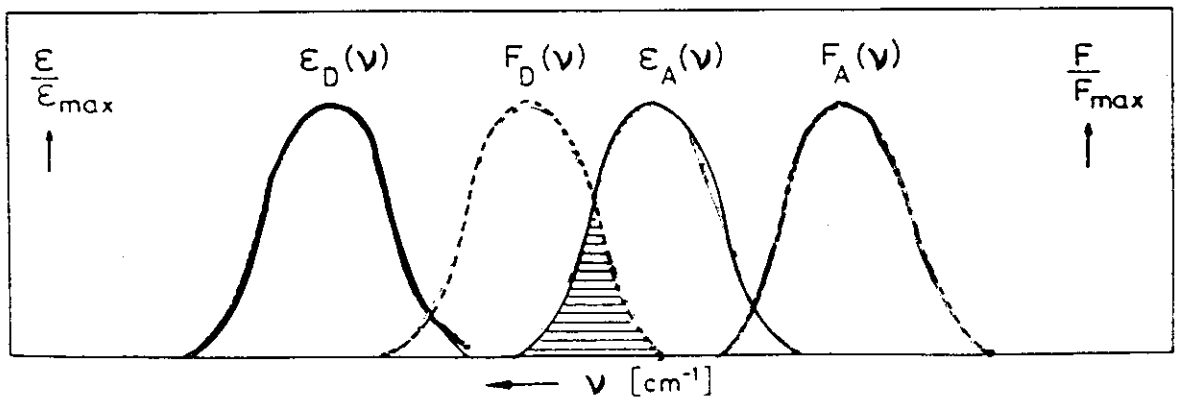

DYE LASERS
(pulsed)

today Excimer- and Nd:YAG - Lasers used for pumping

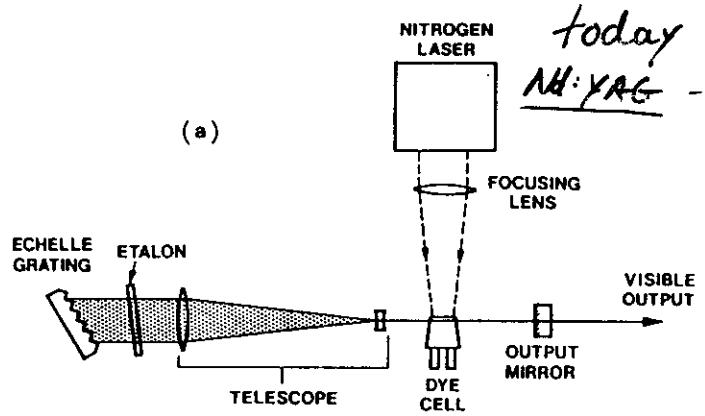

$$M = \frac{\left[1 - \frac{\sin^2\theta}{n^2}\right]^{\frac{1}{2}}}{\cos\theta}$$

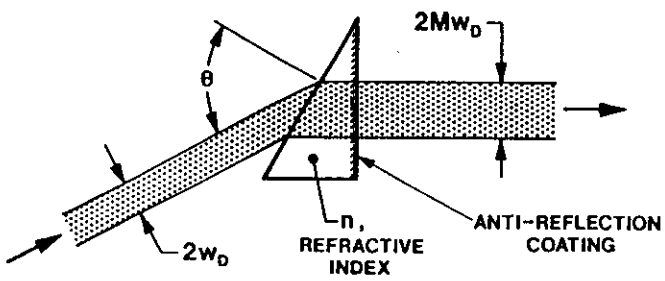

FIG. 5. The original short-pulse tunable dye oscillator. (a) The layout by Hänsch, with an intracavity telescope to increase the resolution of the grating. (b) One-dimensional beam expansion in a prism with high incidence angle on the input face and normal incidence on the exit face. A series of four prisms, arranged for no net dispersion, makes up the "quad-prism expander" that has replaced the Hänsch telescope. [Adapted with permission from Klauminzer, G. K. (1977). *IEEE J. Quantum Electronics* **QE-13,** 103. © 1977 IEEE.]

TUNABLE DYE LASERS

(CW)

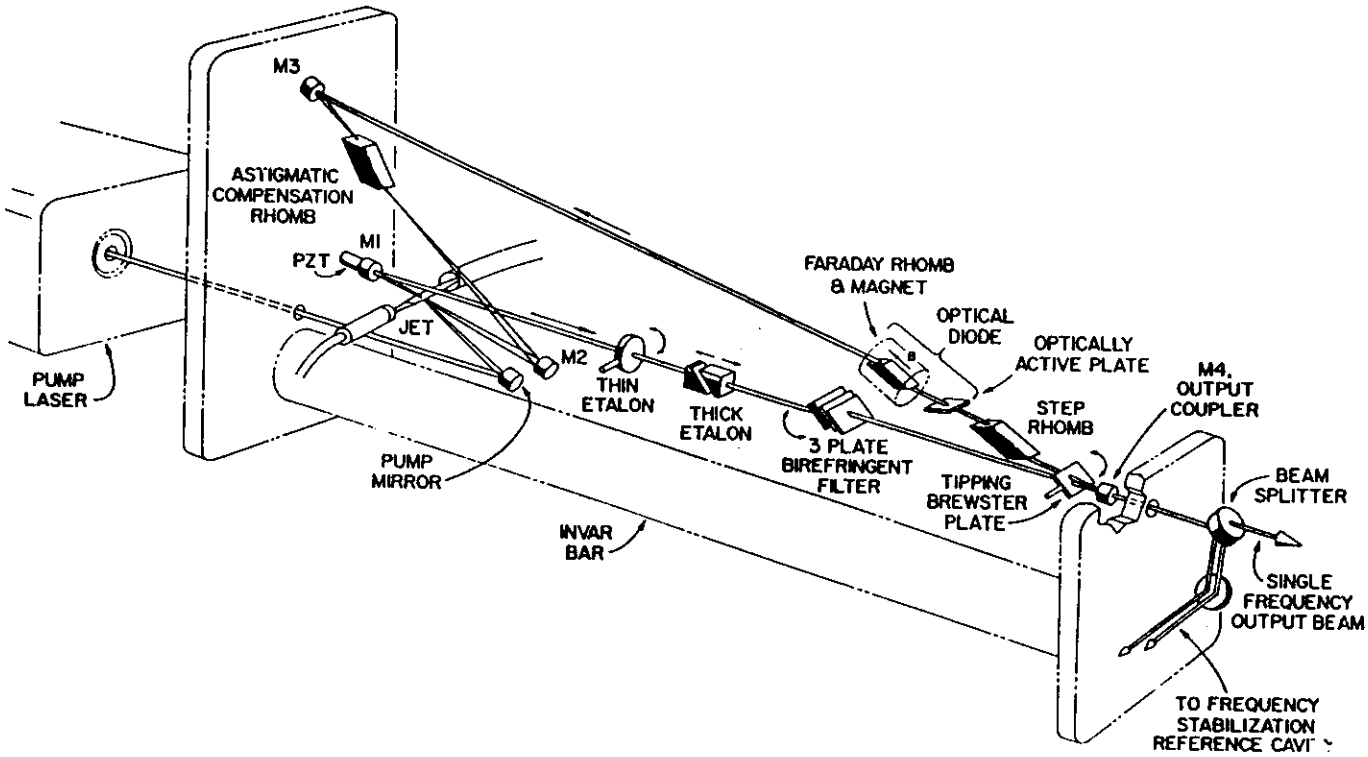

FIG. 10. Tunable single-frequency ring (traveling-wave) dye laser of current design. Spherical folding mirrors M1 to M3 and flat output coupler M4 fold the beam in a figure-eight path, which is traversed in the direction shown by arrows due to the biasing action of the optical diode element. Elements in the horizontal arm lying between M1 and M4 constitute the tunable filter stack, and the output frequency is controlled and the linewidth narrowed by a frequency stabilization servo (whose elements are not shown). (Courtesy of Coherent, Inc., Palo Alto, Calif.)

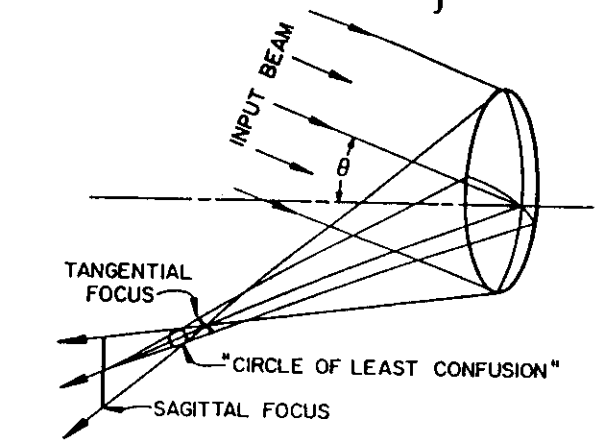

(a)

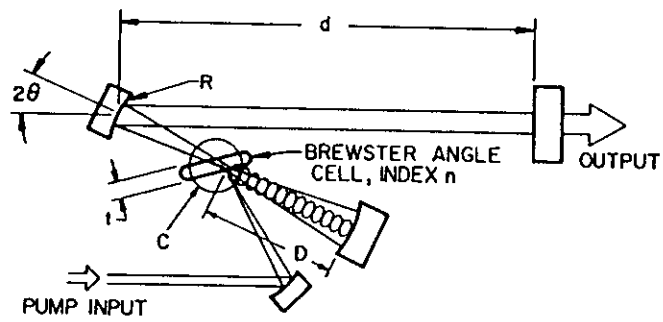

For Compensation:

$$R \sin\theta \tan\theta = 2t \frac{(n^2-1)\sqrt{n^2+1}}{n^4}$$

(b)

FIG. 8. (a) Astigmatism of an off-axis spherical mirror and (b) its compensation by a Brewster plate in a three-mirror focusing cavity, as originally used for standing-wave cw dye lasers.

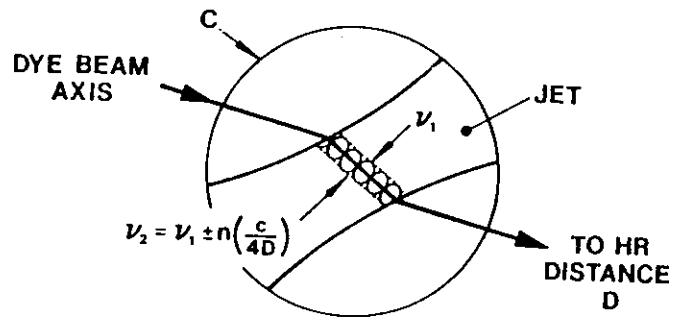

FIG. 9. Enlarged view of the jet, replacing the dye cell inside the circle C of the three-mirror cavity of Fig. 8b, showing the standing waves of the first frequency to lase locally depleting the gain or "burning spatial holes." This leaves gain regions unaddressed and allows a second frequency to lase.

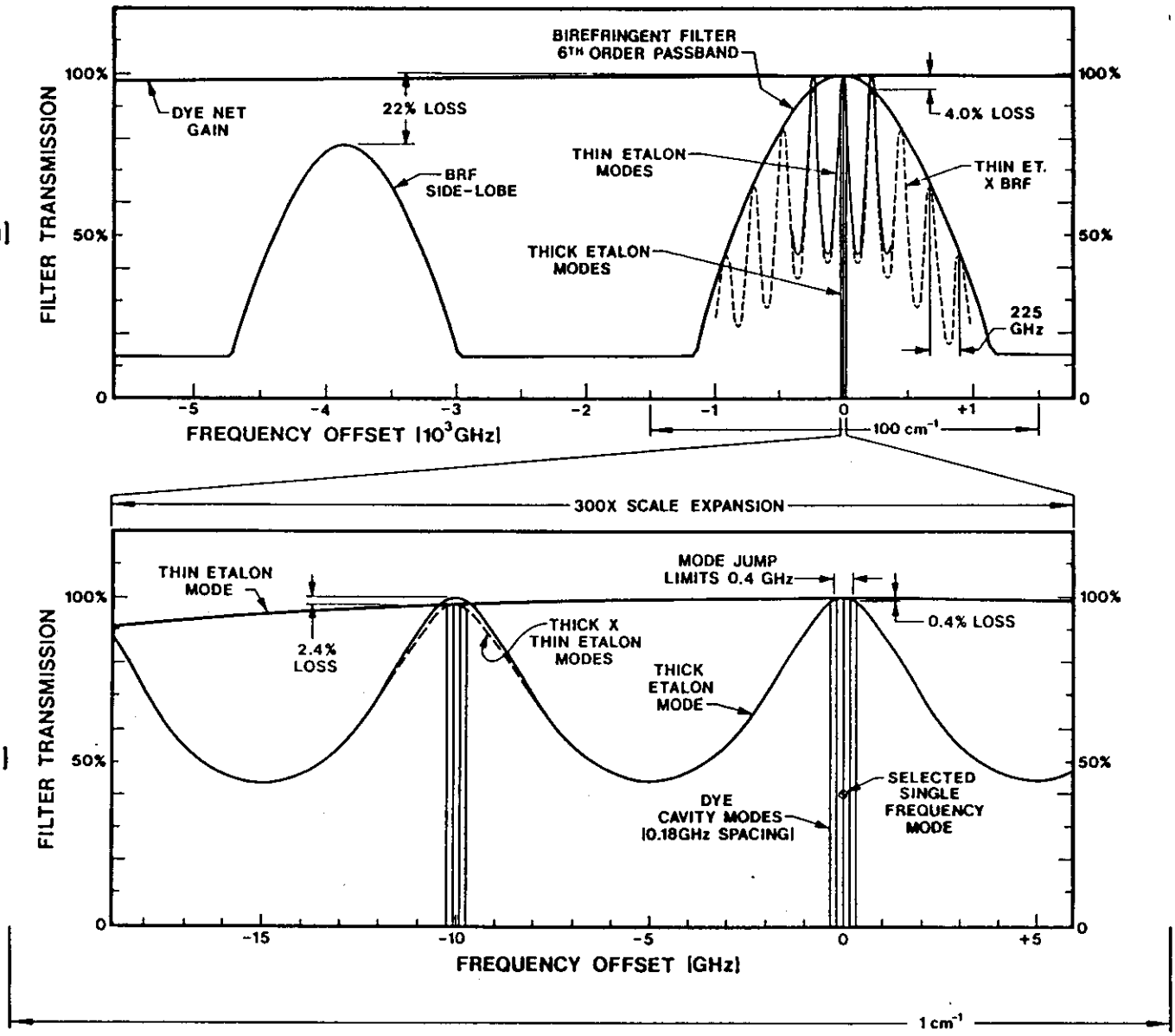
(a)
BIREFRINGENT FILTER
6TH ORDER PASSBAND
DYE NET GAIN
22% LOSS
4.0% LOSS
BRF SIDE-LOBE
THIN ETALON MODES
THIN ET. X BRF
THICK ETALON MODES
225 GHz
FILTER TRANSMISSION
100%
50%
0
-5
-4
-3
-2
-1
0
+1
FREQUENCY OFFSET (10³GHz)
100 cm⁻¹
300X SCALE EXPANSION
(b)
THIN ETALON MODE
MODE JUMP LIMITS 0.4 GHz
2.4% LOSS
THICK X THIN ETALON MODES
THICK ETALON MODE
0.4% LOSS
DYE CAVITY MODES (0.18GHz SPACING)
SELECTED SINGLE FREQUENCY MODE
-15
-10
-5
0
+5
FREQUENCY OFFSET (GHz)
1 cm⁻¹

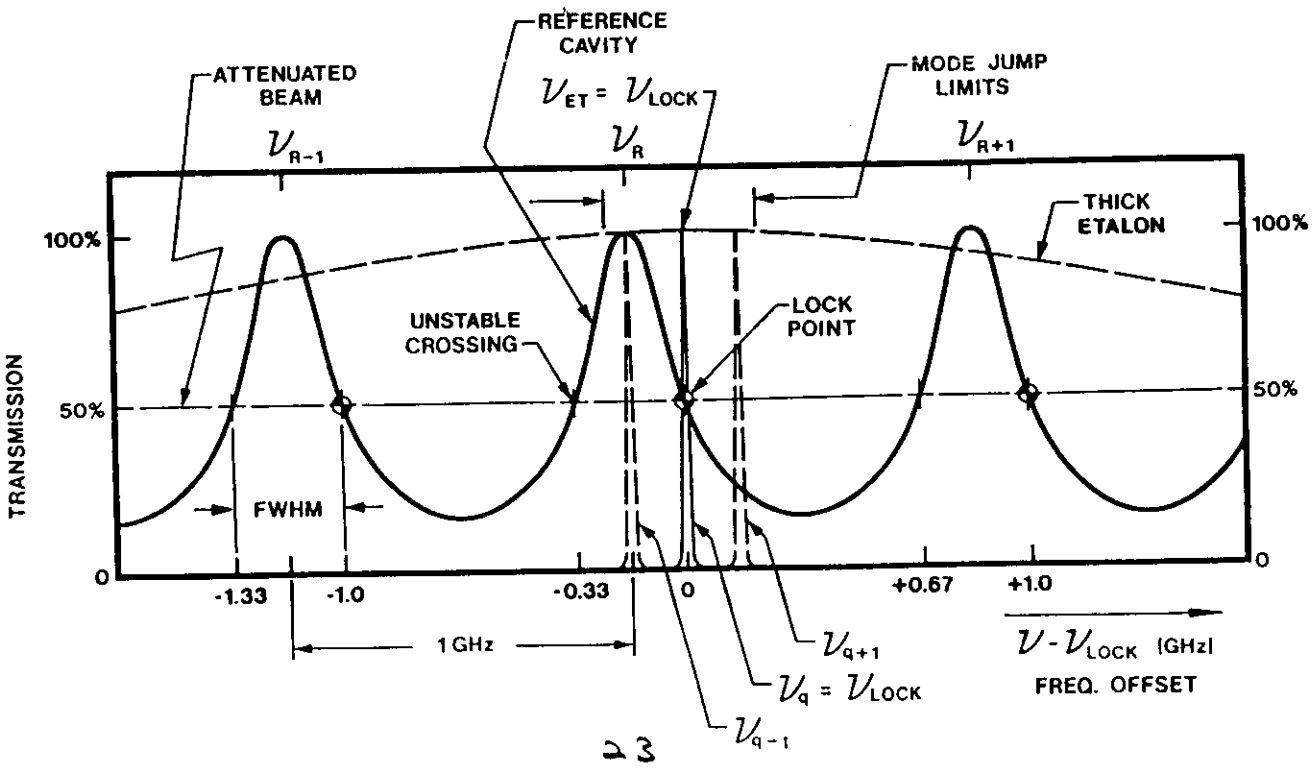
REFERENCE CAVITY
ATTENUATED BEAM
MODE JUMP LIMITS
$\nu_{ET} = \nu_{LOCK}$
ν_{R-1}
ν_R
ν_{R+1}
THICK ETALON
UNSTABLE CROSSING
LOCK POINT
TRANSMISSION
100%
50%
0
FWHM
-1.33
-1.0
-0.33
0
+0.67
+1.0
1 GHz
ν_{q+1}
$\nu_q = \nu_{LOCK}$
ν_{q-1}
$\nu - \nu_{LOCK}$ (GHz)
FREQ. OFFSET

Table 2. Commercially available high-performance CW lasers*

Type	Company	Model	Pump laser	Power out	Tuning range	Linewidth	Comments
Linear	Coherent Inc.	599-01	5-W argon ion	880 mW	400–1000 nm	40 GHz	broadband tunable
	Spectra-Physics	375B	ion lasers models 2016/ 2020/2040	1 W	400–900 nm	<40 GHz with 3-plate BRF	broadband tunable; other tuning elements give broader or narrower linewidth; power stabilizer option
Ring	Coherent Inc.	699-29	7.5-W argon ion	860 mW	400–1000 nm	0.5 MHz	microprocessor controlled; frequency-doubled and broadband (2 GHz, 1.25 W) models available
	Spectra-Physics	380D	ion lasers	550 mW	400–900 nm	0.5 MHz	stabilized single-frequency scanning; broadband (30 GHz) models and frequency-doubling option available

BRF = birefringent filter
* For a complete listing of commercially available high-performance CW lasers, see the *1990 LF World Buyers' Guide.*

Table 1. Pulsed dye-laser performance

Pump laser	Pump wavelength	Output dye energy/pulse	Repetition rate	Comments
Frequency-doubled* Nd:YAG laser	532 nm	up to 150 mJ	up to 50 Hz**	visible pump; pumps red region of visible
Excimer laser	308 nm (XeCl)	up to 80 mJ	up to 400 Hz	XeF and KrF excimer lasers can be used to pump dyes
Nitrogen laser	337 nm	up to 70 μJ	up to 100 Hz (usually 20 Hz)	low-cost, low-energy UV; can use sealed dye cell
Linear flashlamp	broadband	up to 5 J	up to 20 Hz	tunable output from 430 to 750 nm; as rep rate increases, energy decreases; very long pulses (0.4 ms) possible
Coaxial flashlamp	broadband	up to 400 J	up to 50 Hz	tunable output from 220 to 960 nm; as rep rate increases, energy decreases
Copper-vapor laser	510 nm 578 nm	up to 2 mJ	up to 10 kHz	high rep rate; visible pump

* Frequency-tripling available for UV pumping
** Mode-locked Nd:YAG lasers for MHz repetition rates, but low energy/pulse

Table 3. Commercially available ultrafast lasers***

Type	Company	Pump laser	Pulsewidth (fs)	Repetition rate	Energy/pulse (nJ)	Tuning range (nm)	Comments
CW-pumped passively mode-locked	Clark Instrumentation	CW argon-ion	<100	90 MHz	0.1	605–635	CPM laser kit
	Photonetics	CW ion	80	100 MHz	0.2	580–840	
	Femtochrome Research	CW argon-ion	250	80–200 MHz	1	575–625	linear cavity with CPM option
Synchronously pumped mode-locked	Spectra-Physics	doubled mode-locked compressed Nd:YAG	<500	82 MHz*	2.7 (with R6G and 800-mW pump power)	575–880 nm (using 4 dyes)	compressed pump pulse directly generates sub-picosecond pulses in the dye
	Quantronix Inc.	doubled mode-locked Nd:YLF or YAG	<250	76–100 MHz	0.8 (with R6G dy and 1-W pump power)	575–618 (DODCI/DQOCI); 680–700 (DDI)	GVD compensation; vertically mounted sapphire jet nozzle
Hybrid mode-locked	Coherent Inc.	doubled Nd:YAG	220**	76 MHz	3.3	580–900	active stabilization; GVD compensation

*82 Hz is mode-locking frequency of pump laser. With cavity-dumped synchronous pumping, single-shot to 4-GHz operation is possible.
**pulse autocorrelation width
GVD = group velocity dispersion
CPM = colliding-pulse mode-locked
***For a complete listing of commercially available ultrafast lasers, see the *1990 LF World Buyers' Guide.*

Pulsed Tunable Dye Lasers

Pulsed dye lasers: 50% of total dye laser market, thereof

- 50 % excimer laser pumped (308 nm)
- 50 % Nd:YAG laser pumped

- o High spectral resolution - 500 MHz possible - sufficient for sub-Doppler spectroscopy
- o High peak power - > 10 MW possible - allows efficient doubling, and mixing of laser wavelength from VUV to IR
- o High average power (pulse energy x rep rate) - > 15 W possible - allows fast signal processing (gated detection) instead of single photon counting
- o Short pulse duration - << 10 ns possible - allows time resolved spectroscopy of excited electronic states

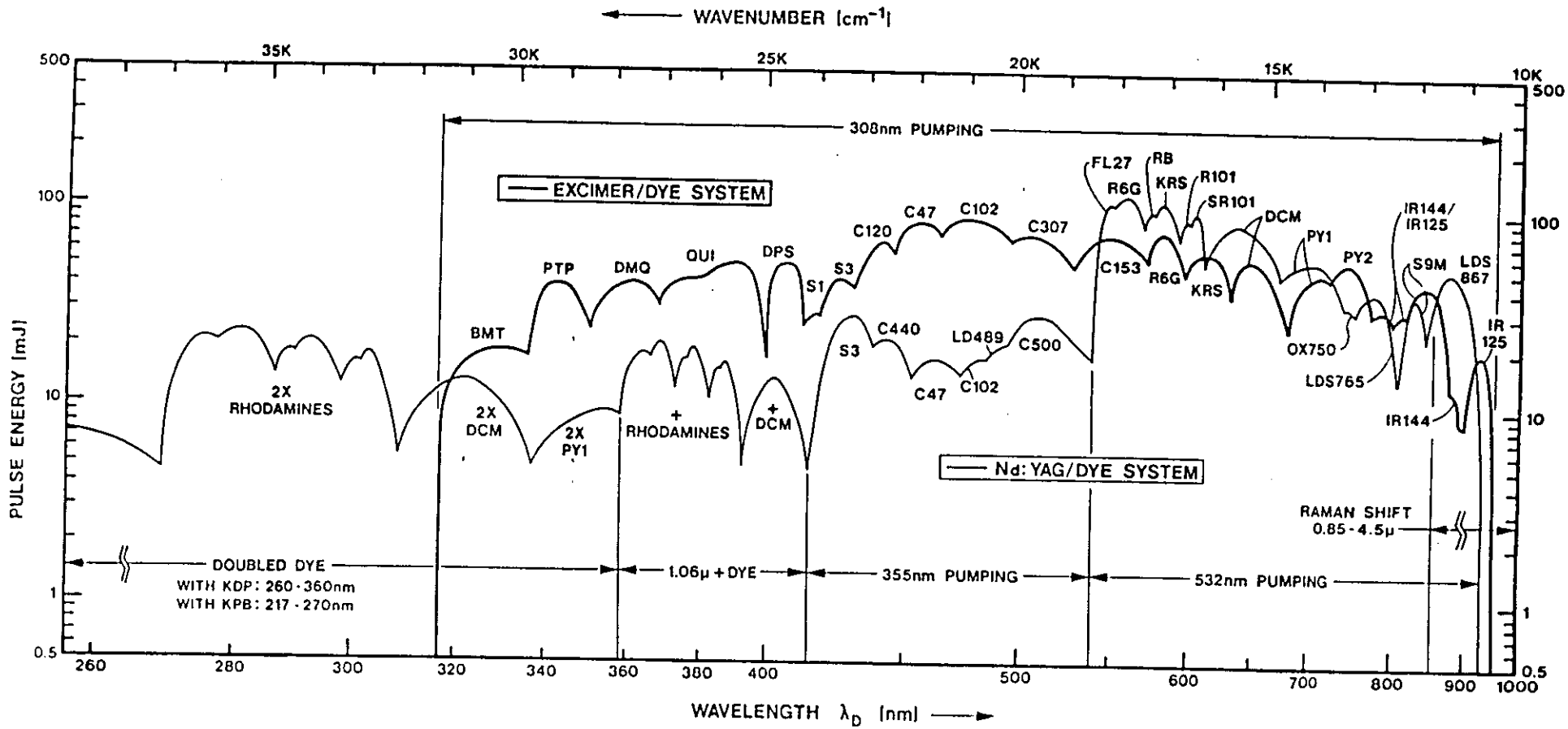

SHORT PULSE DYE TUNING SPECTRUM

Figure 7. Output tuning curves in energy per pulse at low repetition rates for excimer laser pumped (heavy line) and Nd:YAG laser pumped (light line) short pulse dye lasers. Only the upper portion of a dye's tuning curve (above that of the adjacent dyes) is shown. Alternative pumping schemes to those shown are also possible for for the YAG system, with the 266 nm fourth harmonic to pump dyes with 334-387 nm outputs, and with the 1.06 micron fundamental to pump dyes with 1.09 - 1.32 micron outputs.

...excimer data, courtesy of Lambda Physik, Gottingen, West Germany
...Nd: YAG data, courtesy of Quanta Ray, Mountain View, California

- Narrow bandwidth -

- tunable -

Pulsed Dye Lasers

Philosophy of oscillator design:

- Littrow / Hänsch

or

- grazing incidence ?

Shoshan (1977)
Littman (1978)
Saikan (1978)

LITTROW HÄNSCH TYPE OSCILLATOR

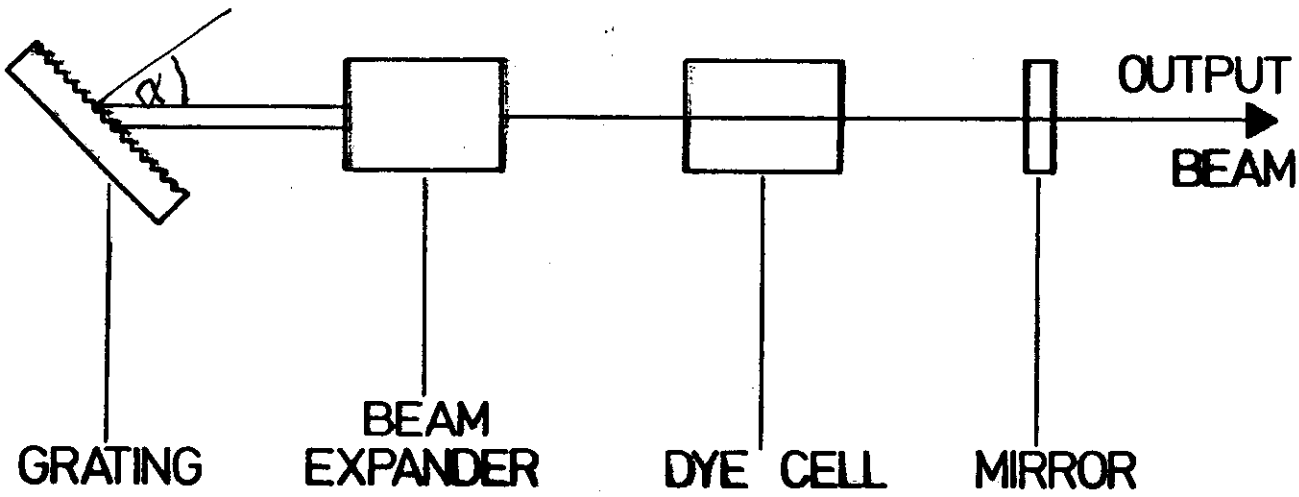

$$\lambda = \frac{2d}{n}(\sin\alpha)$$

United States Patent [19]
Shoshan

[11] 4,229,710
[45] Oct. 21, 1980

[54] WAVELENGTH SELECTOR FOR TUNABLE LASER

[76] Inventor: Itamar Shoshan, 7 Maimon St., Haifa, Israel, 32584

[21] Appl. No.: 921,830

[22] Filed: Jul. 3, 1978

[30] Foreign Application Priority Data

Oct. 21, 1977 [GB] United Kingdom 44006/77

[51] Int. Cl.³ H01S 3/08
[52] U.S. Cl. ..... 331/94.5 C; 350/162 R; 350/168
[58] Field of Search ..... 331/94.5 C, 94.5 D, 331/94.5 L; 350/168, 162 R

[56] References Cited

U.S. PATENT DOCUMENTS

3,684,979	8/1972	Myer et al.	331/94.5 L
3,691,477	9/1972	Janney	331/94.5 C

OTHER PUBLICATIONS

Shosham et al., Narrowband Operation of a Pulsed Dye Laser Without Intracavity Beam Expansion, J. Appl. Phys., vol. 48, No. 11, (Nov. 1977), pp. 4495–4497.
Brannen et al., Far-Infrared Laser Action Using Compound Grating Fabry-Perot Resonators, IEEE J. Quant. Electr., (Feb. 1970), pp. 138–139.

Primary Examiner—William L. Sikes
Attorney, Agent, or Firm—Browdy and Neimark

[57] ABSTRACT

A wavelength selector for use in a laser cavity comprising a diffraction grating mounted at an angle near grazing incidence with respect to the beam travelling away from the excited medium and a reflector which reflects the beam diffracted by the grating back along its incidence path. Wavelength tuning is accomplished by rotating this reflector, while the grating remains fixed. Rotation of the grating provides linewidth variation.

35 Claims, 5 Drawing Figures

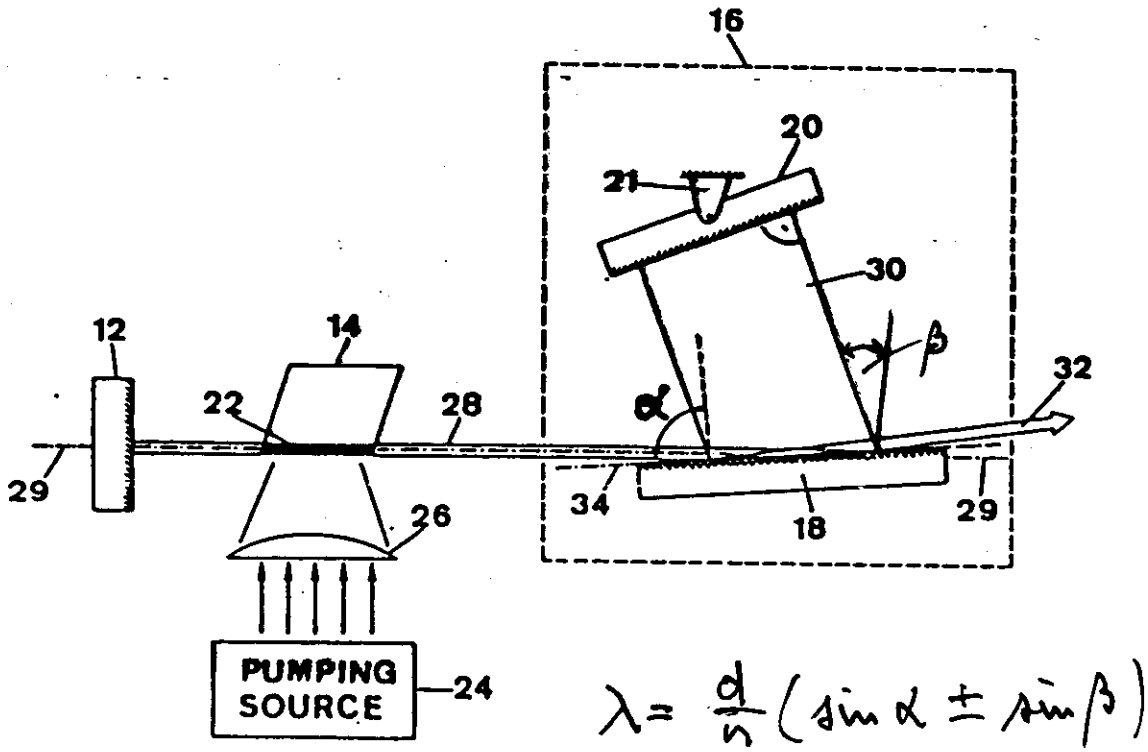

$$\lambda = \frac{d}{n}(\sin\alpha \pm \sin\beta)$$

Single-mode operation of grazing-incidence pulsed dye laser

Michael G. Littman

Research Laboratory of Electronics and Department of Physics, Massachusetts Institute of Technology, Cambridge, Massachusetts 02139

Received May 12, 1978

A variation of the grazing-incidence pulsed dye laser is presented. This laser has been operated in a single longitudinal cavity mode with a single-shot linewidth of less than 300 MHz and a time-averaged linewidth of 750 MHz. The single-mode conversion efficiency of the laser is 2% using Rhodamine 6G dye.

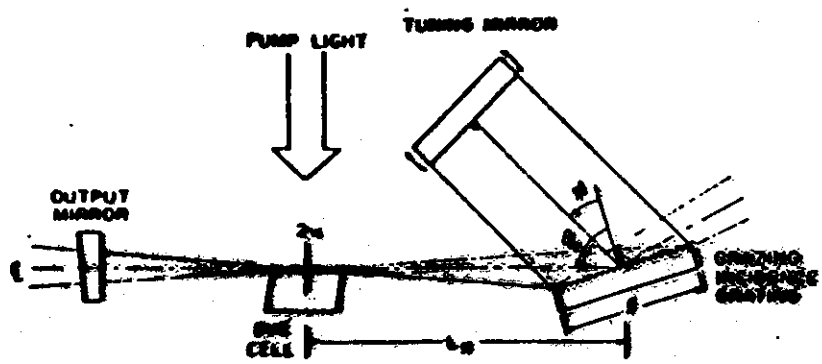

Fig. 1. Schematic of single-grating pulsed dye laser.

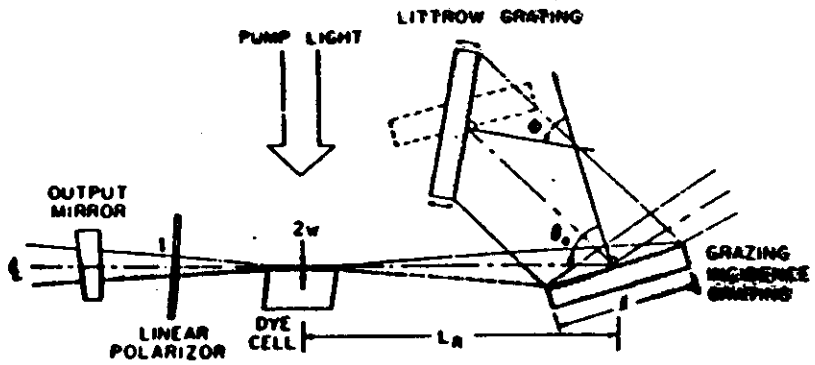

Fig. 2. Schematic of double-grating pulsed dye laser.

Written by:
G. Klauminzer

THE LUMONICS EPD-330 DYE LASER AND A COMPARISON TO THE LAMBDA PHYSIK FL 2002 DYE LASER

I. Introduction

The Lumonics EPD-330 dye laser oscillator is not a new design, but is a rebirth of the design developed independently in 1977 by Littman and Metcalf at MIT, by Moya at Quantel (France), and by Shoshan at Technion (Isreal). Called the "grazing-incidence oscillator," this design uses a grating at a high angle of incidence (>80 degrees) and an outrigger mirror which rotates to tune the wavelength.

The advocates of this design claim numerous advantages over the traditional Hansch oscillator, including simplicity, narrower linewidth without etalons, and constant linewidth (in wavelength units) over the full tuning range of the laser. Lured by these claims, the three leading manufacturers of pulsed dye lasers, Lambda Physik, Molectron, and Quanta-Ray, evaluated this design in detail in 1977 and 1978. Each rejected this design in favor of the Hansch oscillator, concluding that there are severe fundamental limitations to the grazing-incidence oscillator which, while tolerable in a home-made laser, are intolerable in a commercial instrument.

The following discussion describes the Lumonics dye laser in detail, both oscillator and amplifier, and compares it to the Lambda Physik FL 2002. The theory of both oscillators is discussed, followed by unique features of the Lumonics laser and a performance comparison between the Lumonics and Lambda Physik lasers.

II. Design Theory

A. General. Essentially all dye lasers which use a grating follow the standard spectrometer grating equation shown below,

$$n\lambda = d(\sin\alpha \pm \sin\beta) \qquad (1)$$

in which n = grating order
λ = wavelength
d = groove spacing of the grating
α = angle of incidence
β = angle of diffraction (exit angle)
$\pm$ = β on same (+) or opposite (−) side of grating normal as α.

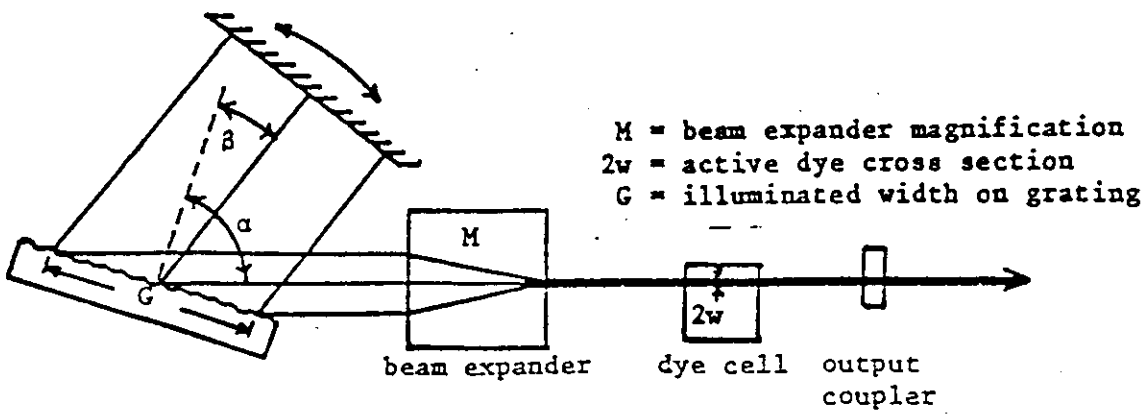

Note that for a Littrow configuration (Hansch oscillator), $\alpha=\beta=\theta$ and (1) reduces to,

$$n\lambda = 2d \sin\theta \qquad \text{(Littrow)} \qquad (2)$$

Equation (1) applies to the Lumonics design, while equation (2) applies to the Lambda Physik design.

The following derivation of linewidth and resolution deals with the more general case of equation (1) in order to preserve the similarities between the two designs. The results are easily modified later for the Lambda Physik laser. The goal of the derivation is to explain how the linewidth and resolution vary with wavelength for each design.

Differentiating (1) yields,

$$n\Delta\lambda = d \cos\beta \, \Delta\beta \qquad (3)$$

and combining terms gives for the linewidth,

$$\Delta\lambda = \frac{\lambda \cos\beta}{(\sin\alpha \pm \sin\beta)} \Delta\beta \qquad (4)$$

Note that the linewidth does not depend on either the grating order or the groove spacing, but only on the grating angle and exit acceptance angle $\Delta\beta$. Of course, the grating angle depends on both n and d, but it is interesting to note their absence in the above expression. By expressing the linewidth in this manner, one can easily see that narrow linewidth is achieved by high grating angles α and β, and by a small exit acceptance angle $\Delta\beta$, analogous to a narrow slit on a monochromator.

This exit acceptance angle can be treated easily if we choose the theoretical minimum value, the divergence of a beam of width G:

$$\Delta\beta = 2\lambda/\pi G \qquad \text{(diffraction limit!)} \qquad (5)$$

Using this expression for $\Delta\beta$, and noting that $G = wM/\cos\alpha$, (3) becomes,

$$\Delta\lambda = \frac{d\,\lambda \cos\alpha \cos\beta}{\pi\, n\, w\, M} \qquad (6)$$

A more important parameter to consider is resolution rather than linewidth. Resolution R is defined as $\lambda/\Delta\lambda$ or $\nu/\Delta\nu$. Re-arranging (6) gives,

$$R = \frac{\pi\, n\, w\, M}{d \cos\alpha \cos\beta} \qquad (7)$$

B. Lumonics EPD-330 Oscillator. The choice of parameters for the Lumonics grazing-incidence oscillator is as follows:

d = 416.67nm (2400 lines/mm holographic grating)
n = 1 (higher orders are not possible)
M = 15 (4-prism expander)
α = 85 degrees
β = -13.2 to +53.5 degrees for 320-750nm range
2w = 0.5mm (approximately; depends on pump energy)

Inserting these numbers into equation (7) gives R = 350,000 at 580nm. But the grating is used double-pass, so this value should be increased by to approximately 500,000, or 2.5 times the observed value of 200,000. This result is not unexpected because the beams are not diffraction-limited, and because for $\Delta\beta$ we used the theoretical minimum value. The important result is that (7) gives the correct functional relationship. Using the observed value, we can now write for the Lumonics oscillator,

$$R_{Lumonics} = 185{,}000/\cos\beta \qquad (8)$$

C. Lambda Physik FL 2002 Oscillator. The choice of parameters is as follows:

d = 1666.7nm (600 lines/mm)
n = 3 to 8 depending on wavelength
M = 66 (4-prism expander)
θ = 42.5 to 72.5 degrees for 320-970nm range
(orders overlap)
2w = 0.5 mm (pproximately; depends on pump energy)

Before we can apply these figures, we must modify expression (5) for $\Delta\beta$ to correct the maximum beam width from G to (wM). The effect is to delete cos α from (7), so that for the Littrow configuration, R is

$$R = \frac{\pi\, n\, w\, M}{d \cos\theta} \qquad (9)$$

Inserting the parameters above gives R = 300,000 at 580nm, or 3 times the observed value of 100,000. Using the observed value, the resolution for the Lambda Physik FL 2002 oscillator is

$$R_{L-P} = 10{,}000\ (n/\cos\theta) \qquad (10)$$

D. Conclusions. Within reasonable limits, equations (7) through (10) accurately describe the resolution as a function of the several parameters. The graph below shows this resolution as a function of wavelength for both designs. The obvious difference between the two is that the Lambda curves are discontinuous, reflecting the use of several grating orders.

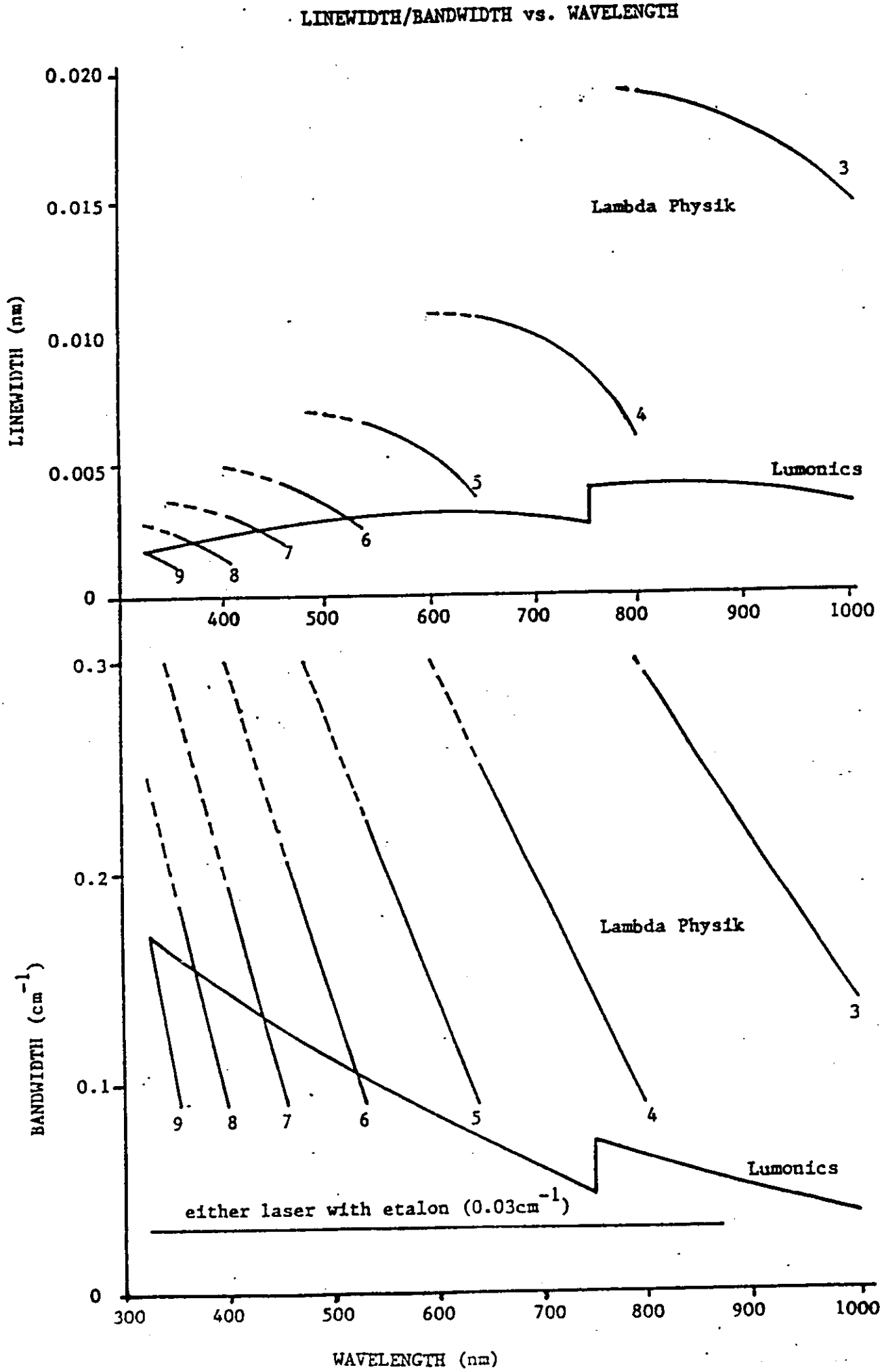
LINEWIDTH/BANDWIDTH vs. WAVELENGTH
LINEWIDTH (nm)
0.020
0.015
0.010
0.005
0
Lambda Physik
Lumonics
3
4
5
6
7
8
9
400
500
600
700
800
900
1000
BANDWIDTH (cm^{-1})
0.3
0.2
0.1
0
Lambda Physik
Lumonics
3
4
5
6
7
8
9
either laser with etalon (0.03cm^{-1})
300
400
500
600
700
800
900
1000
WAVELENGTH (nm)

RESOLUTION vs. WAVELENGTH

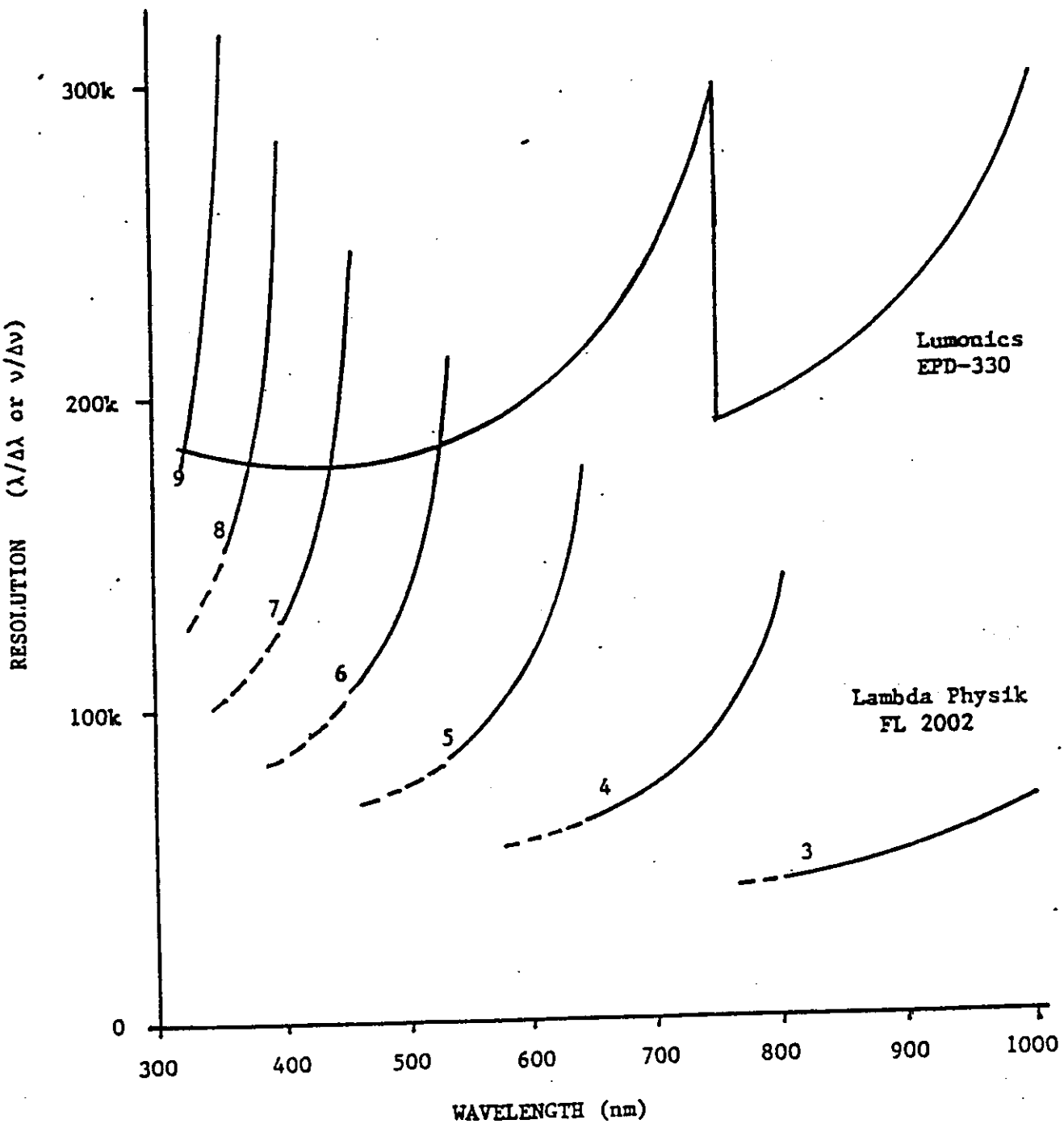

III. Unique Features of the KPD-330

While the Hansch oscillator is generally well-known, the grazing-incidence oscillator used by Lumonics is not as familiar to most readers. This section points out the unique features of the Lumonics oscillator, many of which have an effect on the performance described in the next section.

A. Higher resolution without an etalon.

The resolution R is generally higher than that of the Hansch design because more grating grooves are illuminated. However, there is a limit to the resolution, beyond which frequency jitter, caused by dye inhomogenieties and mechanical vibrations, are significant. Measured figures at 580nm for dye inhomogeniety-related jitter are in the range of 0.02cm-1 for YAG-pumping (532nm) and 0.04cm-1 for UV pumping with an excimer, nitrogen or YAG laser (355nm). Thus the laser bandwidth (without etalon) must remain comfortably above these figures.

B. Two gratings required.

For the 2400 lines/mm grating chosen by Lumonics, the maximum wavelength is 750nm. In order to operate at higher wavelengths, this grating must be replaced by one with 1800 lines/mm. The coarser 600 lines/mm grating in the Lambda Physik design has an upper wavelength limit of 3200nm, far beyond available dyes; thus there is never a need to change the grating.

C. Constant linewidth.

The linewidth (wavelength units) of the Lumonics design is nearly constant over the tuning range of the grating. (In equation (6), the product of variables and cos is almost constant.) This result is simply a peculiarity of the design. If the linewidth is expressed in energy units (properly called "bandwidth"), the result varies by a factor of four over the 320-970nm range (see figures below). Resolution is a better figure of merit than either linewidth or bandwidth.

In the lower figure we can see a peculiarity of the Hansch design - the bandwidth range repeats itself for each order. For future reference, the bandwidth of either oscillator with an intracavity etalon is shown. Incidentally, as displayed in the figure, an etalon is a device with a constant, or near-constant, bandwidth.

D. The Lumonics has a degeneracy point near 415nm at which the grating and outrigger mirror are parallel. On both sides of this wavelength, a second, simultaneous output wavelength occurs along the ray path shown in the figure below. As long as this second wavelength is within the tuning range of the dye, it will compete with the primary wavelength. Clearly all dyes in the 380–450nm region are effected.

An obvious means of eliminating this unwanted wavelength is to rotate the grating about an axis normal to its surface and compensate by tilting the outrigger mirror. While this approach can work at one wavelength, it destroys the fundamental cavity alignment necessary to operate at all wavelengths. Thus the cavity must be re-tuned at other wavelengths. In addition, such an approach introduces an error into the sine drive calibration.

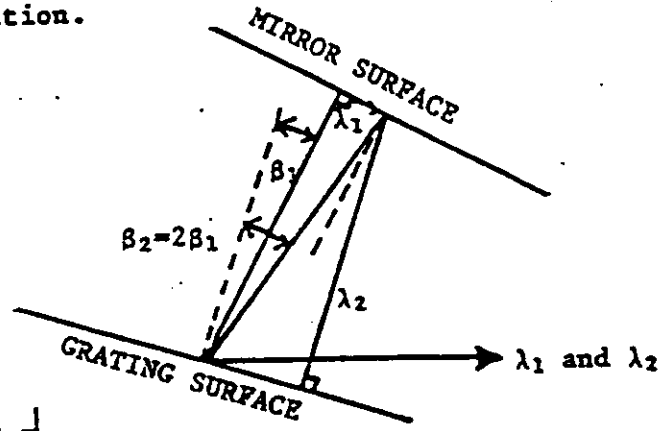

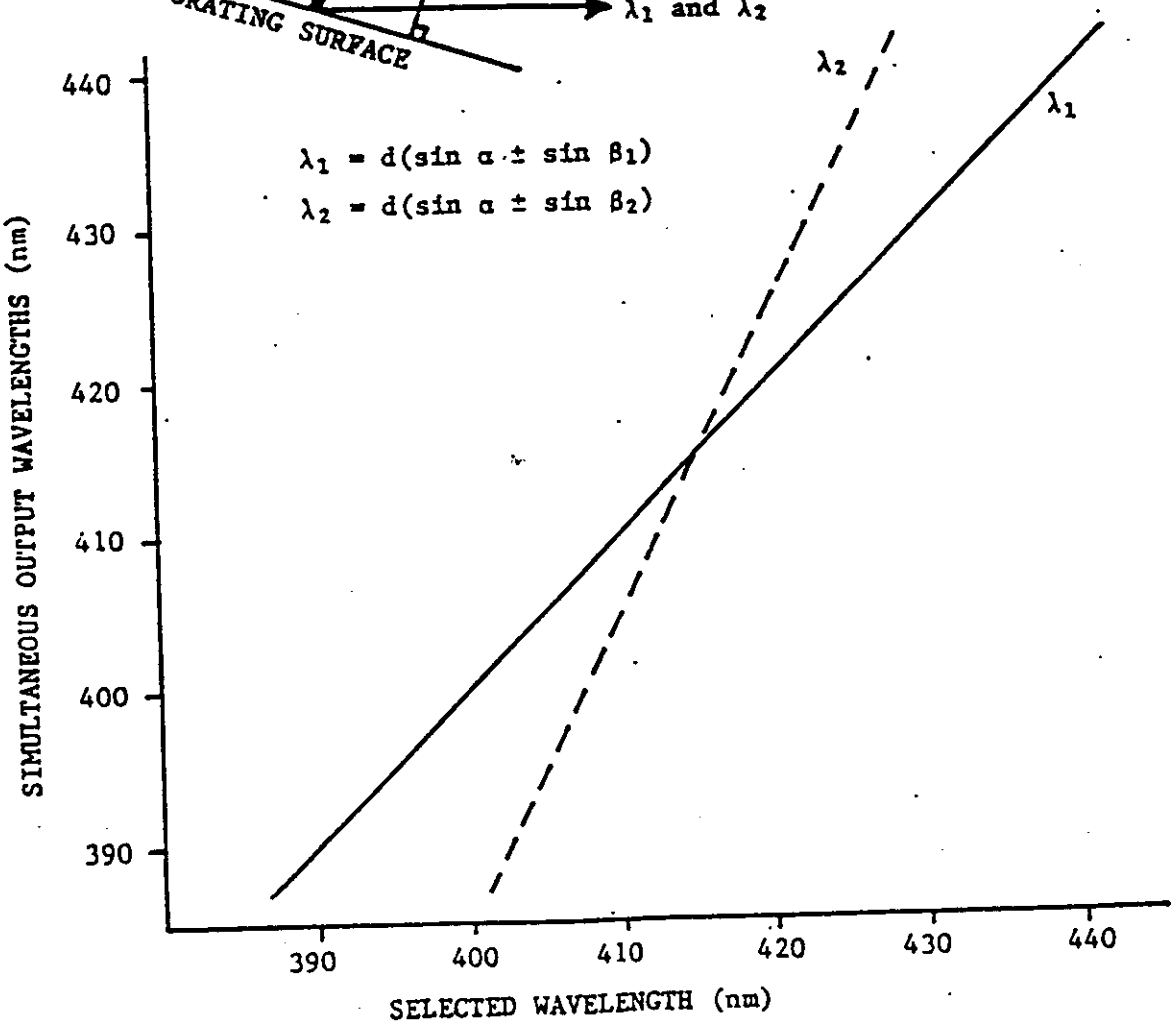

IV. Performance Comparison

A. Linewidth (standard)

At longer wavelengths, the Lumonics linewidth is less than that of Lambda Physik. However, below about 450nm, the Lambda Physik is less on the average. Note that in the Lambda Physik design, there is often a choice of grating orders, one (always the higher one) offering narrower linewidth and the other offering a larger linewidth but generally higher efficiency.

B. Linewidth (optional)

The Lumonics laser has a user-adjustable option of increasing the grating angle about 2 degrees to reduce the linewidth to 0.002nm from 0.003nm. Output efficiency is reduced 30-40%.

The wavelength changes introduced by dye inhomogenieties and mechanical vibrations are now comparable to the laser linewidth, so that extreme caution must be used in interpreting results. At 580nm, the bandwidth is 0.06cm-1, while the jitter may be 0.05cm-1.

The Lambda Physik FL 2002E uses an air-spaced intracavity etalon to reduce the bandwidth to 0.03cm-1. Although the etalon is an expensive component, and requires synchronous scanning with the grating, it has the overriding virtue of extreme frequency stability. Because it is used at near-zero incidence angle, its frequency is virtually insensitive to changes in angle; and because the spacer is made of a zero-coefficient material (as is the grating), its frequency is insensitive to changes in temperature.

Thus the etalon eliminates the frequency jitter inherent in the oscillator, and, in principle, converts it to amplitude fluctuations. But the oscillator is followed by a saturated amplifier, so such fluctuations are attenuated. The result is an output with unmatched frequency stability and amplitude fluctuations no worse than without an etalon. Furthermore, output efficiency is reduced by no more than 10%.

The newest dye laser, model FL 2002EC adds a confocal Fabry-Perot etalon after the oscillator but before the saturated power amplifier. Bandwidth is reduced to a transform-limited value of 0.005cm-1 (150MHz), easily the smallest bandwidth available in any commercial pulsed dye laser.

C. Efficiency

Both standard dye lasers operate with an efficiency of about 10%. Values as high as 14% at 480nm are achieved in both. For the narrow linewidth option, however, the Lumonics efficiency decreases 30-40% while that of the Lambda Physik decreases only 10%.

D. Background (Amplified Spontaneous Emission - ASE)

The Lumonics dye laser uses only a delay line in the amplifier section to reduce ASE to about 3% of the laser output, a result easily achieved in most lasers. As pump powers increase, or as the wavelength is tuned to the blue/UV or the edges of a dye range, ASE increases, often drastically.

The Lambda Physik FL 2002, in addition to a delay line, incorporates a spectral filter after the oscillator ("Lambdapure" filter) to eliminate virtually all the broadband background coming from the oscillator dye cell. The result is a maximum integrated ASE background of 1% anywhere in the spectrum, and typically less than 0.1% at the peak of rhodamine 6G. This background is a factor of 10 lower than that of any other commercial laser.

E. Frequency sensitivity

Having mentioned that frequency jitter is common to all dye oscillators (without etalon), we now calculate the angular "perturbation" required to change the wavelength an amount equal to the linewidth. All figures are at 580nm for convenience.

For the Lumonics laser, we use equation (4):

$$\Delta\lambda = 380\ \Delta\beta\ (\text{nm}) \tag{11}$$

Inserting the linewidth value of 0.003nm,

$$\Delta\beta = 8\ \mu\text{rad} \tag{12}$$

For the Lambda Physik laser, we use (4) with $\alpha=\beta=\theta$: :

$$\Delta\lambda = 165\ \Delta\theta\ (\text{nm}) \tag{13}$$

Inserting the linewidth value of 0.006nm,

$$\Delta\theta = 36\ \mu\text{rad} \tag{14}$$

There are two results to these calculations:

1. Without regard to linewidth, the Lumonics oscillator is roughly a factor of two more sensitive to angular perturbations than the Lambda Physik laser. This result applies not only to frequency jitter, but to alignment sensitivity as well.

2. The Lumonics oscillator is roughly a factor of four more sensitive to perturbations producing a shift equal to the linewidth.

Of course, as the linewidth of any dye laser is narrowed, it becomes more sensitive (again, only without etalon). The point is, that whatever the design, normal perturbations should be a small fraction of the linewidth.

F. Beam quality

Beam quality of a pulsed dye laser is difficult to describe quantitatively. Normally, indirect measures are used.

Lumonics describes up to 20% conversion efficiency when frequency doubling in KD*P. However, most pulsed dye lasers, including the FL 2002, will achieve this figure.

Lambda Physik prefers Raman shifting efficiencies as a better measure of beam quality. An equivalent but far easier technique is to measure the pulse energy required to break down air with a lens of 50mm focal length. For the FL 2002, the energy is 5mJ at 580nm, a figure which may not be achieved by even YAG-pumped dye lasers. Thus the beam quality of the FL 2002 is indeed "near diffraction-limited."

V. Conclusions

The Lumonics EPD-330, with its grazing-incidence design, is in principle an excellent approach to achieving high performance at low cost. However, the significant defects are numerous:

A. Frequency jitter a large fraction of the bandwidth.

B. Extreme mechanical sensitivity.

C. A second wavelength near the degeneracy point.

D. Limited range with one grating.

E. High background ASE.

All of these defects would either vanish or be less significant if the laser were limited in bandwidth to about 0.2cm-1, similar to the FL 2002, and an etalon were used to achieve narrower bandwidth. The claim that it can equal the performance of the FL 2002E without using an etalon is simply untrue. When dealing with bandwidths much below 0.2cm-1, only an etalon can overcome the limitations imposed by frequency jitter and provide a stable, reliable output beam. The manufacturers of over 90% of the commercial pulsed dye lasers in use today agree with this statement.

Further Reduction of Laser bandwidth

1) Intra Cavity Etalon technique
   (Zoom technique)

2) Short cavity grazing incidence design

3) Extended oscillation time with
   long pump pulses

The ultimate :

— Single (longitudinal) Mode Laser

Fabry-Perot Interferometer

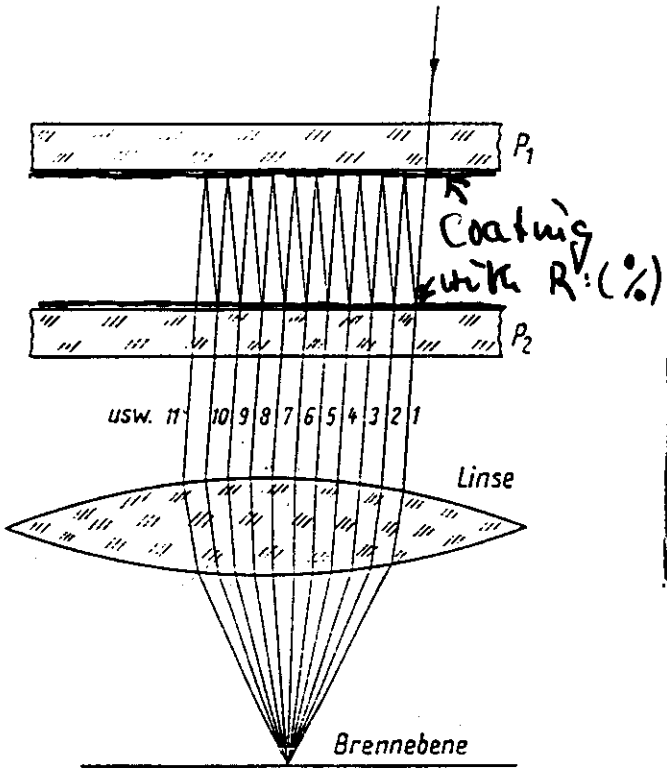

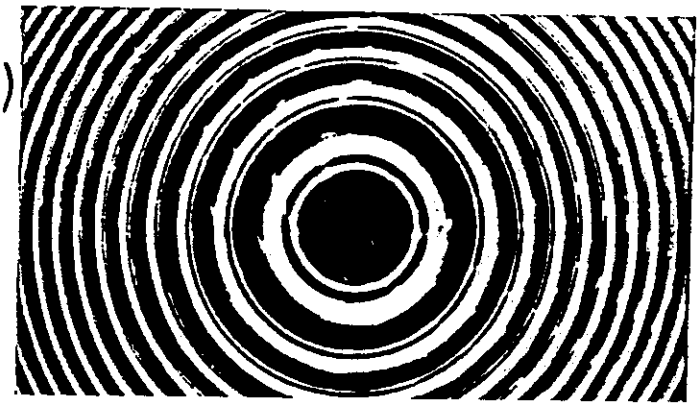

$$\frac{d\lambda}{d\alpha} = \lambda \tan\alpha$$

$$m\lambda = 2nd\cos\alpha'$$

$= \Delta\lambda_F$

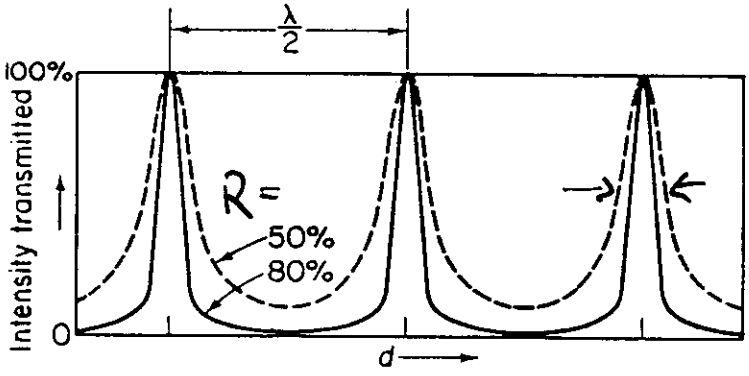

$$\delta\lambda = \Delta\lambda_F / F$$

$$F = \frac{\pi\sqrt{R}}{1-R}$$

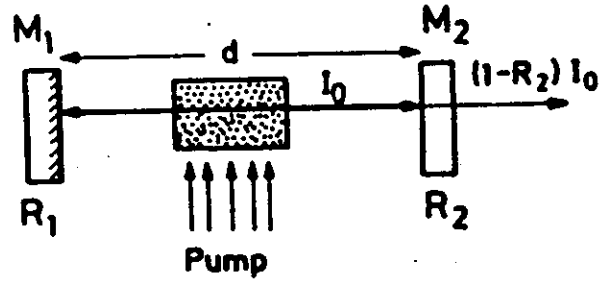

Linewidth narrowing by intra cavity etalon:

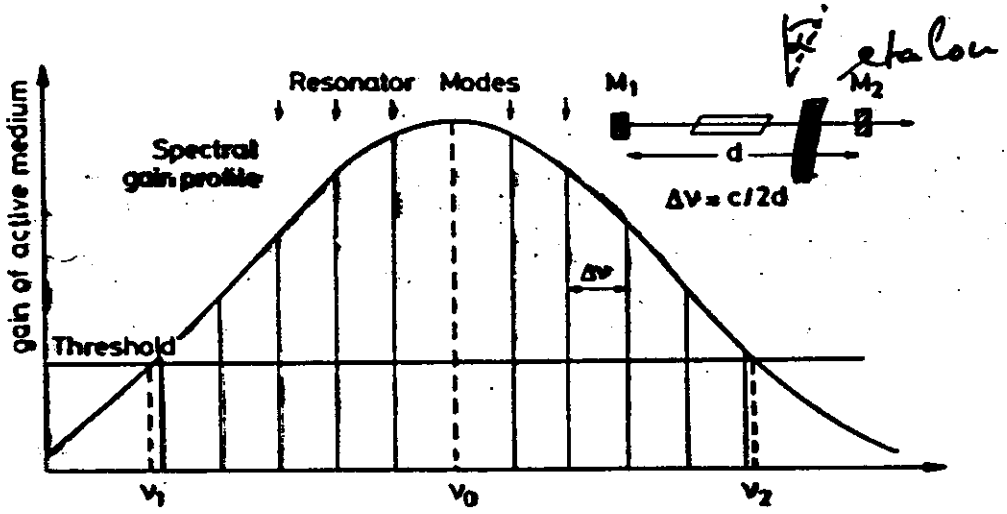

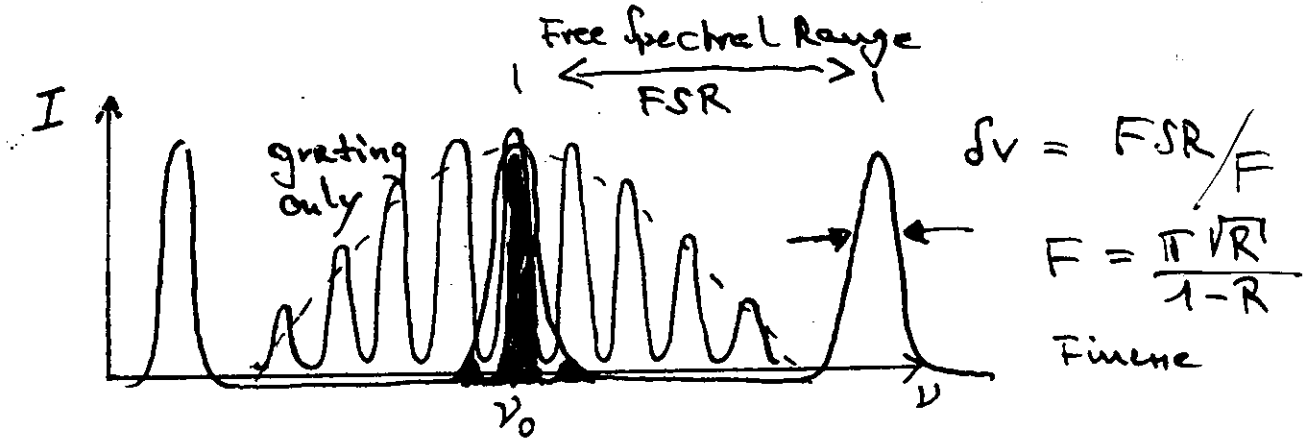

$$\delta\nu = FSR/F$$

$$F = \frac{\pi\sqrt{R}}{1-R}$$

Finesse

Etalon tuning by tilting the etalon:

$$d\lambda = \lambda \tan\alpha \, d\alpha$$

(synchro scan of etalon/grating!)

Fig. 8: Bandwidth of LPD 3002E measured with a confocal Fabry Perot monitor etalon (FSR = 0.1 cm^{-1}) during pressure tuning of the laser.

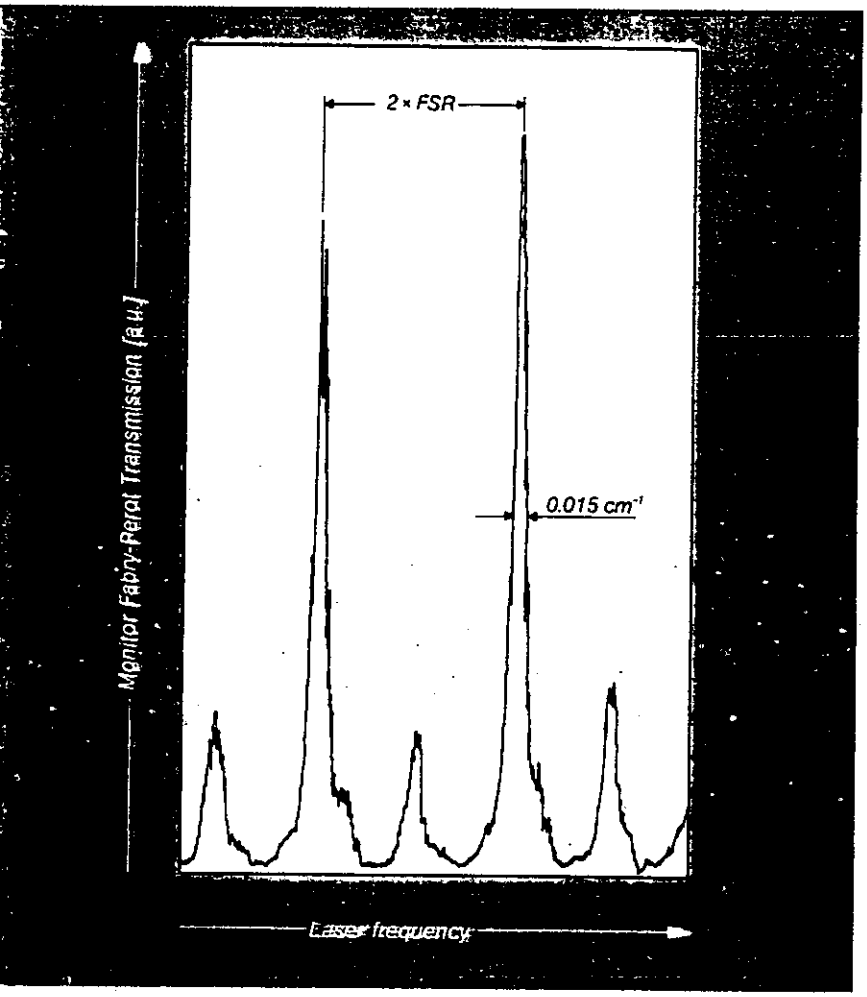

The concept of optional use of an etalon gives more flexibility during operation. In case of need the etalon can be removed and a broad spectral range can be scanned at lower resolution but higher scan speed. In this way, a survey of a spectrum can be obtained within a few minutes.

Single-Mode Operation of Pulsed Dye Lasers

B. Burghardt, W. Mückenheim, D. Basting
Lambda Physik, P.O.Box 2663, D-3400 Göttingen, FRG

In large domains of laser spectroscopy narrow-bandwidth probes are an imperative requirement, with single-mode lasers being the ideal instruments. cw-lasers satisfying this desire are commercially available but, if not complemented by pulsed amplifiers, they deliver only low output power, and the costs of such systems are almost inversely proportional to their bandwidth. Pulsed dye lasers, usually pumped by excimer or Nd:YAG lasers are already suited for many applications and, therefore, present in every spectroscopy laboratory. However, with exception of a few sophisticated devices they oscillate on several modes.

This drawback can be overcome by reducing the cavity length (Littman design /1/) such that even a rather broad spectral distribution would not cover more than one longitudinal mode, or by reducing the bandwidth via extended pulse duration, which is the appropriate approach for a Hänsch-type /2/ oscillator. This way, being subject to the present paper, offers the unique opportunity of automatic ASE-suppression by utilizing the grating twice /3/. While in the past this way was merely of academic interest, because pump lasers of sufficient pulse duration were not easily accessible, meanwhile a suitable excimer laser, emitting pulses of 300 ns duration at 308 nm /4/, has been made commercially available (Lambda Physik, EMG 602).

For an oscillator equipped with an intracavity etalon, the advantage gained by extended pulse duration can be estimated under some simplifying conditions as follows. The single-pass transmission function of the etalon is, for large finesse F, given by

$$T(\nu) = \left(1+\left(\frac{2F}{\pi}\sin\frac{\nu-\nu^*}{F\Delta\nu_o}\,\pi\right)^2\right)^{-1} \qquad (1)$$

with ν^* a frequency of maximum transmission and $\Delta\nu_o$ the width of the single-pass transmission function. With no regard to amplification and loss processes or hole burning in the laser cavity but assuming a constant amplitude $T(\nu^*) = 1$ and negligible divergence of the radiation, the halfwidth $\Delta\nu_N$ of the transmission function after N cavity roundtrips is determined by

$$T(\nu^* + \Delta\nu_N/2)^{2N} = 1/2\ . \qquad (2)$$

Expanding the sine and taking only the linear term we get

$$\Delta\nu_N/\Delta\nu_o = \sqrt{2^{1/2N}-1} \qquad (3)$$

which, for large N, can be written

$$\Delta\nu_N/\Delta\nu_o = \sqrt{\ln 2/2}\ /\sqrt{N}. \qquad (4)$$

More interesting for practical applications is the time-averaged bandwidth $\langle\Delta\nu_N\rangle$. According to (3) it can be calculated from

$$\langle\Delta\nu_N\rangle/\Delta\nu_o = N^{-1}\sum_{k=1}^{N}\sqrt{2^{1/2k}-1} \qquad (5)$$

which, again for large N, may be approximated by means of (4) by

$$\langle \Delta\nu_N \rangle / \Delta\nu_o = \sqrt{\ln 2/2}\; N^{-1} \sum_{k=1}^{N} k^{-1/2}. \qquad (6)$$

Applying the condition $N \gg 1$ for a last time, the sum in (6) can be approximated by $2\sqrt{N} - \sqrt{2} \approx 2\sqrt{N}$ yielding

$$\langle \Delta\nu_N \rangle / \Delta\nu_o = \sqrt{2\ln 2}\,/\sqrt{N}. \sim 1/\sqrt{\Delta t} \quad \text{(Pulse duration)} \qquad (7)$$

Thus, the final as well as the time-averaged bandwidth reduce in proportion to the inverse square root of the number of cavity roundtrips.

The length of common dye laser oscillators lies between 30 and 40 cm. Therefore, the distance between longitudinal modes ranges from 0.4 to 0.5 GHz. When equipped with an intracavity etalon and pumped by 20 ns pulses, a bandwidth of about 1 GHz is obtained. Hence, two or three modes will usually oscillate. An increase to 200 ns pulse duration is obviously sufficient, to reduce the bandwidth by a factor of 3, permitting only one single longitudinal mode to oscillate.

Due experiments have been performed by using a Hänsch-type dye laser of 2.3 ns roundtrip time and 440 MHz mode separation. The single pass transmission function determined by the intracavity etalon is about $\Delta\nu_o$ = 2 GHz. The dye laser was pumped either by an ordinary excimer laser of 18 to 20 ns pulsewidth or by a precursor of the EMG 602, delivering pulses of 220 ns duration at 308 nm. In both cases the duration of the dye laser output was reduced, namely to 16, 18 and 170 ns respectively. In addition, the time-averaged bandwidth over the first 5 ns was measured by means of a streak camera, when the ordinary excimer laser was used. The results are given in Fig. 1. It is obvious that during the first 20 ns several modes can oscillate ($\Delta\nu_s$ = 0.8 GHz), while a pulse duration of 200 ns or more guarantees single mode operation ($\Delta\nu_{ns}$ = 0.3 GHz), if the dye laser frequency is chosen such that one mode lies near the center of the transmission function. This condition, however, can be satisfied, e.g., by adjusting the cavity length of the dye laser via a piezo-driven mirror mount.

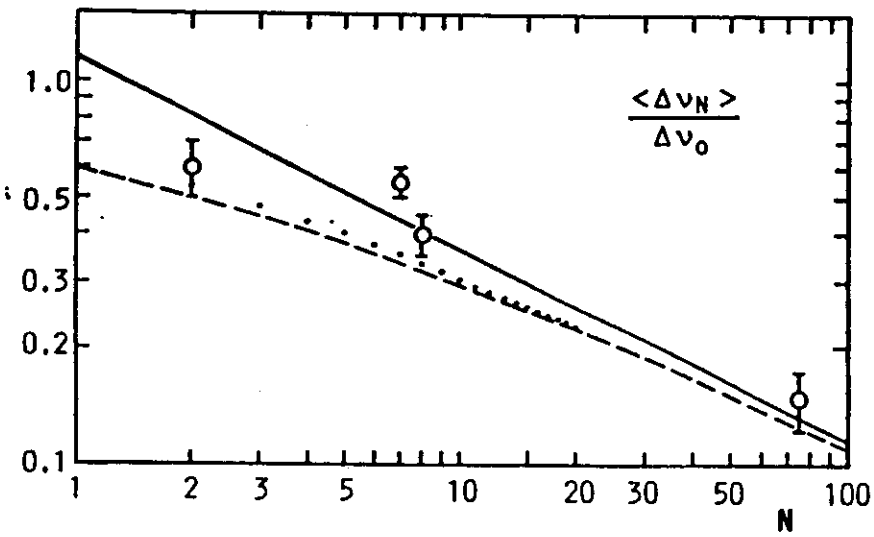

Fig. 1 Normalized average bandwidth $\langle \Delta\nu_N \rangle / \Delta\nu_o$ versus number of roundtrips N. The error bars do not include a +/- 20 % uncertainty in $\Delta\nu_o$. Theoretical curves:
..... Eq. (5),
----- Eq. (6),
——— Eq. (7).

References

/1/ M. G. Littman and H. J. Metcalf, Appl. Opt. 17 (1978) 2224
/2/ T. W. Hänsch, Appl. Opt. 11 (1972) 895
/3/ H. Bücher, U.S. Patent 4399540
/4/ P. Klopotek, U. Brinkmann, D. Basting and W. Mückenheim, CLEO '87, Baltimore, Digest of Technical Papers p. 326

FL3002E

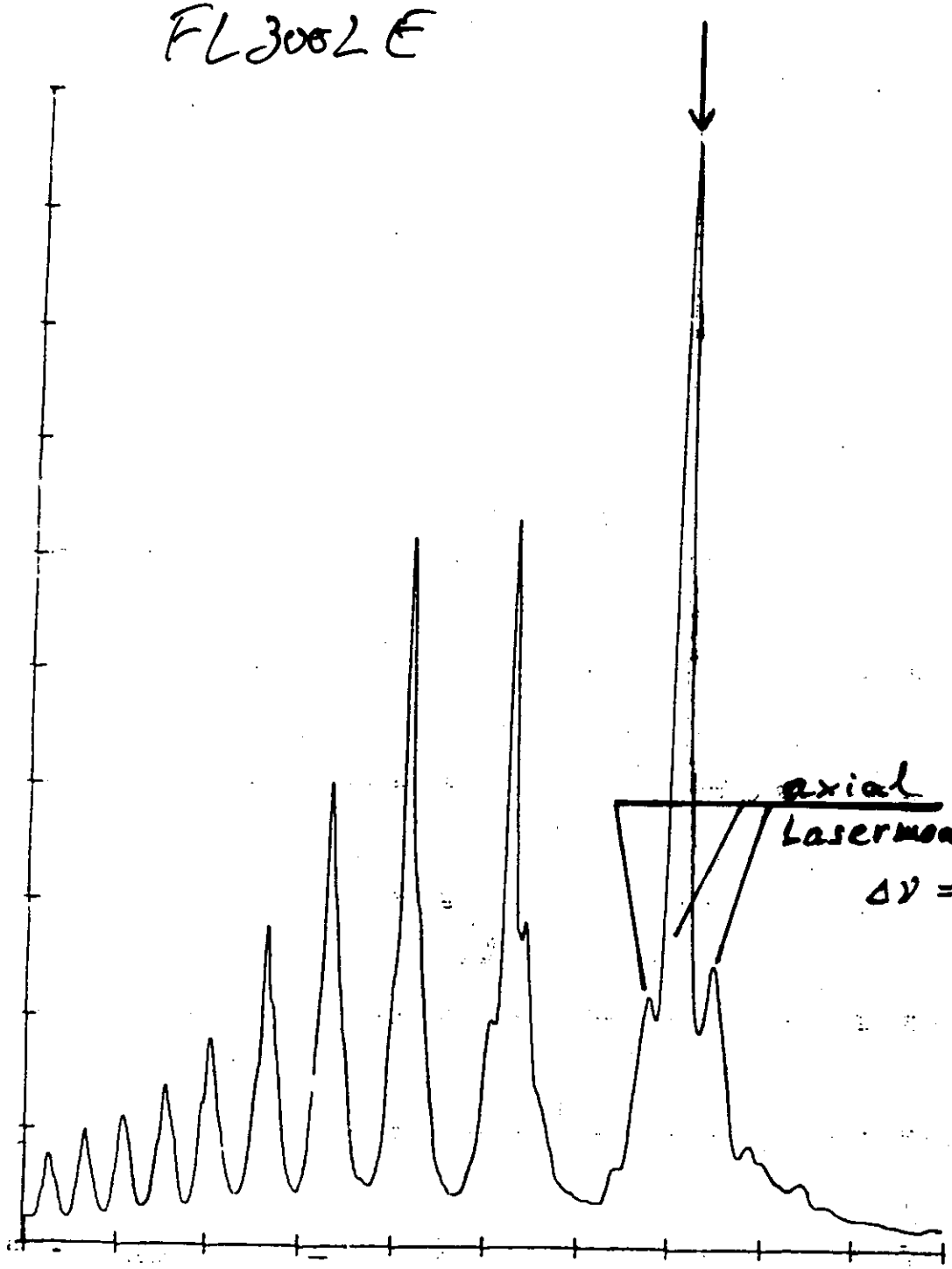

14.12.83 Bgl.

<u>nearly single mode laser oscillation:</u>

$\Delta\lambda \triangleq 250$ MHz

$\tau_{Puls} = 70$ µs

Littman 1981 Single Mode Dye Laser

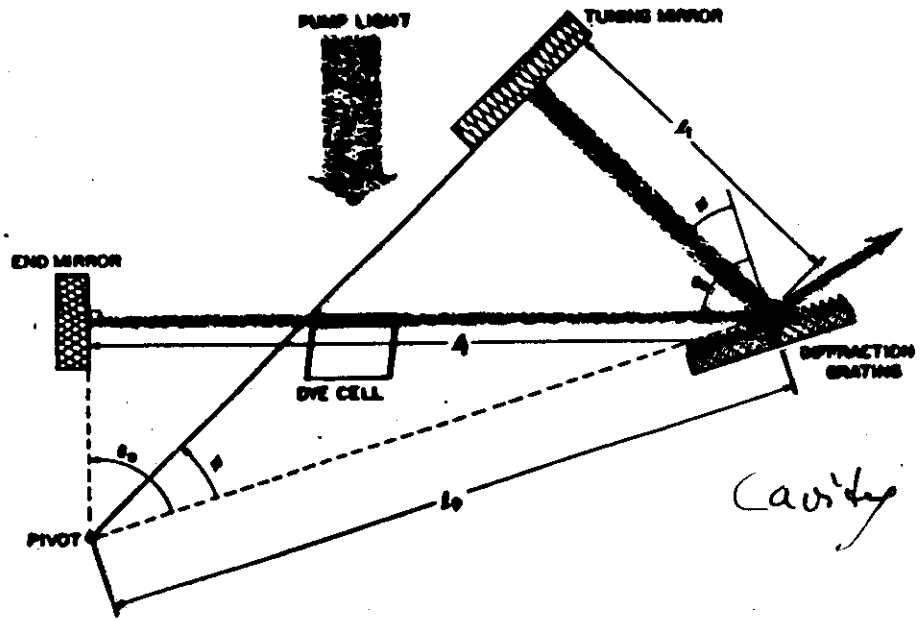

Cavity length < 10 cm

Fig. 1. Grazing-incidence pulsed dye laser with self-tracking geometry. (The pivot position as shown is correct only if the optical path length of the dye is equal to its physical length.)

500 MHz Bandwidth

(conversion efficiency ~ 2%)

continuous tuning range

~ 30 cm⁻¹ without mode

hopping

Advantages of Etalon vs. grazing incidence technique:

1) Etalon only used when looking for spectral details (Zoom function)

A <u>30 cm^{-1} scan</u> at 0.03 cm^{-1} bandwidth and 0.003 cm^{-1} resolution requires <u>10^4 pulses</u>!
(at 10 Hz → > 15 min scanning time)

2) Intracavity Etalon is inherently more stable in λ $\quad \delta\lambda \sim \tan\alpha \, \delta\alpha$

Very accurate control on α!

High Resolution Laser Bandwidth Measurement Using Confocal Monitor Etalon

(fringe mode)

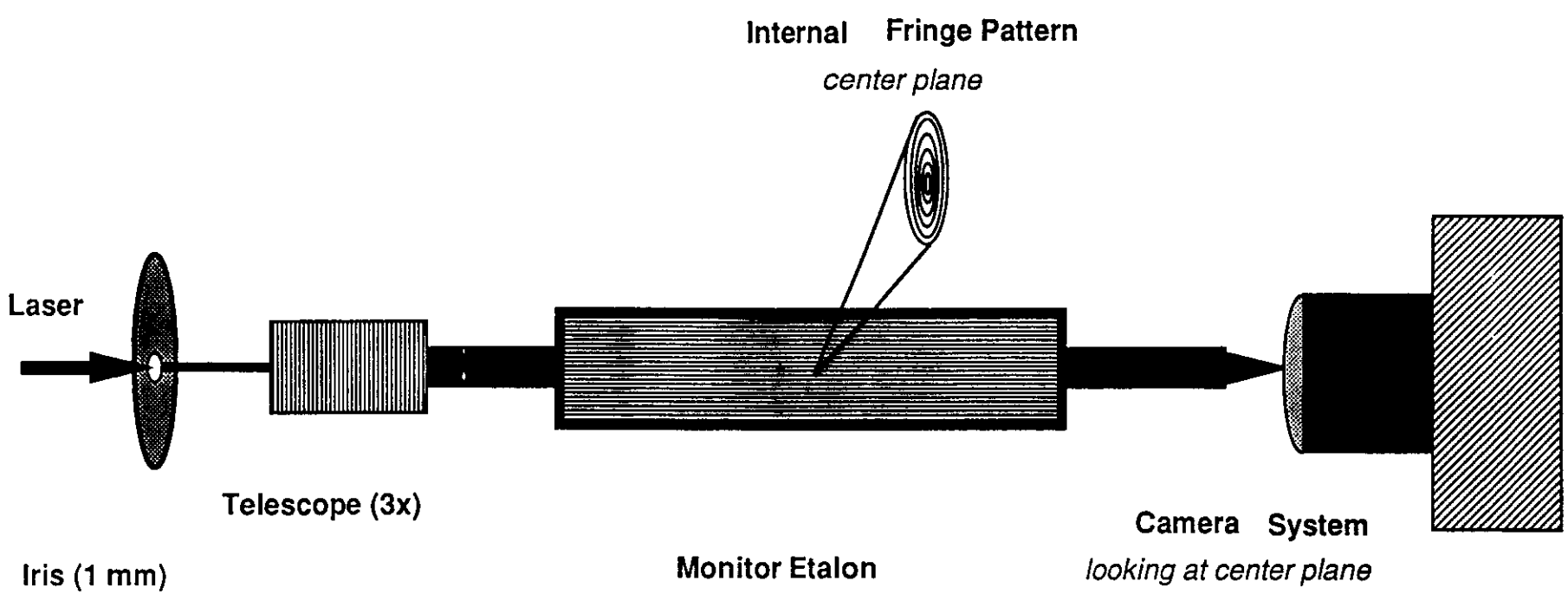

Other important features of good dye lasers

1) Wavelength stability and reproducibility
   - mechanical {vibrations affect grating, etc...}
   - thermal {change of refractive index $\Rightarrow$ affects diffraction on prism, grating}
   - pressure {dito ; $\lambda_0 = n\lambda$ }

2) Amplitude stability
   - mechanical { see above }
   - dye circulator design {fast, laminar dye flow required to avoid thermal and turbulence effects on laser beam }

3) Spectral purity
   - High Q-resonator design
   - ASE filtering
     (Amplified Spontaneous Emission)

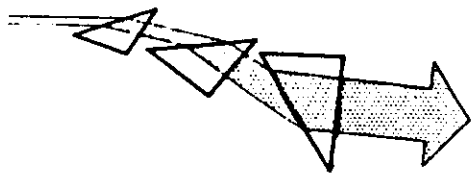

Fig. 2. Three-prism up–up–down beam expander. This configuration is optimal for achromatic three-prism beam expanders.

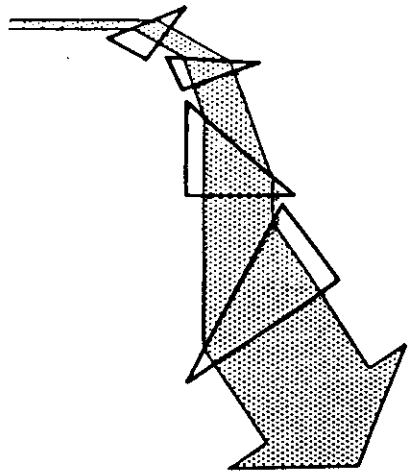

Fig. 3. Four-prism up–up–up–down beam expander. This configuration is optimal for achromatic four-prism beam expanders of a single material with total magnification $\gtrsim 10$ and probably also for lower magnifications.

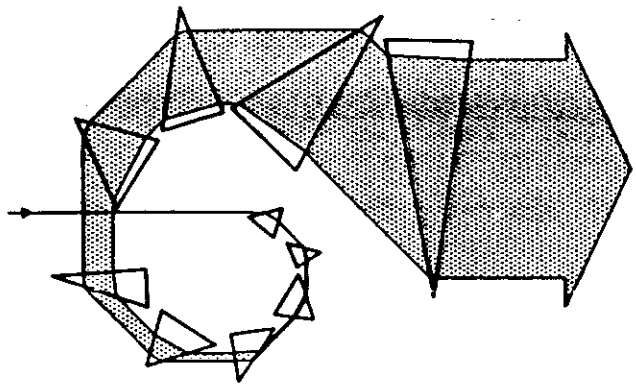

Fig. 4. N-prism up–up . . . up–down beam expander. This configuration is optimal for achromatic single-material prism beam expanders of moderate to large magnification, specifically, for magnifications greater than about $[2 - 1/(2^{N-1} - 1)]^N$. In addition, if each prism magnification is 2, such a device achieves a total magnification of 2^N, a dispersion of $1/2^{N-1}$ that of a single prism, and a transmission of 98% per prism.

Prism Beam Expander

Example: 7 prisms; magnification=230

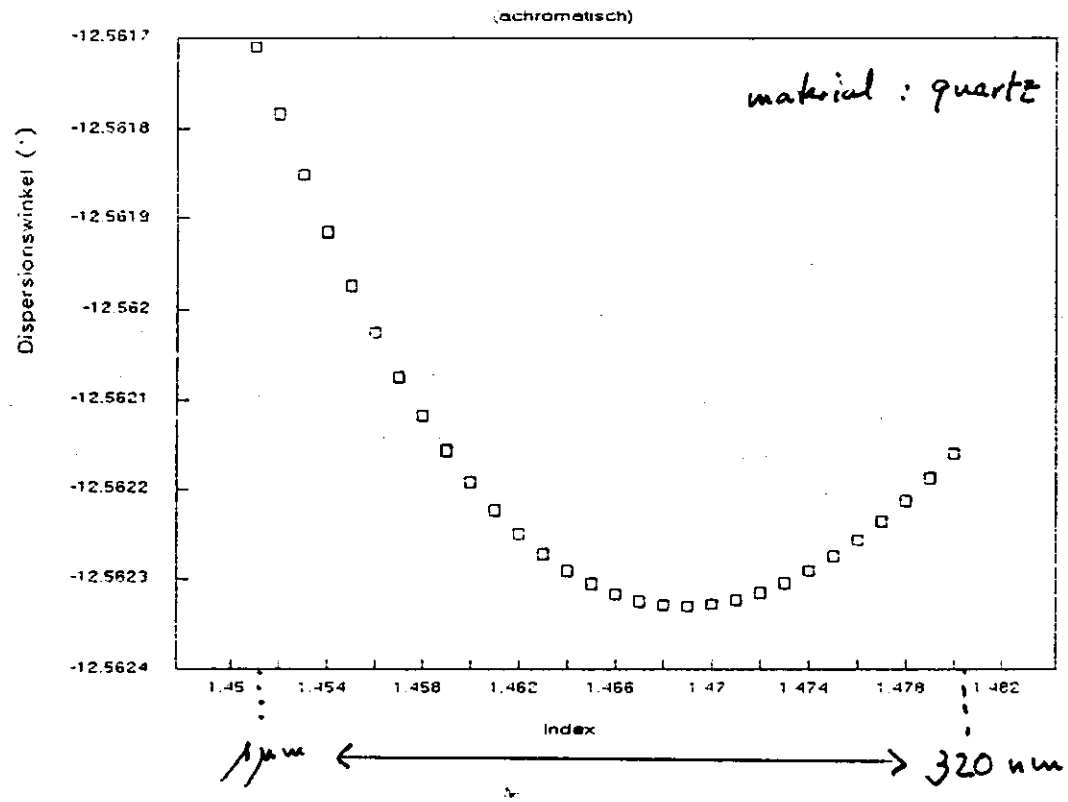

Contribution to total angular dispersion:

$$\frac{d\Theta}{d\lambda} = \left(\frac{d\Theta}{d\lambda}\right)_{Prism} + \left(\frac{d\Theta}{d\lambda}\right)_{grating}$$

ideally $\equiv 0$ for whole wavelength range

Excimer-pumped dye laser with high beam quality

D. J. Brink and C. J. van der Hoeven

National Physical Research Laboratory, Council for Scientific and Industrial Research, P. O. Box 395, Pretoria 0001, Republic of South Africa

(Received 2 April 1984; accepted for publication 12 August 1984)

A novel design for a dye cuvette used in an excimer-pumped dye laser is described. The cuvette consists of a thin-walled quartz tube illuminated equally from four sides. This, combined with the focusing action of the dye-filled tube, results in a homogeneous excitation of the central core of the dye volume and a near TEM (00) output beam is obtained at moderate repetition frequencies. Sufficient data are provided to allow interfacing of the cuvette with standard oscillator-amplifier arrangements.

INTRODUCTION

Pulsed dye lasers excited by high-energy excimer lasers are well known and widely used. These lasers offer short (~10 ns), high peak-power pulses at wavelengths ranging from the ultraviolet to the near infrared. Although they have been successfully employed in a wide range of applications they suffer from one major drawback, namely, that they are transversely pumped from one side only.[1-3] This leads to a nonuniform illumination over the cross section of the excited volume. In addition, the highest gain occurs right on the inner face of the one cuvette side wall, leading to severe diffraction effects in most amplifier configurations.

We have developed a novel pumping scheme which eliminates the problems mentioned to a large extent and which yields an output pulse closely resembling a TEM(00) intensity distribution.

Such a high beam quality should be especially useful in nonlinear applications such as frequency mixing and stimulated Raman scattering.[4]

I. THEORY OF OPERATION

The principle of operation is based on a recently reported technique,[5] where a cylindrical dye volume is illuminated equally from four sides. Instead of using a 90° prism with a small hole as dye cuvette, we used two flat dielectric-coated mirrors to split the pump beam into four equal parts. This allowed us to use a strategically placed, thin-walled tube as dye cuvette. The arrangement is illustrated in Fig. 1.

Although the system seems very similar to the prism cuvette,[5] its performance differs in two important respects. First, the dye-filled tube acts as a very short focal-length cylindrical lens, which focuses the pump light into the dye. This increases the pump intensity towards the tube center and thus, to some extent, compensates for absorption losses.

Taking, to a first approximation, the gain coefficient to be proportional to pump-light intensity and to dye concentration, one can compute relative gain profiles over the cross section of the cuvette tube by simple ray tracing. For example, in a cuvette with its axis parallel to the z-axis, the gain coefficient $g(x,y)$ at an arbitrary point (x,y) in the dye is given by

$$g(x,y) \propto \sum_{i=1}^{4} (\Delta d_i / \Delta d'_i) \exp(-\alpha l_i),$$

where Δd is the width of a narrow probe beam aimed at (x,y) outside the cuvette, $\Delta d'$ is the probe-beam width at the point (x,y), α is the absorption coefficient, and l is the propagation length in the dye. The first term depicts the increase in intensity due to focusing of the light. The summation is taken over the four beams shown in Fig. 1.

We assumed, to a first approximation, α to be proportional to dye concentration and independent of intensity. A simple absorption experiment with a rhodamine 6G sample in the excimer beam showed this assumption to be valid to within a few percent for the range of pump-light intensities and concentrations employed in this work.

A number of such computer-generated gain profiles are shown in Fig. 2. The influence of dye concentration can be seen in Fig. 2(a). We used the product αR, with R the radius of the dye column, as a measure of concentration. It is evident that lower concentrations give a better gain distribution. However, this also leads to a lowered absorption efficiency and gain. One will therefore have to decide on a compromise between conversion efficiency and beam quality.

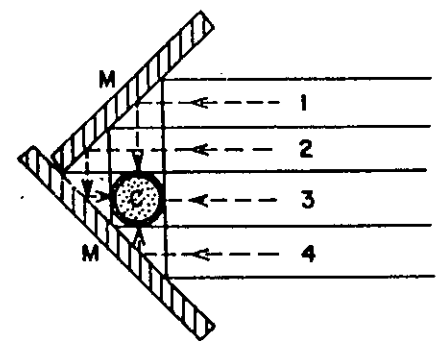

FIG. 1. Outline of the pumping geometry showing the two dielectric-coated mirrors M and the cuvette C. The arrangement divides the pump beam into four equal parts shown as 1 to 4.

 0034-6748/84/121948-04$01.30

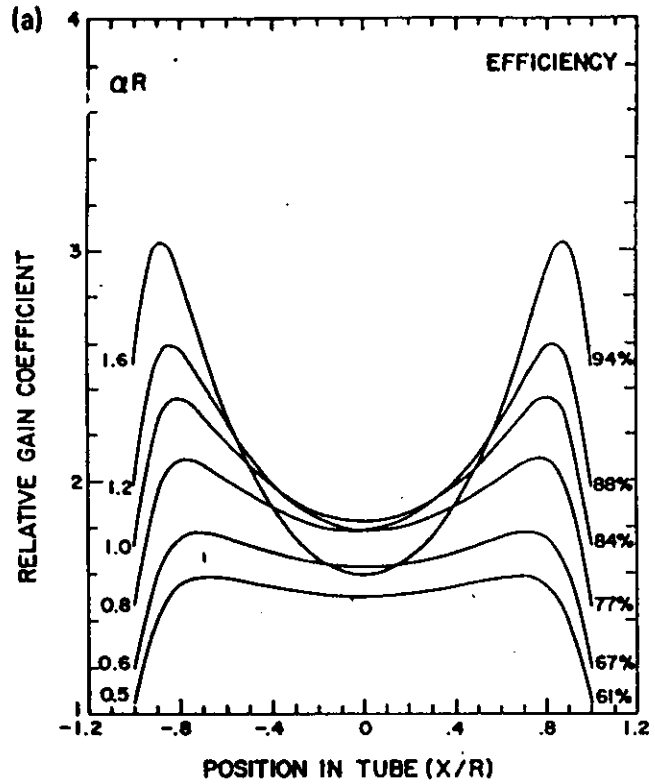

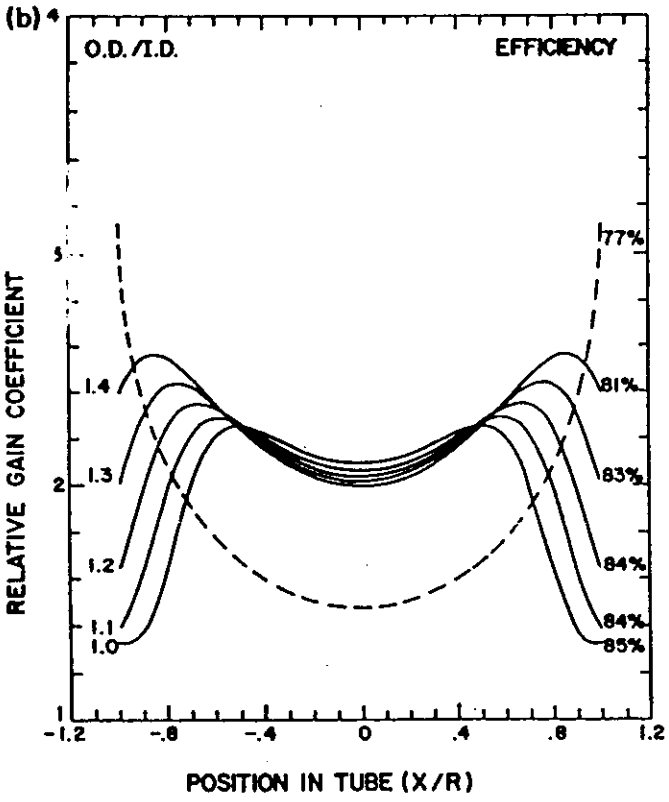

FIG. 2. (a) Calculated relative gain profiles for various values of absorption coefficient. Ratio of tube outer diameter to inner diameter is 1.2. Tube inner radius is R. Gain coefficients are calculated along an axis parallel to one of the pump beams across the diameter of the tube. (b) Calculated gain profiles for different wall thicknesses. Dye concentration corresponds to $\alpha R = 1$. Ratios of outer to inner diameters are indicated on the left. Dashed curve represents the no focusing case. Profiles are calculated along the same axis as in Fig. 2(a).

In Fig. 2(b) the effect of a finite wall thickness is shown. Due to the focusing effect of the cuvette most of the pump light enters the dye solution even at a ratio of outer diameter to inner diameter as large as 1.4. From a mechanical point of view a ratio of 1.2 is already entirely acceptable. The gain near the cuvette walls is considerably lower than the peak value deeper in the dye. This is also a result of the focusing effect and it has a very important bearing on beam distortion due to diffraction effects from the tube walls. The significance of this effect can be appreciated when comparing the gain profiles with the case where no focusing occurs (dashed curve). In the prismatic cuvette[5] the dye refractive index is lower than that of the prism resulting in a slight negative focusing, which is even worse.

The second advantage of the present design is that it is comparatively easy to interchange cuvette tubes. This is necessary to optimize the performance when using different dyes with different gain characteristics.

II. EXPERIMENTAL DETAILS

A schematic layout of the complete laser system is shown in Fig. 3. An EMG 201 XeCl excimer laser from Lambda Physik was used as pump source. This provided 500-mJ pulses at 308 nm with repetition frequencies up to 25 Hz.

The system utilizes conventional side-pumped oscillator and preamplifier stages. This was chosen because an impractically narrow tube will be required to yield sufficient gain at the relatively low pump intensities (5%–10% of the available excimer power) used here. In this way the system is also relatively insensitive to dye and concentration changes.

By placing the final amplifier ~60 cm away from the first stages only the central lobe of the preamplifier output can be selected as input to the main amplifier. Any small intensity variations across this lobe get ironed out by saturation effects in the last amplifier.

The oscillator was fitted with a broadband dielectric-coated flat end reflector, a four-prism beam expander, and a 300-grooves /mm echelle grating blazed at 63°. The beam-expander prisms were specially manufactured for this application from a high refractive-index glass (Schott La-SF9)

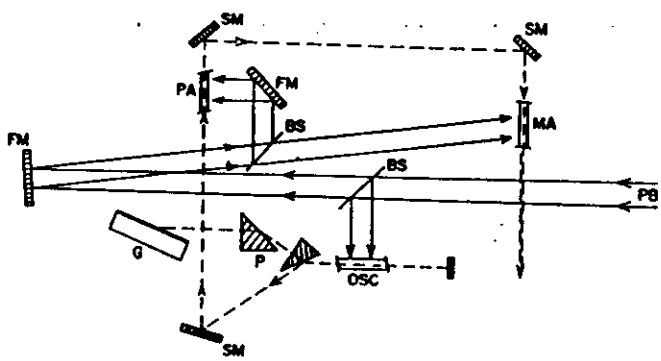

FIG. 3. Schematic layout of the complete laser system showing oscillator (OSC), preamplifier (PA), main amplifier (MA), beam expander (P) (only two prisms shown), grating (G), folding mirrors (FM), beam-steering mirrors(SM), beam splitters (BS), and pump beam (PB).

57

J. Phys. E: Sci. Instrum., Vol. 18, 1985. Printed in Great Britain

Dye cell design for high-efficiency amplifier of high beam quality

P Simon and N Juhász
JATE University, Department of Experimental Physics, H-6720 Szeged, Dóm tér 9, Hungary

Received 7 March 1985

Abstract. A novel amplifier cell design for high-power pulsed-laser-pumped dye laser systems is presented. High spatial quality of the amplified dye laser beam and fairly large energy efficiency is expected.

Nowadays high-power excimer and Nd:YAG lasers are commercially available for pumping amplifiers in dye laser systems. The different pumping arrangements generally used, however, have led to some problems. With longitudinal pumping, the excited state absorption of the dye molecules causes considerable loss of pump energy. While using the standard transverse pumping arrangement, the exponential attenuation of the pump light leads to bad output beam quality and may cause damage to the windows. Bethune reported a novel dye cell which could produce a high-quality output beam, but to the detriment of the utilisation of the pump energy (Bethune 1981).

Here we present a design of a new dye cell, which can produce more homogeneous excitation with higher efficiency than that of Bethune's. The heart of the design is shown in figure 1. The dye solution flows through a hole drilled along the axis of a 90° fused silica cone. The pump beam enters the cone perpendicular to its base. After total internal reflection the pump beam is deflected towards the axis, ensuring uniform illumination of the dye solution from each side, and providing sufficient of a focusing effect to approximately compensate the exponential attenuation of the pump beam.

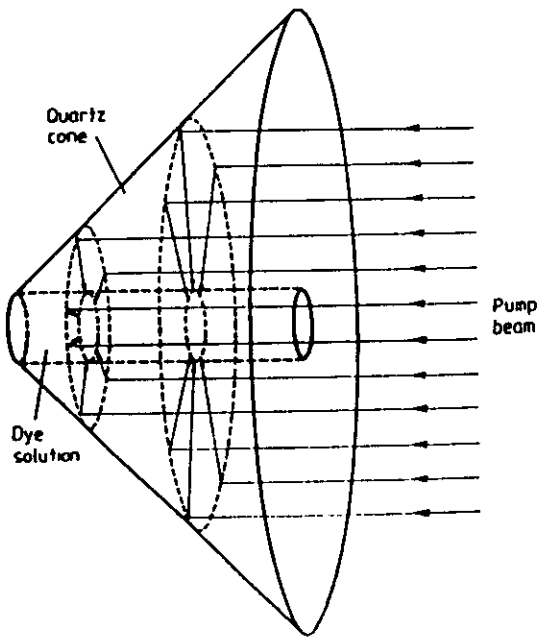

Figure 1. Schematic diagram of the conic dye cell. The active medium is illuminated from all sides.

In order to compare the prismatic and conic cells, let us define two figures of merit, one of which accounts for the utilisation of the pump energy, while the other represents the homogeneity of the pump intensity distribution. Let η be the ratio of the absorbed energy to the total pump energy (in percentage terms):

$$\eta = \frac{\text{absorbed pump energy}}{\text{total pump energy}} \times 100$$

and let h be the ratio of the portion of the area where the pump intensity differs by less than 10% from its minimum value to the total area of the cross section of the active medium (also in percentage terms):

$$h = \frac{\text{area}((I - I_{\min})/I_{\min} < 10\%)}{\text{total area}} \times 100.$$

We assume that in both cells there is perfect index matching between the fused silica and the solvent of the dye. The pump intensity at each point in the absorbing medium is determined by beams coming from four sides in the prismatic cell, and by two counterrunning beams in the conic cell. We calculated the values of η and h as functions of the absorption coefficient of the dye solution, α, for both cells. In our calculations the pump energy was 100 mJ at 308 nm, the pump pulse duration was 15 ns, the diameter of the excited medium was 6 mm, the length of the amplifier was 20 mm, and we used the molecular parameters of R6G. The results are shown in figure 2. It can be seen that with the prismatic cell, for an efficiency of 70%, the homogeneity and, as a consequence of this, the quality of the output beam are rather poor, while in the conic cell the homogeneity has a fairly high maximum value. The other advantage is that the value of the absorption coefficient corresponding to the highest homogeneity is about four times as high as it is in the prismatic cell. This helps the absorption of the pump light to become nearly complete.

By a slight modification we can make use of another advantage of the conic cell. Note, that the pump power increases along the excited medium from the apex to the base of the cone. When the cylindrical space for the dye is replaced by a conical one, the cross section of which increases as the pumping increases, the cell will approach an 'ideal' amplifier which has the following properties:

(i) the pump energy density is uniform along the length of the amplifier;

(ii) the cross section of the amplifier increases as the amplified signal passes through it so as to keep the number of photons emerging from unit area uniform.

The former condition ensures that no part of the active medium should be excited to an extreme degree, while the latter is necessary so that the depletion of the excited state should be complete enough, while at the same time the temporal distortion of the amplified pulse can be kept negligible (Bor *et al* 1983).

A theoretically collinear pump beam would result in extremely high pump intensity near the axis. In practice, however, it is avoided by the natural divergence of the pump light. The defocusing effect can be enhanced – if necessary – by appropriate tailoring of the pump beam.

Finally we can conclude that the homogeneity of the conic dye cell is fairly good and at the same time its efficiency is more than 90%. Using an excimer laser as a pump source some

0022-3735/85/100829 + 02 $02.25

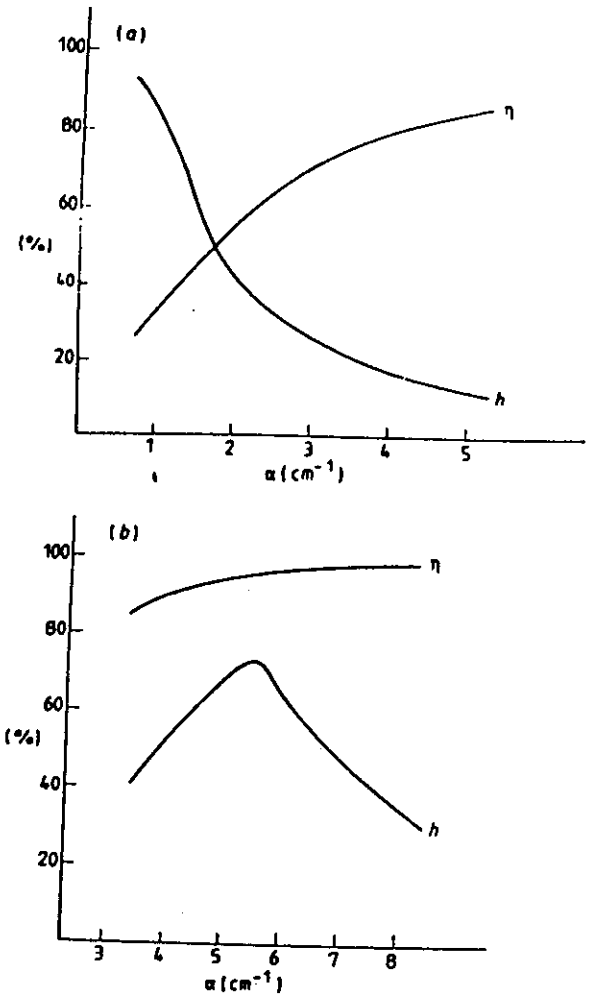

Figure 2. The efficiency (η) and homogeneity (h) of (a) the prismatic cell and (b) the conic cell as functions of the absorption coefficient (α) of the dye.

additional loss occurs owing to the transformation between the rectangular beam profile and the circular pump inlet aperture of the cell. But even then the efficiency and homogeneity of the conic cell are better than that of the prismatic one.

Acknowledgment

The authors gratefully thank Dr J Hebling and Dr S Szatmári for their helpful discussions and Dr G Szabó, Dr B Rácz and Dr J Klebniczki for critical reading of the manuscript.

References

Bethune D S 1981 Dye cell design for high-power low-divergence excimer-pumped dye lasers
Appl. Opt. **20** 1897

Bor Zs, Rácz B and Schäfer F P 1983 N_2 laser pumped ultrashort pulse amplifier.
Sov. J. Quantum Electron. **12** 1050

J. Phys. E: Sci. Instrum., Vol. 18, 1985. Printed in Great Britain

Semi-automatic determination of scattering vector in small-angle light scattering

B Koyuncu† and J C Earnshaw
Department of Pure and Applied Physics, The Queen's University of Belfast, Belfast BT7 1NN, Northern Ireland

Received 4 February 1985, in final form 22 March 1985

Abstract. An electronic system is described for semi-automatic determination of the scattering vector in small-angle light-scattering experiments. The method is simple and capable of complete automation. It has been applied to small-angle scattering from thermal fluctuations of liquid surfaces and typical results are presented.

1. Introduction

Small-angle light scattering finds widespread use in characterising the properties of molecular systems. The dynamic properties are accessible via quasielastic scattering, for which the incident and scattered wave vectors are $|k_i| \simeq |k_s|$. One specific application is the determination of the physical properties of fluid interfaces via the spectrum of light scattered by thermally excited fluctuations of the interface (e.g. Her and Meunier 1974, Byrne and Earnshaw 1979).

It is essential to the correct analysis of any light-scattering experiment that the scattering vector K be accurately determined. This is particularly true at small scattering angles ($\Delta\theta$) when K is rapidly varying:

$$K = k_i - k_s$$
$$= 2k_0 \sin(\Delta\theta/2)$$

for quasielastic scattering ($k_0 = 2\pi/\lambda$). This note describes a novel electronic technique for determination of K which is then applied to an example of fluid interfacial scattering to illustrate its usefulness.

2. Light-scattering system

Only the essential details of our heterodyne spectrometer (figure 1) need be given (cf Byrne and Earnshaw 1979). Light from a He–Ne laser ($\lambda = 632.8$ nm, TEM_{00} mode) was spatially filtered to ensure a gaussian intensity profile, to expand the beam, and was then focused to cause it to converge slowly. The laser beam was incident upon the water–air interface just above the critical angle. A coarse diffraction grating (G) set normal to the laser beam provided heterodyne reference beams of controllable intensity at various small angles from the main laser beam. The lens L_3 caused the various diffracted beams to cross at the liquid surface (i.e. the grating is imaged there) and focused them in the detector plane. Light scattered out of the zero-order beam mixed with the various diffracted beams. A single diffraction order was selected for detection by a pinhole before the detector. This type of local oscillator has advantages for inaccessible scattering volumes (Hård and Nilsson 1979).

† Present address: Physics Department, University of Kuwait, PO Box 5969, Kuwait.

0022-3735/85/100830 + 04 $02.25

III) Beam profile of FL 3002

Measurements taken by OMA at 2m distance from laser
Dye.....Rh 6G

a) Horizontal profile

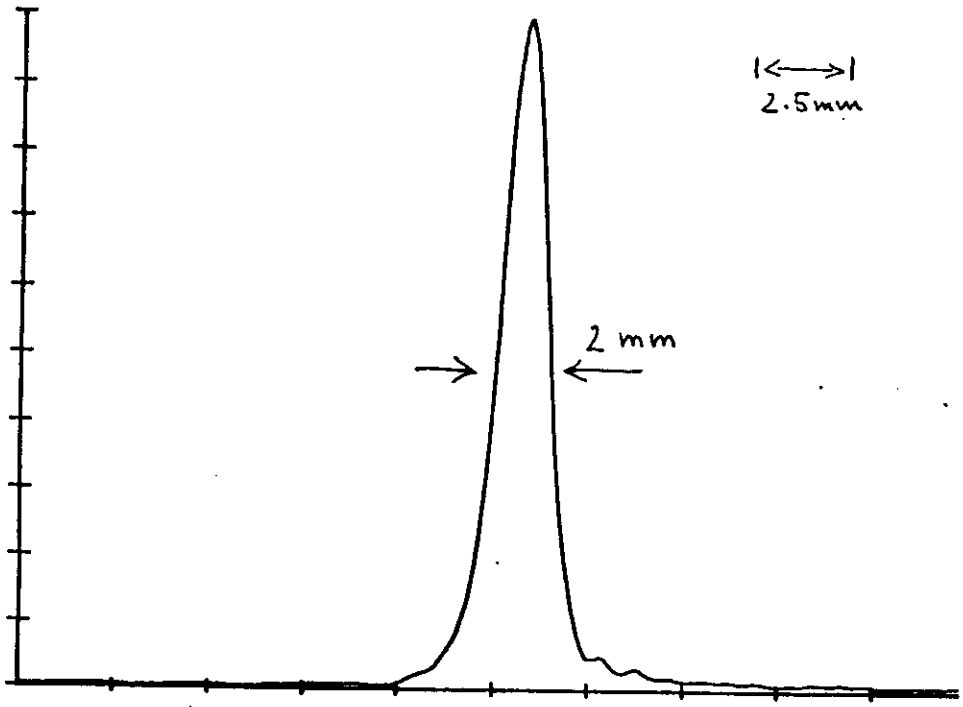

b) Vertical profile

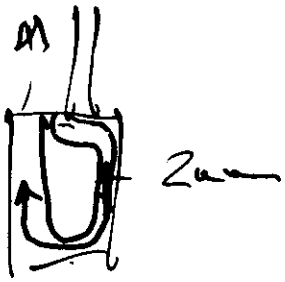

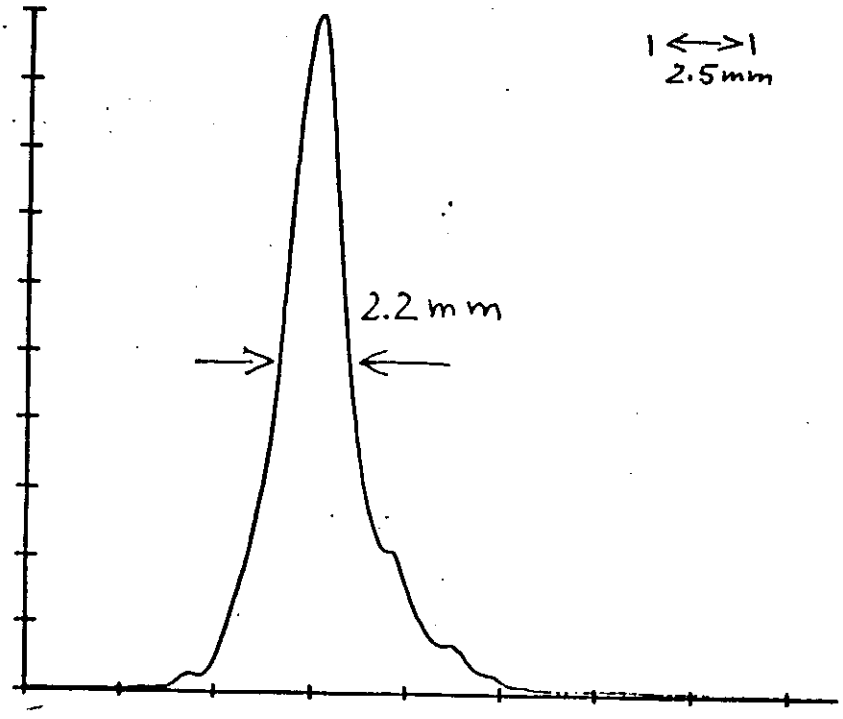

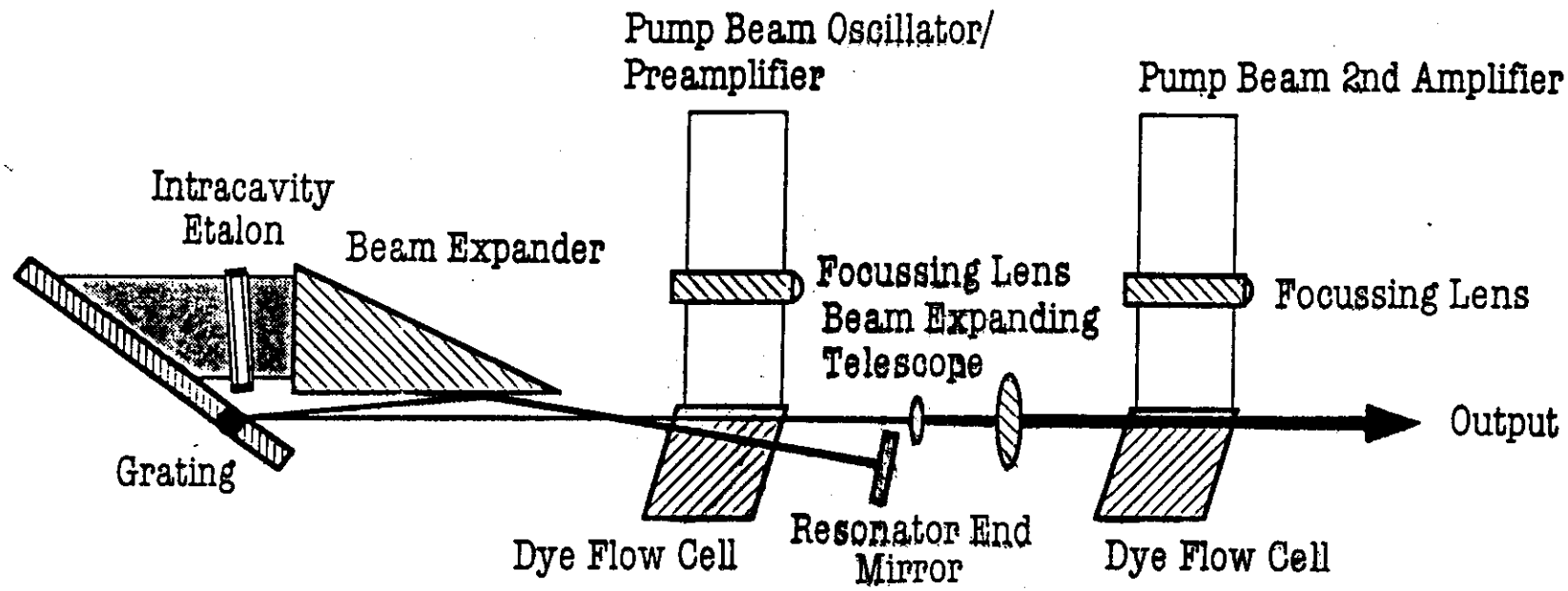

General design FL 3002 E dye laser

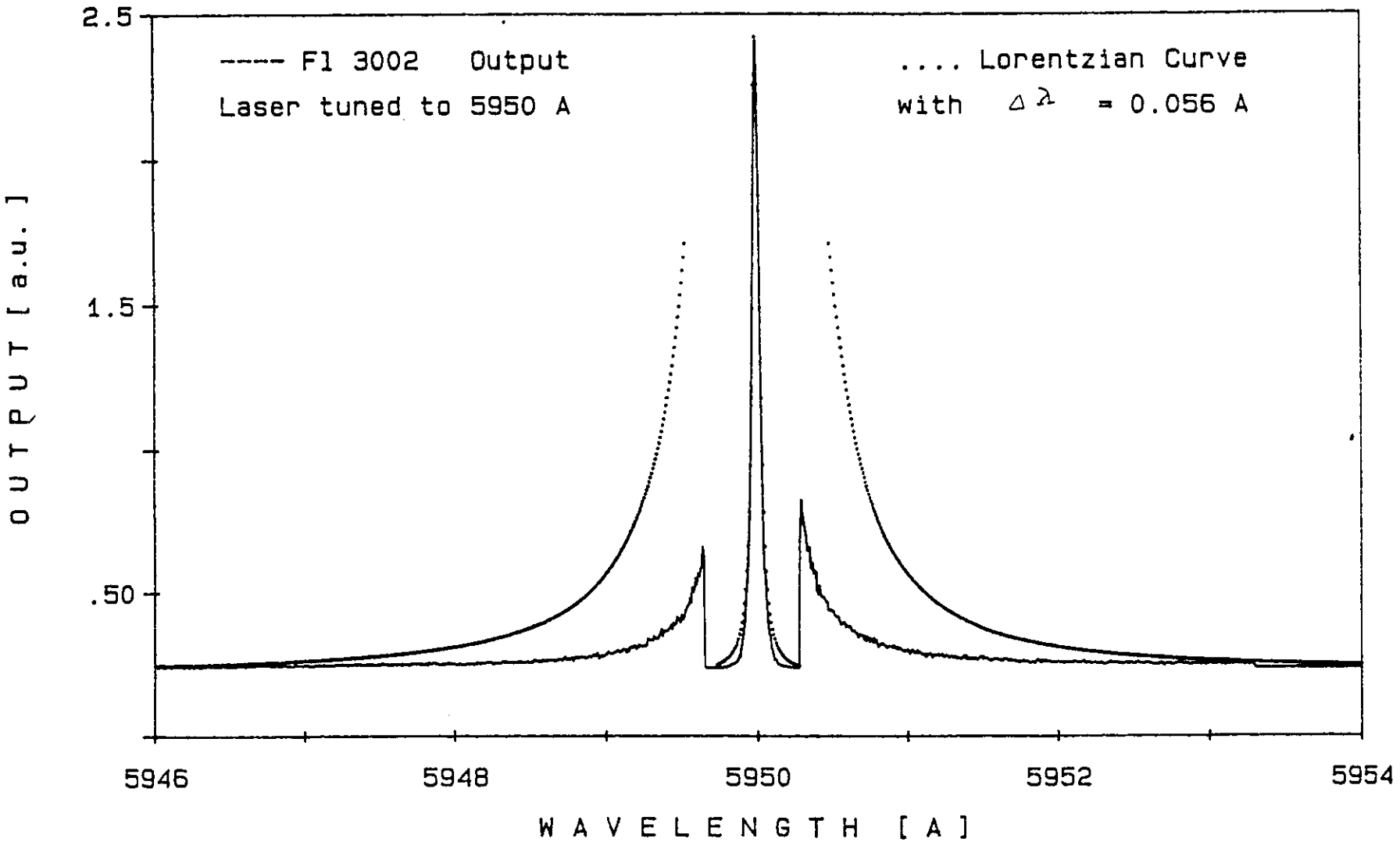
2.5
1.5
.50
----- F1 3002 Output
Laser tuned to 5950 A
.... Lorentzian Curve
with Δλ = 0.056 A
OUTPUT [a.u.]
5946
5948
5950
5952
5954
WAVELENGTH [A]

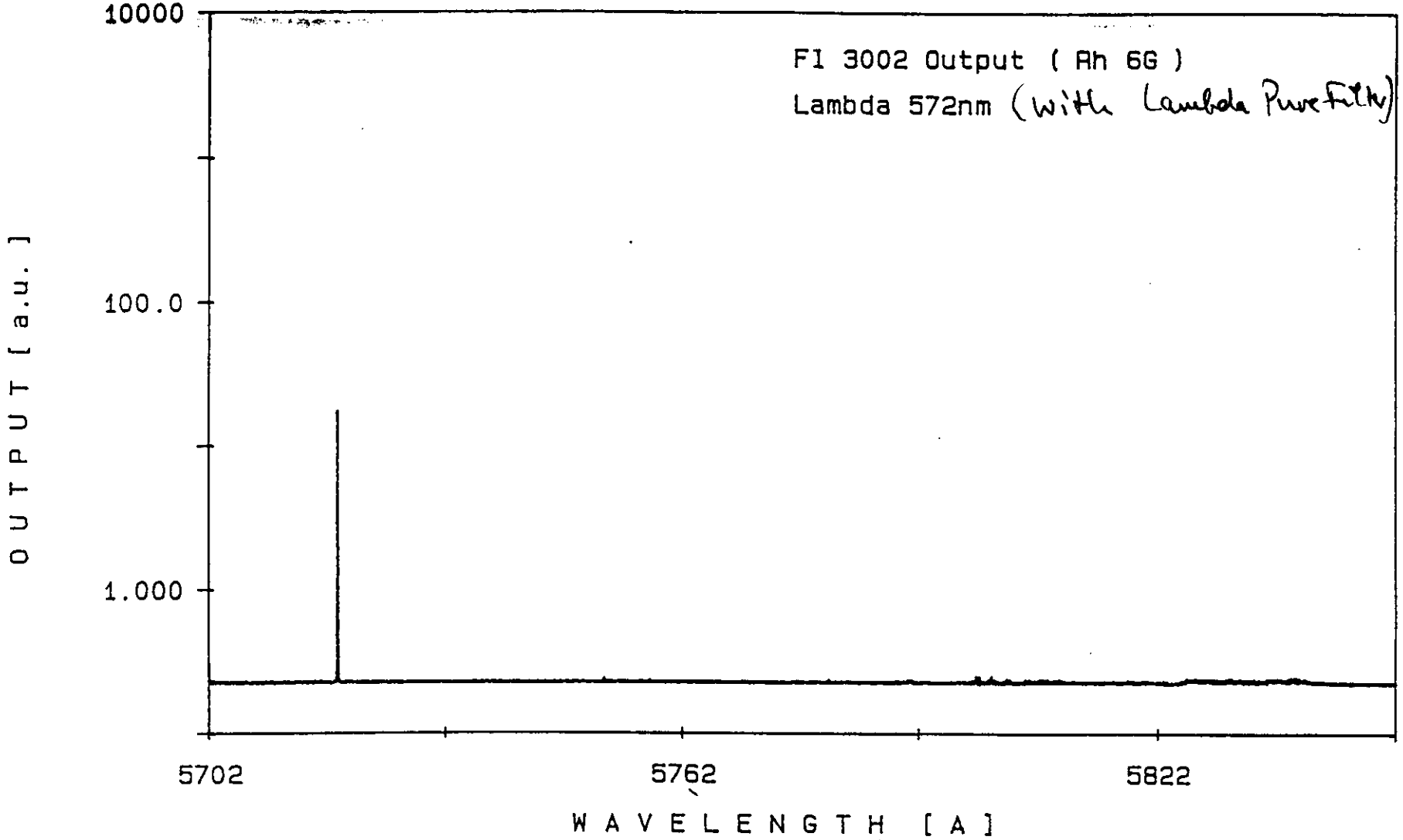
10000
100.0
1.000
OUTPUT [a.u.]
FI 3002 Output (Ah 6G)
Lambda 572nm (with Lambda Pure Filter)
5702
5762
5822
WAVELENGTH [A]

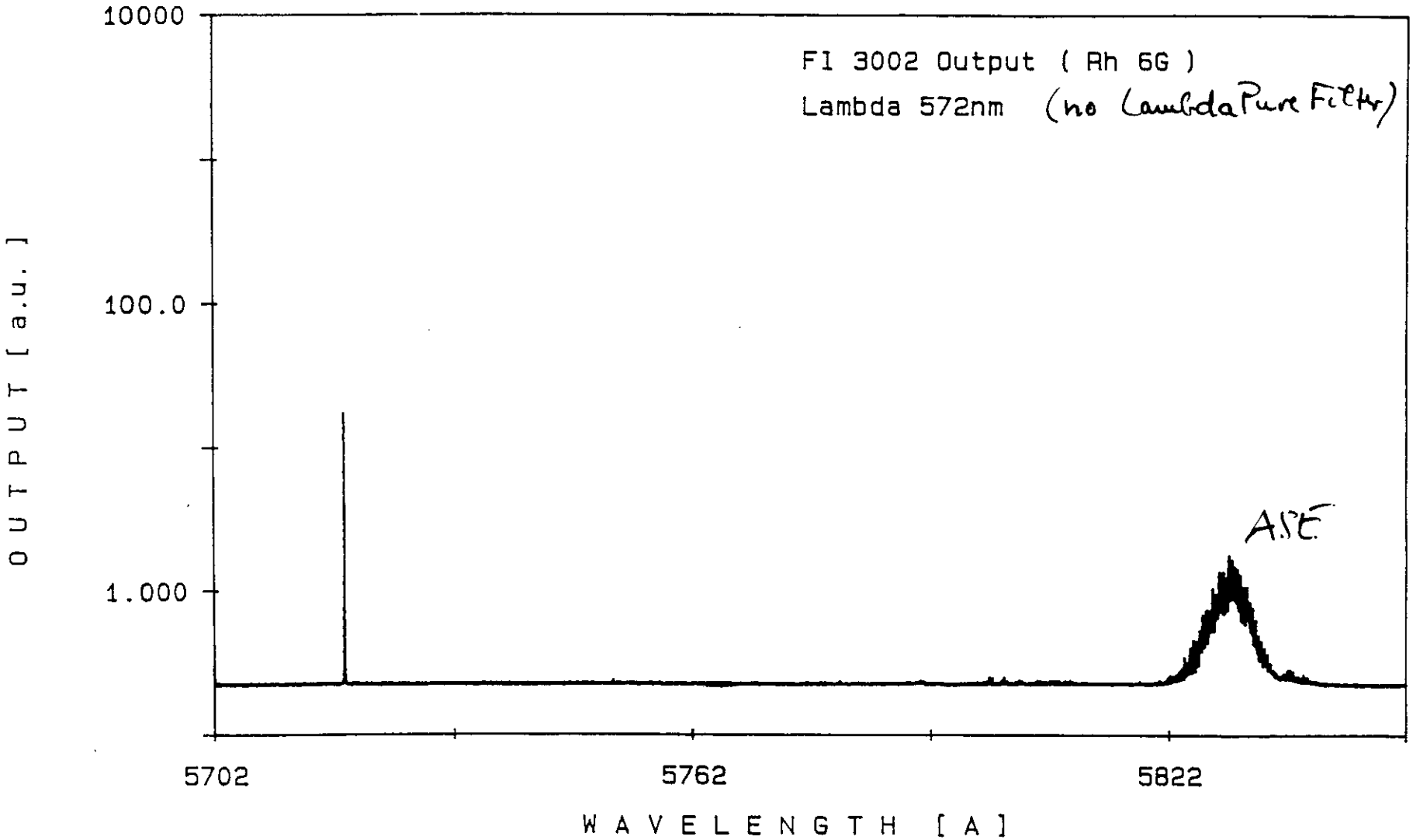
FI 3002 Output (Rh 6G)
Lambda 572nm (no LambdaPure Filter)
ASE
10000
100.0
1.000
OUTPUT [a.u.]
5702
5762
5822
WAVELENGTH [A]

Commercial Dye Lasers

— State - of - the - art

Combination of:

a) best choice of technical principles

b) sophisticated engineering

c) ease of use

LPD 3000

LPD 3000

The Dye Laser Generation of the Future

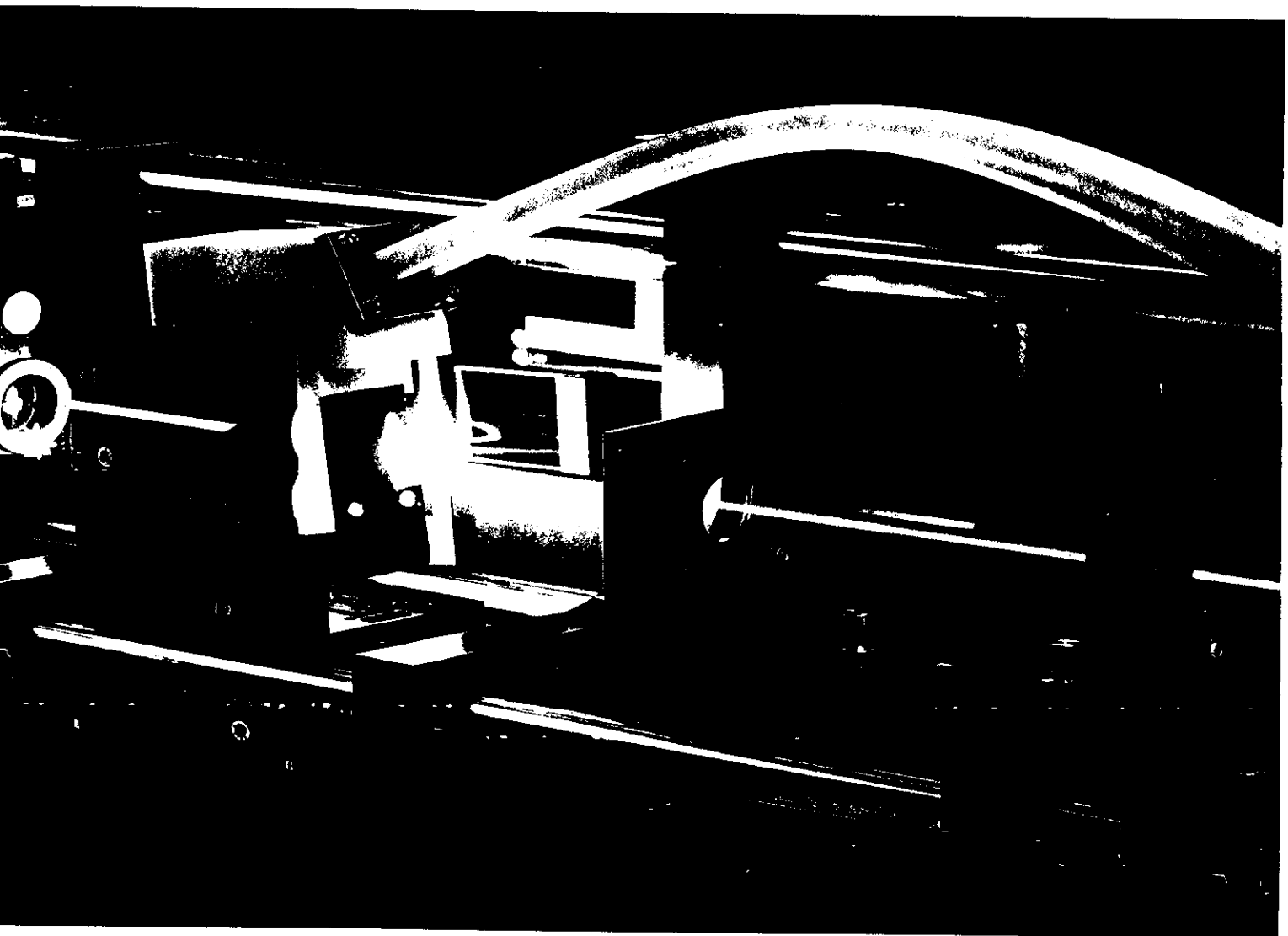

LAMBDA PHYSIK
LASERTECHNIK

LPD 3000
All the advantages at a glance

The latest generation of a long line of pulsed dye lasers, LAMBDA PHYSIK's new LPD 3000-series, benefits from more than 15 years of experience. The LPD 3000 combines the advantages of the well known FL 3000-series with numerous innovative improvements.

Oscillator configuration
The oscillator design guarantees broad tunability with only one single grating. It has a high diffraction efficiency, high frequency accuracy and low spectral bandwidth.

LAMBDAPURE®-filter
This automatic filtering process developed by LAMBDA PHYSIK guarantees optimum spectral purity and extremely low ASE-background.

Mechanical stability
All parts of the dye laser are placed in a mechanically very stable multi-rod system. This concept ensures very good wavelength accuracy at highest thermal stability.

Oscillator/preamplifier combination
One dye cell functions economically both as oscillator and amplifier, just being pumped in different regions at different times. This results in highest conversion efficiencies at lowest background.

Optimized amplifier configuration
By using separate dye circulations for the oscillator/preamplifier and for the main amplifier optimization of the dye concentration is possible. This results in highest pulsed dye laser efficiency.

Etalon concept
Use of an etalon for low bandwidth operation results in additional frequency stabilization. That makes the LPD 3000 more than ten times less sensitive to mechanical vibrations, temperature changes and refractive index inhomogeneities within the laser beam compared with other low bandwidth lasers. The easy removable etalon insures a high flexibility for low resolution survey scans and high resolution detailed scans.

Ease of use
All optical components of the LPD 3000 are clearly arranged in a mechanically very stable three-rod system. Only a few alignment screws need to be addressed. An integrated HeNe-laser allows proper positioning of the dye laser to the excimer laser.

Control of the system is achieved by a removable remote control.

High degree of automation
The internal microprocessor assures optimized drive speed with fully synchronized continuous path control. This way a much faster data acquisition is possible. Convenient software ensures on-line remote control of the laser by a host computer via an IEEE 488 interface.

Free choice of a pump laser
The LPD 3000 can be alternatively pumped with high efficiency by an excimer, Nd:YAG, nitrogen or copper-vapor laser.

Dye circulating unit
Sturdy dye cell mounts allow exchange of the cuvette without realignment. This way fast change between different tuning ranges is possible. Repetition rates of up to 1000 Hz with excimer pump lasers and several kHz with copper vapor lasers at high conversion efficiencies are possible when using an optimized high flow dye circulating unit.

Tuning range 189 ... 2000 nm
Conversion to the VUV or NIR with good efficiency is achieved by frequency-doubling and Raman-shifting.

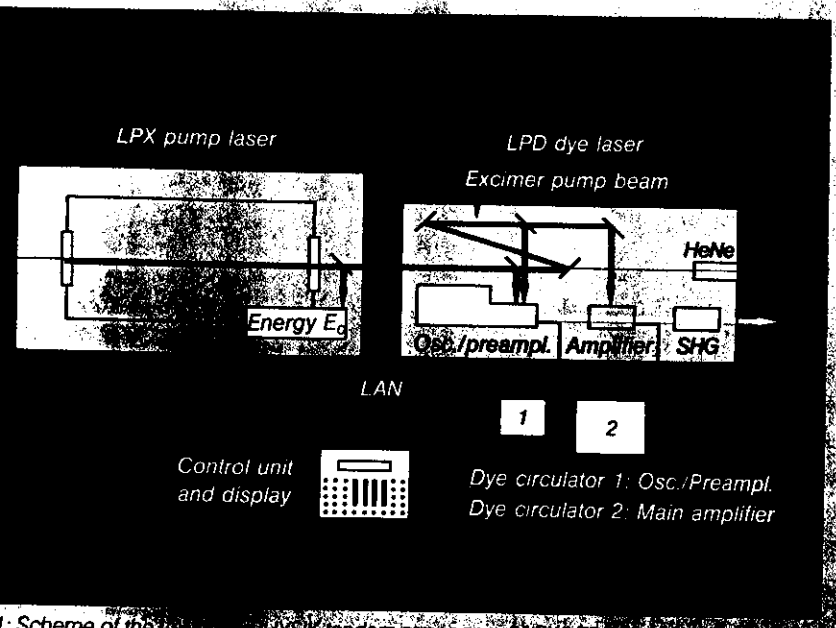

1: Scheme of the LAMBDA PHYSIK tandem arrangement LPX/LPD 3000

LPX pump laser (XeCl) type	Pump energy [mJ]	max. Rep.-rate [Hz]	max. average power [W]	Dye laser LPD 3002 (C102) Pulse energy [mJ]	max. average power [W]
LPX 120i	200	200	32	30	4
LPX 210i	400	100	40	65	5
LPX 325i	600	250	120	100	15

Characteristics of LPX/LPD 3000 systems

```
462.000 << 575.000 <--  580.675  --> 610.000 >> 787.000     1.000

LAMBDA PHYSIK LPD 3000 GRATING SCAN:

          ENTER LOWER END OF SCAN INTERVALL:   575.000 [nm]
          ENTER UPPER END OF SCAN INTERVALL:   610.000 [nm]
          ENTER SCAN STEP:                       1.000 [nm]
          ENTER DWELL TIME:                       .500 [s]
          ENTER NUMBER OF SCANS:                   10
          ENTER DELAY TIME:                       .200 [s]
          ENTER NEW CURRENT WAVELENGTH:        580.675 [nm]

          TRG.ON    BURST MODE    REP.RATE: 100 Hz   PLS./BURST: 10

SET          F3  SET SCN.RNG F5  TRG.ON/OFF  F7  CONT/BURST  F9  SET GRTG.ORD
START SCAN   F4  SET CRNT.WL F6  TRG.PARAM   F8  BREAK       F10 GO TO LOCAL
```

Menu driven control software (based on the software package ASYST™, to be ner supplied)

LAMBDA PHYSIK system concept: LPX/LPD 3000

- *integrated system concept (design, beam height, alignment and control of the whole system)*
- *system optimized pumping laser*
- *integrated automation of the whole system by integration of the LPD 3000 into the fiber optic network of the LPX excimer laser.*

Excimer-pumped dye laser

- *nearly all dyes can be directly pumped by one of the excimer lines. There is no need for complex and expensive frequency conversion techniques*
- *broad fundamental tuning range UV-NIR*
- *high pulse energy*
- *variable and high pulse repetition rate from 1 to 1000 Hz*
- *simple handling of the complete system*

LAMBDACHROME® laser-grade dyes

All laser dyes are synthesized and tested by experienced LAMBDA PHYSIK scientists. Specifications are guaranteed.

LPD 3000
Configuration and operation

LAMBDA PHYSIK's LPD 3000 dye lasers consist of an oscillator, preamplifier and main amplifier.

Oscillator design

The oscillator determines the quality of radiation and is therefore the most important and sensitive part of a dye laser system. The LPD 3000 oscillator consists of:

- *a grating for wavelength selection,*
- *an achromatic prism beam expander for narrowing the bandwidth,*
- *a dye flow cell containing the active medium and*
- *an end mirror coated for the whole spectral range to be covered.*

See figure 3 for a schematic diagram.

The LPD 3000 uses the grating in the retro-reflective or Littrow-position. With this oscillator concept, moderate grating angles (≦75°) can be used. This allows lower frequency jitter, higher grating efficiency and less sensitive operation than other oscillator concepts such as grazing incidence operation, where the grating is set to almost 90°, and tuning has to be performed by an additional mirror.

Littrow-scheme dye lasers have the advantage that there is no need for any grating replacement with subsequent calibration procedures: the entire spectral range (320 ... 970 nm) can be covered by one single grating. Multiple wavelength output as known from grazing-incidence systems does not occur.

LAMBDAPURE® filter

*In addition to bandwidth and tuning accuracy, the LPD 3000 achieves highest spectral purity. The output of a conventional dye laser includes some background emission with spectral distribution around the maximum of the tuning range. Most of this background originates in the oscillator itself, where spontaneously emitted photons can be amplified due to the high gain (**ASE** = **A**mplified **S**pontaneous **E**mission). In conventional dye lasers this ASE leaves the oscillator through the outcoupling mirror without being suppressed or filtered out and is thus further amplified in the following amplifier stages of the dye laser.*

The special outcoupling system of the LPD 3000 dye laser series and the use of an additional automatic filtering process ("LAMBDAPURE® filter") avoids all these problems: The oscillator output is decoupled at the entry surface of the prism beam expander and reflects from the grating again before reaching the next amplifier (figure 3). This leads to a substantial suppression of ASE (figure 4). Synchronization of the oscillator wavelength and the filter center wavelength is guaranteed by the fact that the dye laser beam coming from the oscillator hits the grating at the location of its rotational axis (so called LAMBDAPURE® point) with an appropriate angle of incidence.

Preamplifier

Use of this patented configuration from LAMBDA PHYSIK also means that one dye cell can economically function both as an oscillator dye cell and as an amplifier dye cell which is simply pumped in a different region. The dye cell functions in this way as a preamplifier. For pumping of the preamplifier a laser beam with exactly defined delay is used (figure 3). This also reduces a major part of the ASE background originating at the beginning of oscillation. That is the second major innovation in the LAMBDAPURE® concept. The LAMBDAPURE® system results in a drastic reduction of ASE background to less than 10^{-3}. It should be mentioned that highest ASE suppression can be achieved at the wings of the tuning curves (figure 4). The usable spectral range can thus be extended.

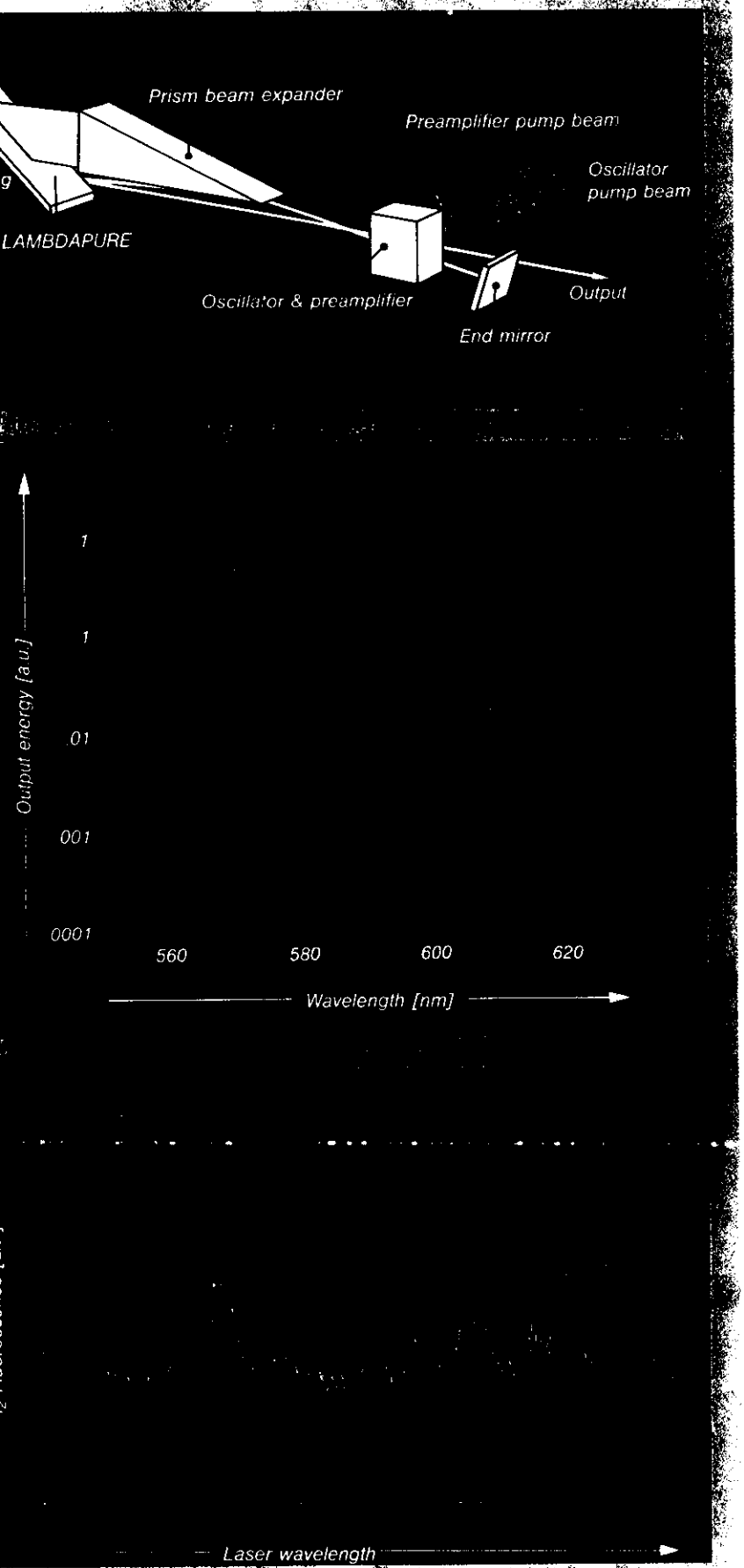

Fluorescence spectra of I₂ measured by the LPD 3002E at different room temperatures

Mechanical and thermal stability LPD 3000

During the development of the LPD 3000 dye laser series, special attention was paid to the mechanical stability and precision of the apparatus. All optical components are placed in a stable three-rod system. All parts of the oscillator which require the highest mechanical and thermal stability are enclosed in a hermetically sealed and mechanically rigid metal block with provisions for temperature as well as pressure stabilization. In addition, the grating is made on a substrate of low thermal expansion (zerodur) and is driven by a especially checked and calibrated precision sine-drive. This allows very high absolute and relative wavelength accuracy as well as highest temperature stability (figure 5).

40

LPD 3000
Configurations

LPD 3001

The LPD 3001 is the basic model of the new dye laser family. In combination with the LPX 100 excimer laser series of LAMBDA PHYSIK or other pump lasers with medium pulse energy, this compact dye laser system is an ideal light source of high spectral purity for applications which require tunable dye laser radiation of medium energy and power.

The design is the same as described above (figure 3). The LPD 3001, like the other models of the LPD 3000 series, is supplied with AR-coated pump optics for pumping with XeCl excimer lasers. Other pump optics are optionally available.

LPD 3002

The LPD 3002 is the high performance model of the LPD 3000 series. An additional amplifier has been added to the basic configuration described above (figure on page 7/8).

A beam expanding telescope behind the preamplifier matches the dye laser beam to the larger active volume in the main amplifier. This - in combination with the possibility of optimizing the dye concentrations for oscillator/preamplifier and main amplifier separately - results in the highest pulsed dye laser efficiency available (for excimer pumping up to 20%, for Nd:YAG pumped red dyes up to 35%).

Linewidth and ASE-suppression measured with a high resolution grating monochromator as shown in figure 7 present a convincing argument.

Pumped by an excimer laser of high pulse energy and high average power the LPD 3002 delivers high pulse energies (up to 100 mJ) and high average powers (more than 10 W). These peak values could be realized by the development of special high flow dye circulating units (figure 14).

LPD 3002E

The LPD 3002E is the narrow-bandwidth version of the LPD 3002 dye laser. The system incorporates an intracavity etalon by which the bandwidth is reduced to $\leqq 0.04\ cm^{-1}$. Figure 8 shows the checkup with a confocal Fabry Perot-interferometer.

Installation and removal is a matter of minutes and does not require cavity realignment. Contrary to other commercial dye lasers with intracavity etalon, the LPD 3002E requires only one etalon for bandwidth narrowing. This etalon has three different selectable dielectric coatings on one common substrate and covers the entire spectral range.

Due to the high number of cavity roundtrips during the excimer laser pump pulse (even more favorable when using an LPX 605i long pulse excimer laser), single-mode operation is possible (s. D. Basting et al., SPIE vol. 912, 87 (1988)).

Automatic tuning can be achieved either by synchronously tilting grating and etalon with the aid of the control electronics or optionally by changing the pressure inside the resonator housing.

LPD 3002
Optical design

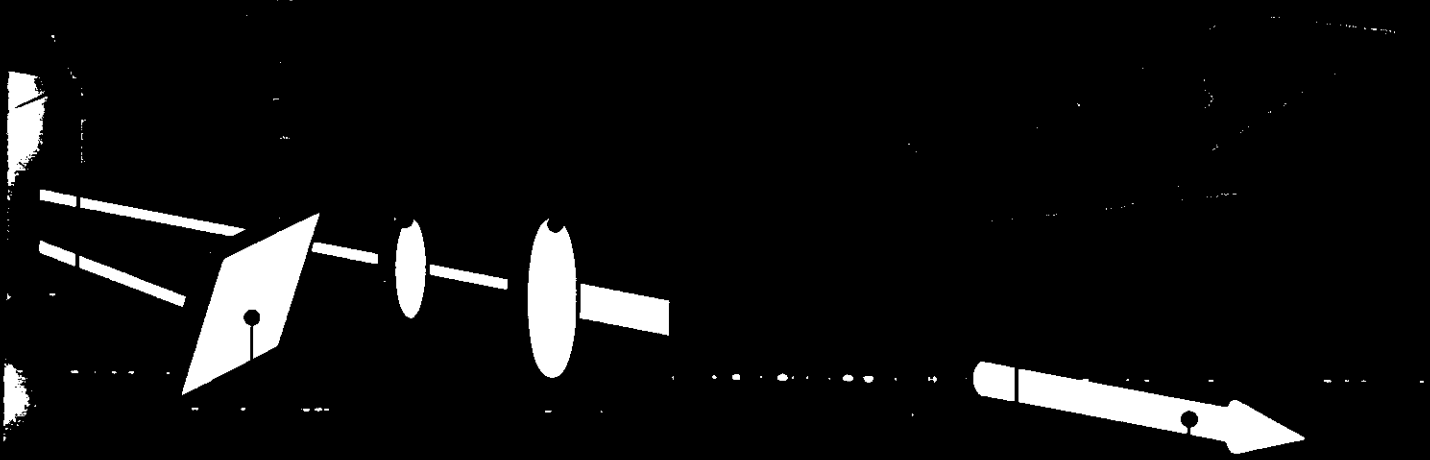

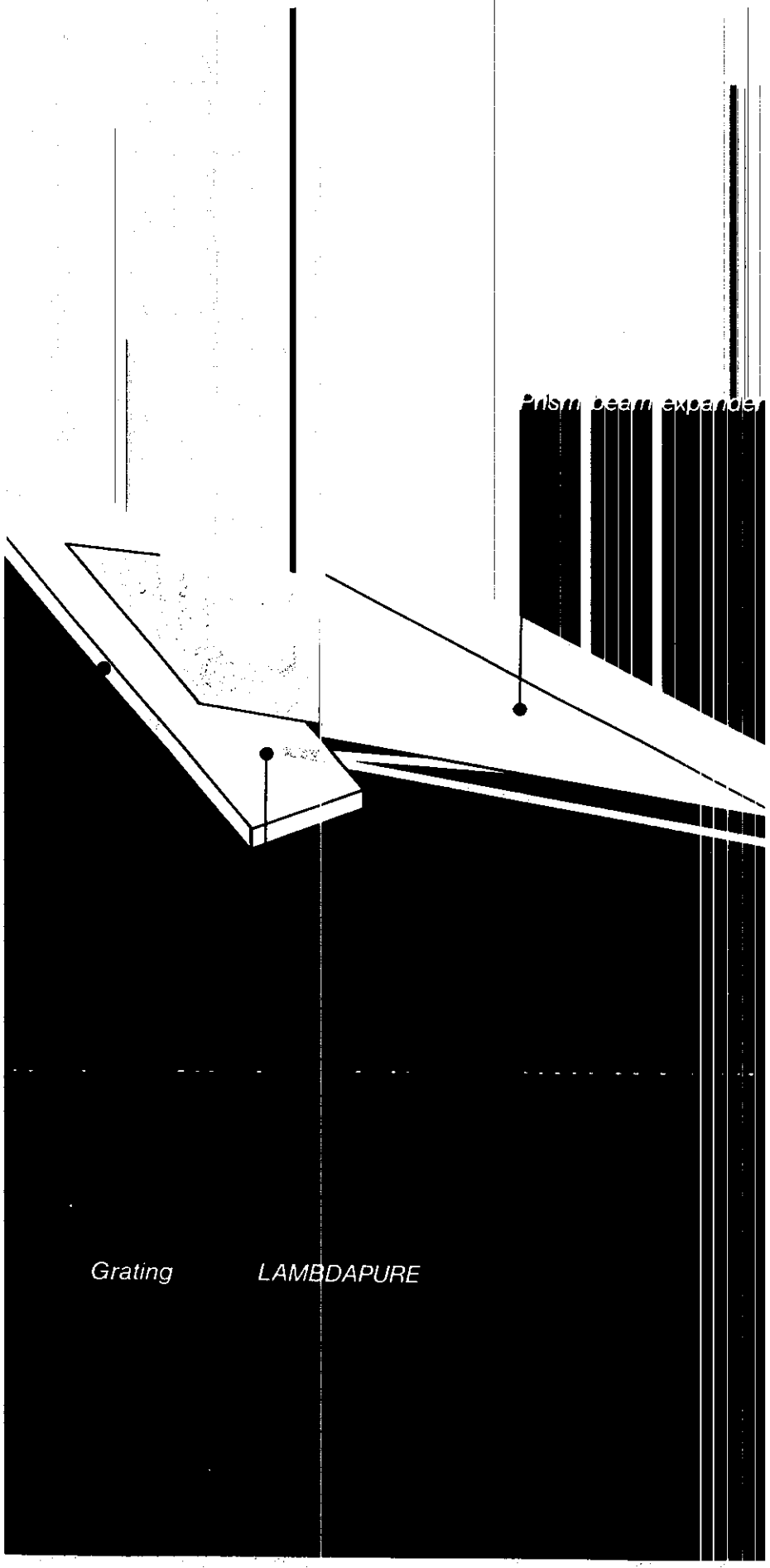
Prism beam expander
Grating
LAMBDAPURE

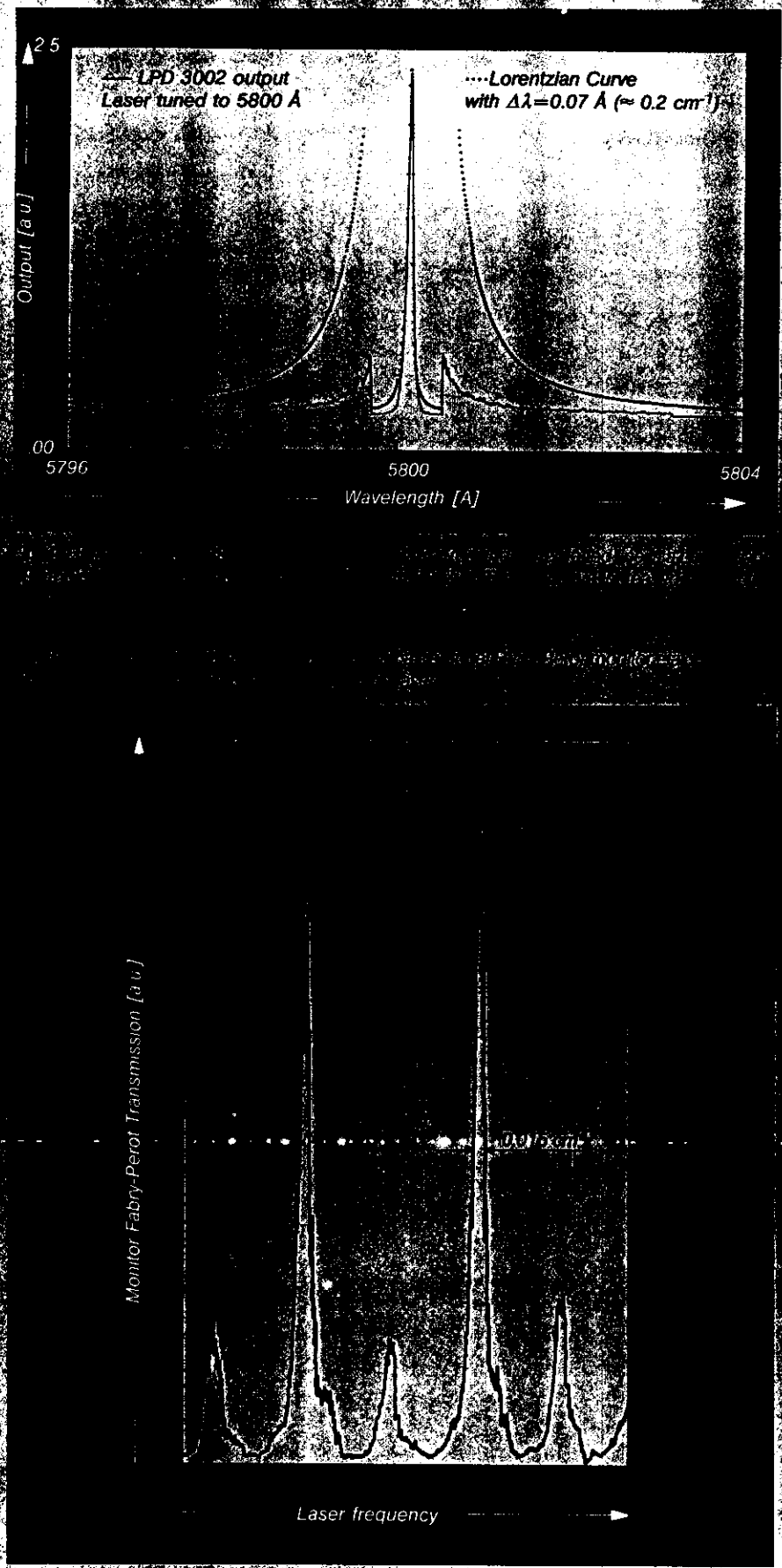

Use of an etalon inside the resonator for low bandwidth operation results in additional highest frequency stabilization. Each frequency jitter is converted to amplitude fluctuations of the oscillator which are compensated by the following amplifier stages operating in saturation.

The concept of optional use of an etalon gives more flexibility during operation. In case of need the etalon can be removed and a broad spectral range can be scanned at lower resolution but higher scan speed. In this way, a survey of a spectrum can be obtained within a few minutes.

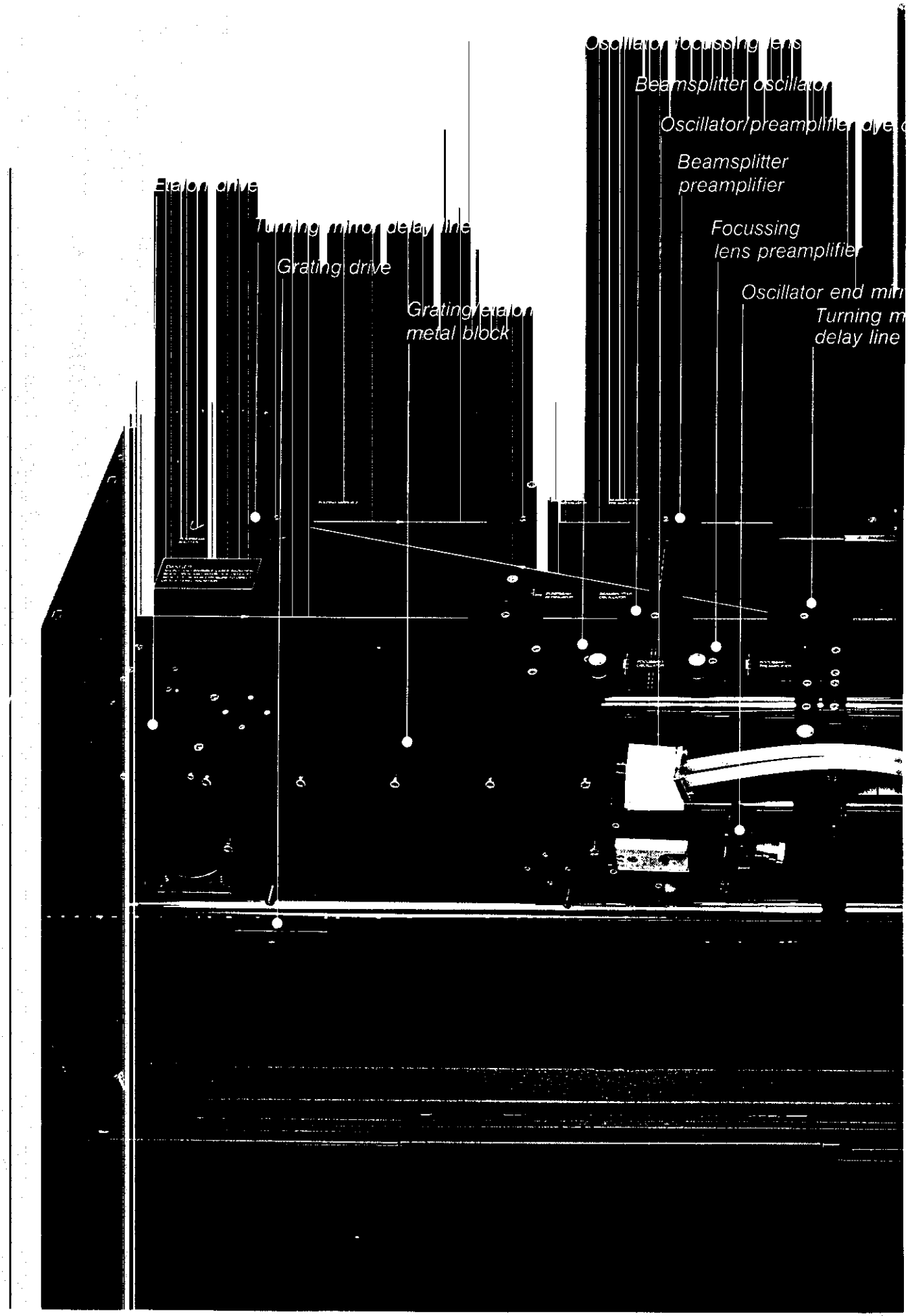
Oscillator focussing lens
Beamsplitter oscillator
Oscillator/preamplifier
Beamsplitter preamplifier
Etalon drive
Turning mirror delay line
Grating drive
Focussing lens preamplifier
Oscillator end mir
Grating/etalon metal block
Turning m
delay line

LPD 3002
Mechanical and optical design

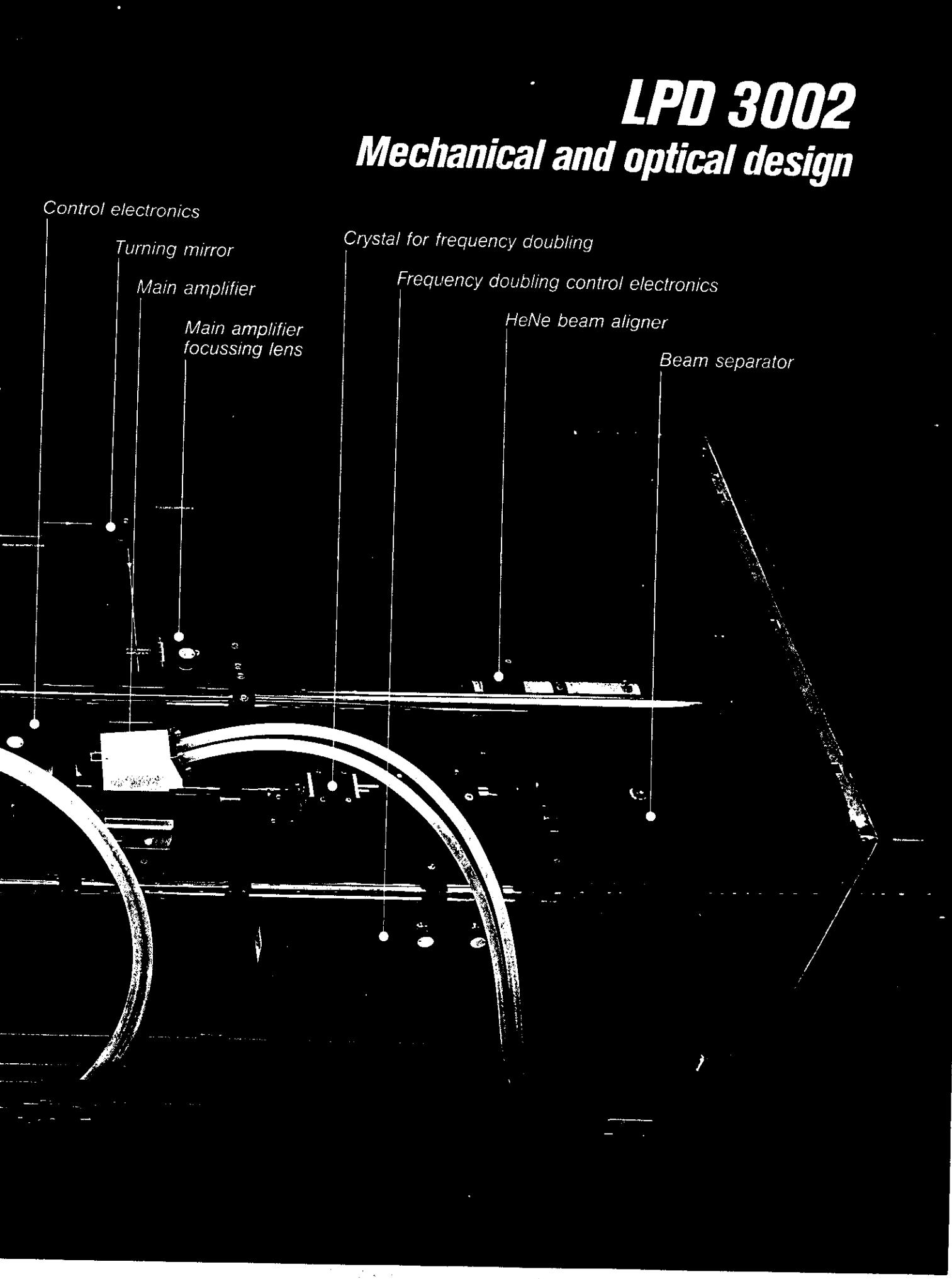

LPD 3000
Control concept

The LPD 3000 comes equipped with a microprocessor as standard. This microcomputer unit offers maximum flexibility and ease of use. It can be easily removed from the dye laser housing (figure 11) and can be used at any distance from the laser.

Integrated control unit

The concept of continuous path control allows fast and synchronous scan of the three drives for grating, etalon and crystal. This allows the scan speed to be increased drastically. The microcomputer offers the following programmable operation:

- *automatic wavelength calibration during initial set-up,*
- *actual wavelength display in nm (LPD 3002E additionally in cm^{-1} or GHz),*
- *continuous path controlled scan to a preselected wavelength,*
- *enhanced scan speed,*
- *automatic scan between two preselected wavelengths with preselected scan speed,*
- *automatic scan between two preselected wavelengths with preselected step width at maximum speed and output of selectable number of laser pulses after each step (burst mode),*
- *automatic determination of the optimum grating order, and*
- *crystal tuning during frequency doubling and mixing with automatic crystal/grating synchronization.*

The additional following features are included in the FL 3002E:

- *automatically synchronized multiple etalon scan across the entire dye tuning range,*
- *crystal tuning with automatic grating/etalon/crystal synchronization.*

The high frequency accuracy of the microcomputer controlled wavelength tuning of the LPD 3002E is demonstrated by an iodine absorption spectrum in figure 10. Comparing the real distance between two absorption lines with the wavelength displayed on the microcomputer screen, the error is less than 0.02 cm^{-1} over a tuning interval of 4 cm^{-1}.

Fiber optic local area network technology

A totally new control concept has been adapted in the LPD-series.

The LPD 3000 can be integrated via a corresponding interface into the fiber optic local area network (LAN) of LAMBDA PHYSIK's LPX excimer lasers. This technology connects distributed intelligent control modules via a single fiber optic communication ring. Controlled by decentralized microprocessors with electronic safety circuits (watchdogs), this concept guarantees that the system is always operated under safe conditions. By using the LAN-interface, the LPX pump laser can be controlled completely from the microprocessor of the LPD dye laser. Pumping with constant pulse energy can be of special interest and is simply performed by the new concept.

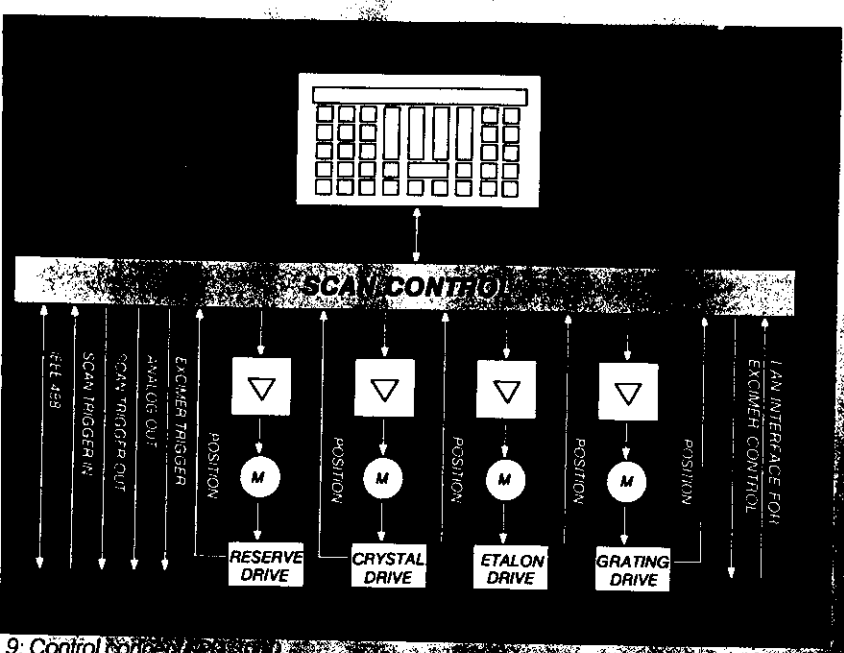

9: Control concept

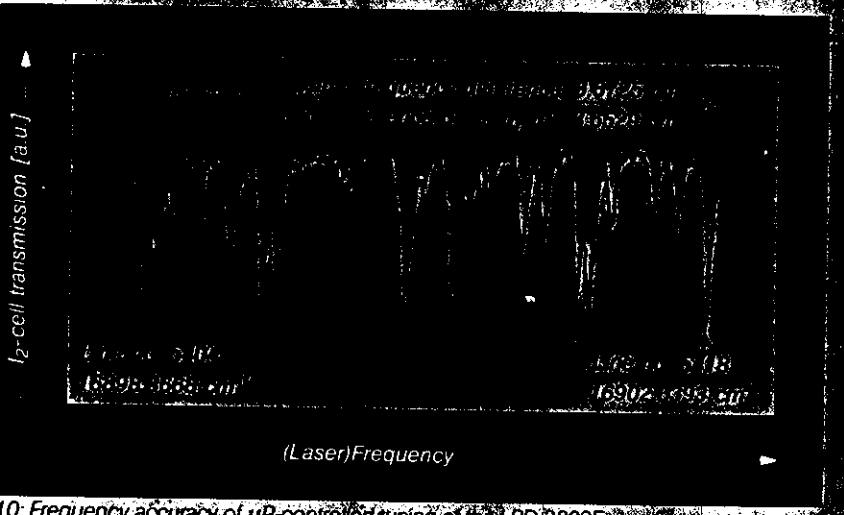

10: Frequency accuracy of µP-controlled tuning of the LPD 3002E

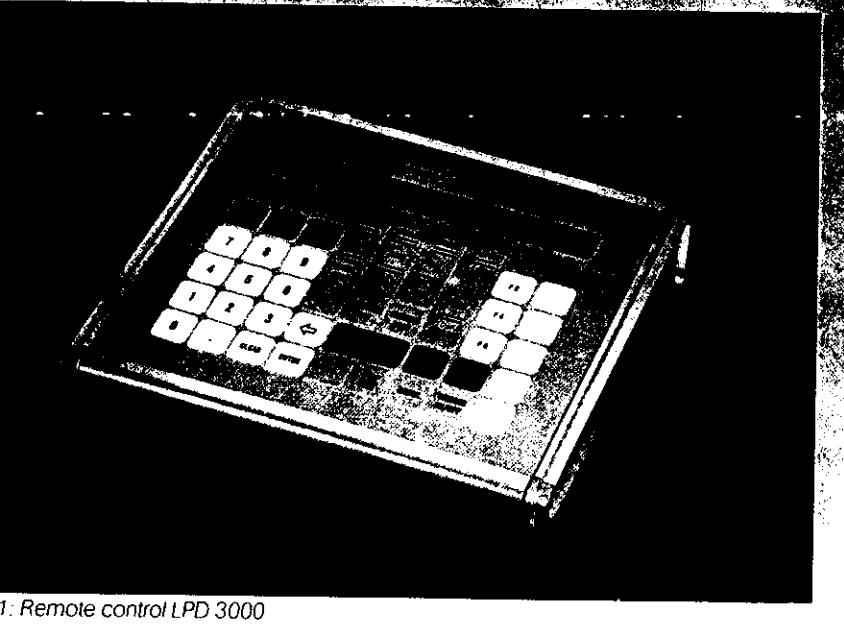

1: Remote control LPD 3000

IEEE 488-Bus

The easy-to-use IEEE parallel bus interface has been designed for comfortable integration of the LPD 3000 into computer controlled experiments. Via this interface and with the help of correspondingly adapted software (e.g. ASYST™) all actual laser parameters can be set on-line by a host computer. In addition, experimental results can be analyzed immediately (figure 2).

Additional interfaces

- *wavelength proportional analog signal output with selectable sensitivity (e.g. for a chart recorder),*
- *scan trigger in/out*
- *trigger out for other pump lasers or experimental set ups.*

48

LPD 3000
Wavelength extension

The LPD 3000 in its basic configuration emits in a fundamental tuning range of 320 - 970 nm (figure 12). This range can be extended with high conversion efficiencies and good beam parameters to other spectral regions either by

- *frequency doubling (**SHG** = **S**econd **H**armonic **G**eneration),*
- *frequency mixing (**SFG** = **S**um **F**requency **G**eneration) or*
- ***R**aman **S**hifting (**RS**).*

SHG generation

With additional frequency doubling accessories the UV-region from 205 nm to 335 nm can be covered with good conversion efficiencies of up to 30% and pulse energies of up to 10 mJ (figure 13). Due to its excellent properties (high non-linear coefficient, high damage threshold, wide transparency range and low temperature dependence), Beta-Barium-borate (β-BBO) is one of the outstanding materials for frequency doubling.

The LPD 3000 uses:

- *BBO I (290 - 220 nm),*
- *BBO II (221 - 205 nm) and*
- *KDP (335 - 265 nm).*

The conversion efficiency can be enhanced by use of an additional Glan-Foucault polarizer.

For automatic wavelength tuning, the angle between crystal axis and dye laser beam axis must be continuously controlled to maintain phase-matching conditions. This "crystal tracking" is done automatically with the microcomputer, which has the complete angular trajectory of each crystal stored in its memory. To compensate for variations of the individual crystal, LAMBDA PHYSIK has developed an interactive program which allows the computer to adapt the stored parameters to the actual working conditions. This approach, in combination with the mechanically stable set-up, guarantees optimum UV output without a complicated servo-system.

Automatic beam displacement correction is achieved by an additional quartz block which rotates synchronously with the doubling crystal.

Separation of fundamental and harmonic is accomplished by using a Pellin-Broca prism set.

SFG generation

The accessible UV-tuning range can be extended to approximately 198 nm by sum frequency generation (SFG). Two frequency conversion crystals together with the corresponding control unit are needed. In the first crystal (BBO I or KDP) the SHG (2ω) of the dye laser radiation is generated. This SHG is mixed in a second crystal (BBO II) with the fundamental dye laser radiation (ω), resulting in the sum frequency (3ω) (figure 13, region "SFG I").

*Tunable dye laser output in the **even deeper UV range down to 189 nm** (figure 13, region "SFG II") can be obtained when using two LPD 3000. A frequency doubled dye laser (BBO I-crystal) is set to a fixed wavelength in the UV while the other tunable dye laser works in the NIR. Both laser beams are mixed colinearly in an external additional BBO II-crystal. (see LAMBDA HIGHLIGHTS No. 8, Dec. 1987).*

Raman shifting

The RS 75 Raman-cell from LAMBDA PHYSIK can be used for shifting the wavelength in the IR to approximately

- *1100 nm (1st Stokes, efficiency >25%) or*
- *2000 nm (2nd Stokes).*

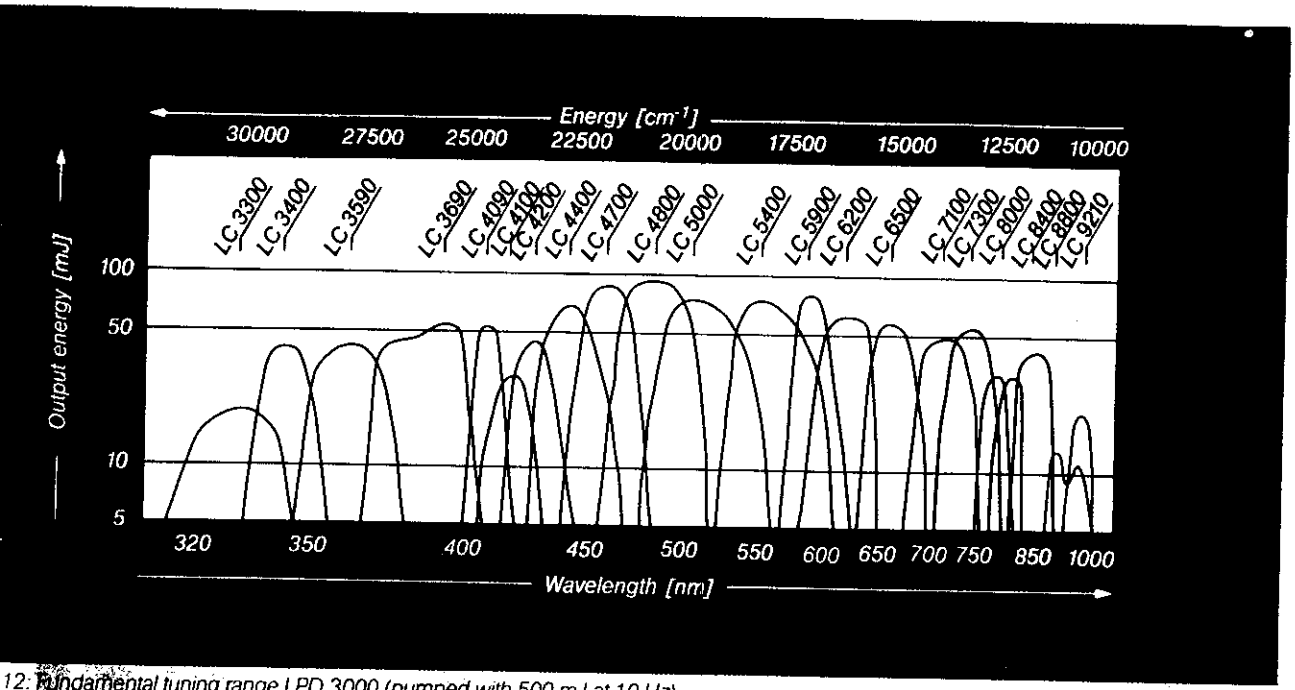

12: Fundamental tuning range LPD 3000 (pumped with 500 mJ at 10 Hz)

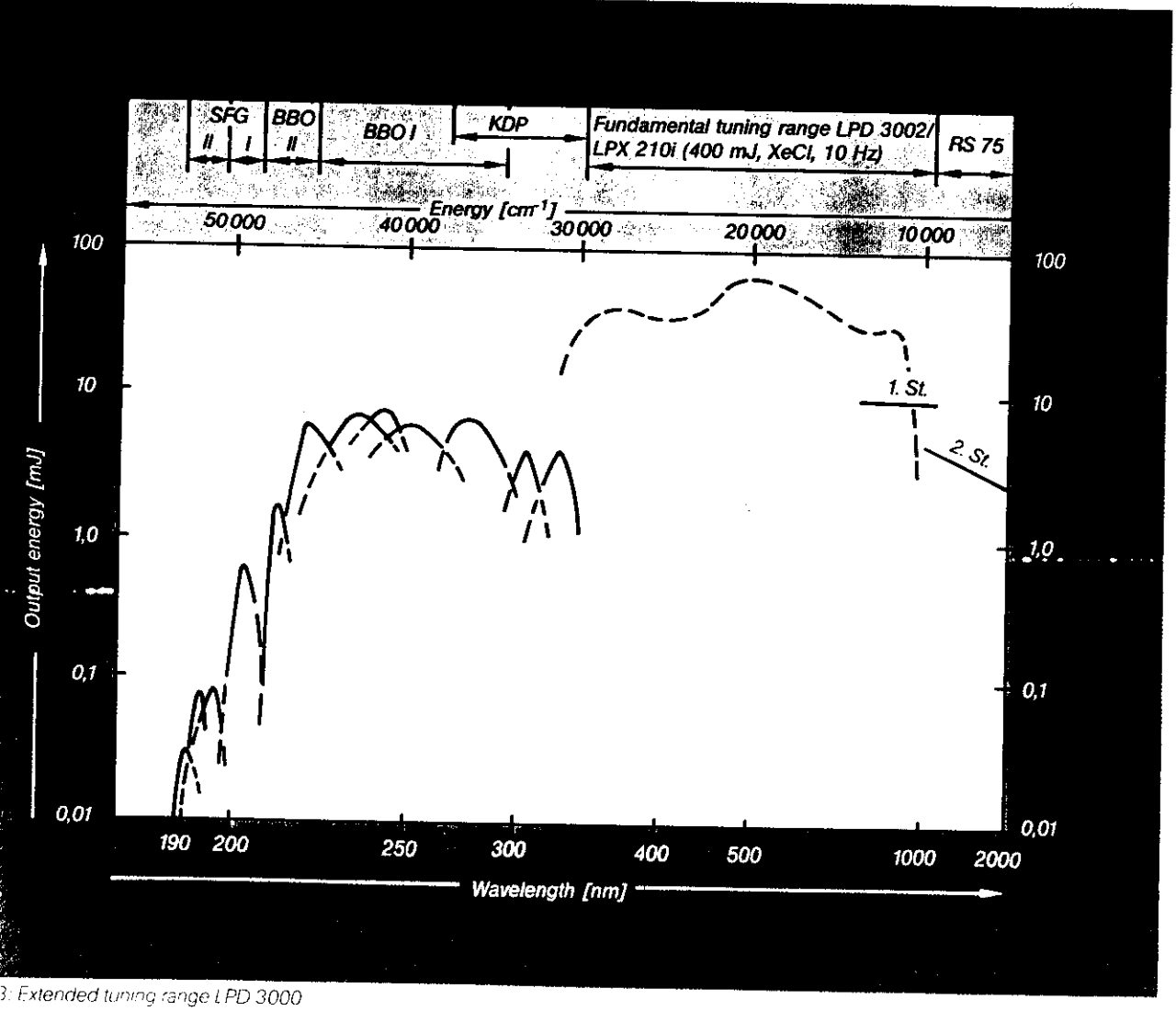

3: Extended tuning range LPD 3000

LPD 3000
Accessories

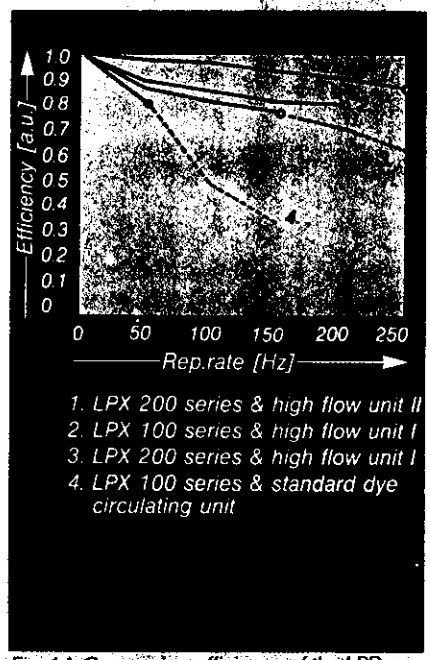

Fig. 14: Conversion efficiency of the LPD 3002 with different dye circulating units.

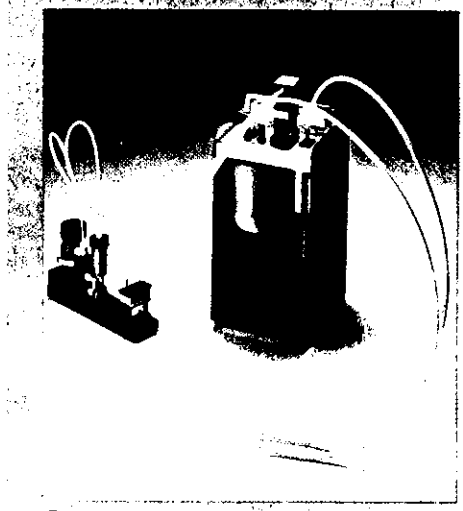

Fig. 15: Dye circulating unit (standard, up to 25 Hz)

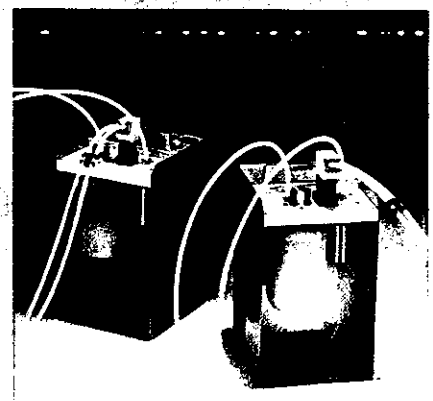

Fig. 16: High flow dye circulating unit I

Pump optics
Besides the standard XeCl pump optics, the following sets are available:
- *optics for pumping with a Nd: YAG laser (2nd or 3rd harmonic),*
- *optics for pumping with a Cu vapor laser (LPD 3001) and*
- *optics for pumping with a KrF or XeF excimer laser (LPD 3002).*

Dye circulating units
These units consist of one (LPD 3001) or two independent dye circulators. Each dye circulator consists of a flow cell, pump, filter housing, dye reservoir and tube connections. Depending on output energy and power of the pump laser, the following configurations are available:
- *dye circulator (max. 100 Hz) for oscillator/preamplifier of the LPD 3001,*
- *standard dye circulating unit (max. 25 Hz) for oscillator/ preamplifier and main amplifier of the LPD 3002,*
- *high flow dye circulating unit I for pulse repetition rates >25 Hz and average pump powers <40 W and*
- *high flow dye circulating unit II for high pulse repetition rates and average pump powers exceeding 40 W.*

SHG accessory
- *frequency doubling control,*
- *frequency doubling crystals KDP, BBO I, BBO II (in hermetically sealed cell),*
- *compensators (depending on crystal),*
- *beam separator (mounted Pellin Broca prisms) and*
- *polarizer (Glan Foucault air spaced polarizer).*

SFG accessory
Complete set of electronics, mechanics, optics and doubling crystals for the spectral range 207 - 189 nm.

Additional accessory
- *pyroelectric detector for pulsed dye lasers (max 25 Hz pulse rep.rate),*
- *Fabry Perot monitor etalon, three zoned broadband coating for use in the range 320 - 860 nm,*
- *set of aluminum coated broad-band filters (190 - 1100 nm, max. power density 1 MW/cm^2),*
- *set of neutral density filters, colored glass (400 - 1100 nm, max. power density 100 MW/ cm^2) and*
- *RS 75 Raman shifter.*

LPD 3000
Specifications

Dye laser model	LPD 3001	LPD 3002	LPD 3002E	
Wavelength range				
XeCl pumped	320-970	320-970	332-860	[nm]
SHG/SFG		189-335		[nm]
Conversion efficiency				
XeCl pumped				
PTP (343 nm)	6	10	9	[%]
Coumarin 102 (475 nm)	13	17	14	[%]
Rhodamine 6G (581 nm)	8	14	12	[%]
Styryl 9 (840 nm)	5	8	7	[%]
Nd: YAG pumped*				
Rhodamine 6G (570 nm)	–	35	30	[%]
Pyridin 1 (690 nm)	–	20	–	[%]
Peak power	up to 20 MW, depending on pump source and dye			
Average power	up to 15 W, depending on pump source and dye			
Bandwidth**	≦0.2	≦0.2	≦0.04	[cm^{-1}]
Tuning range		dye limited		[Å]
Wavelength reproducibility	±6.3	±6.3	±1.1	[mÅ]
Absolute wavelength accuracy		±0.5		[Å]
ASE-background	$<10^{-3}$	$<4x10^{-3}$	$<10^{-2}$	
Pulse width	similar to pump laser or slightly shorter			
Amplitude stability	similar to pump laser			
Divergence (typ.)	1.5	0.5	0.5	[mrad]
Beam diameter (typ.)	———	2.5	———	[mm]
Frequency stability	<0.05	<0.05	<0.01	[cm^{-1}/°C]

* 2nd harmonic (532 nm), E≦300 mJ, with excimer-like pulse shape
** time averaged value

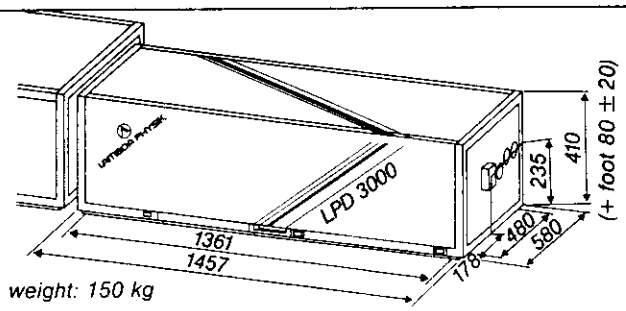

weight: 150 kg

82

VISIBLE AND INVISIBLE LASER RADIATION

AVOID EYE OR SKIN EXPOSURE TO DIRECT OR SCATTERED RADIATION

Max. average power
50% of pump source
Max. energy/pulse
50% of pump source
Pulse duration
Less than or equal to pump source
Principle radiation: 100 nm - 10 µm
CLASS IV LASER PRODUCT
This product complies with DHHS performance radiation standards.

Lambda Physik GmbH
Hans-Boeckler-Strasse 12
D-3400 Goettingen, W-Germany
Tel. (0551) 6938-0
FAX (0551) 68691

Lambda Physik Inc.
289 Great Road
Acton, Ma 01720; USA
Tel. (800) 262-1100
FAX (508) 263-4296

printed 02/90

Lambda Physik Marubun Inc.
8-1 Nihombashi, Odemmacho
Chuo-Ku;
Tokyo, 103; Japan
Tel. (03) 639-9871
FAX (03) 661-7433

● MODEN- KOPPLUNG

alias **MODEN - SYNCHRONISATION**

"mode - locking"

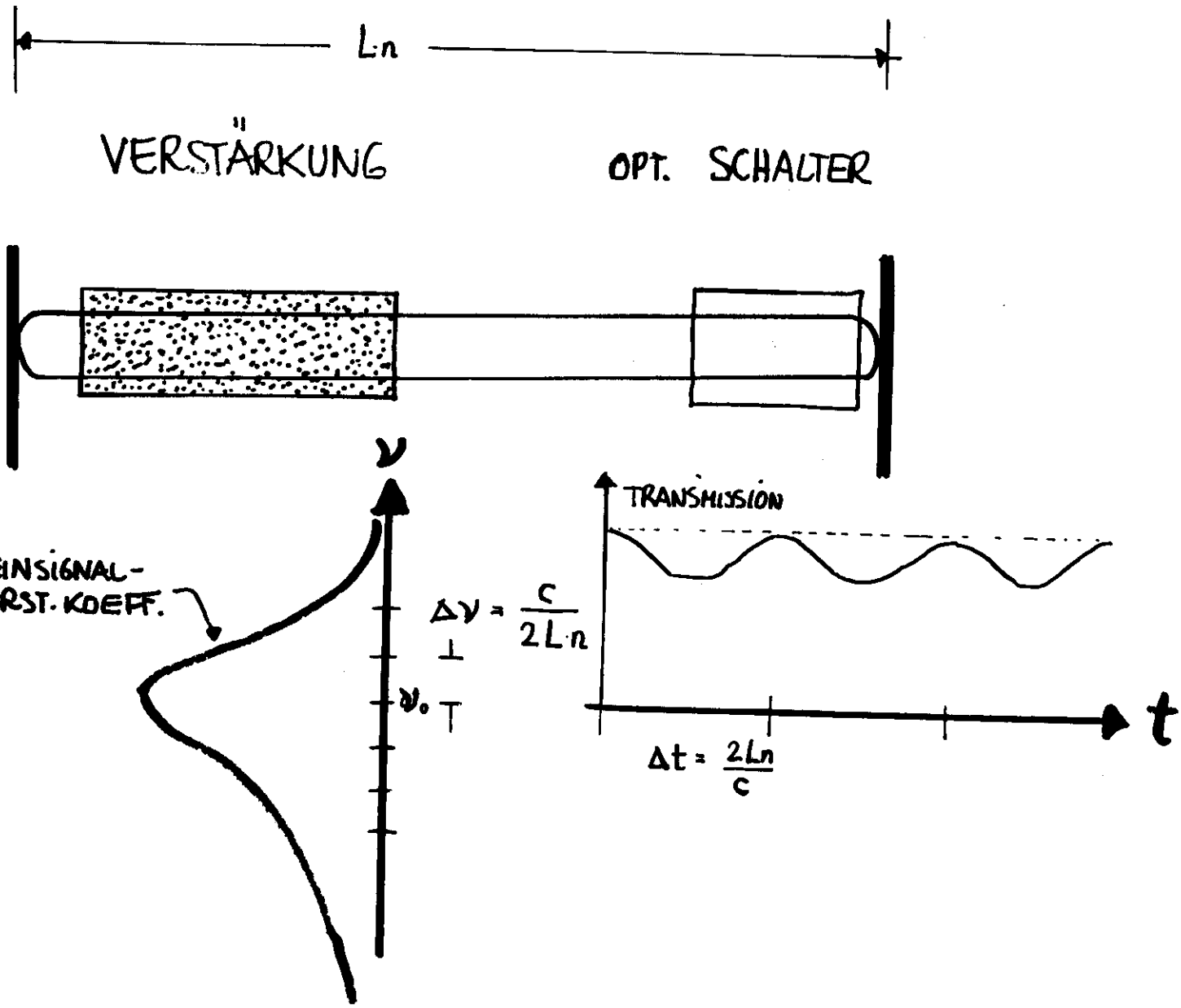

KEINE PHASEN KORREL.

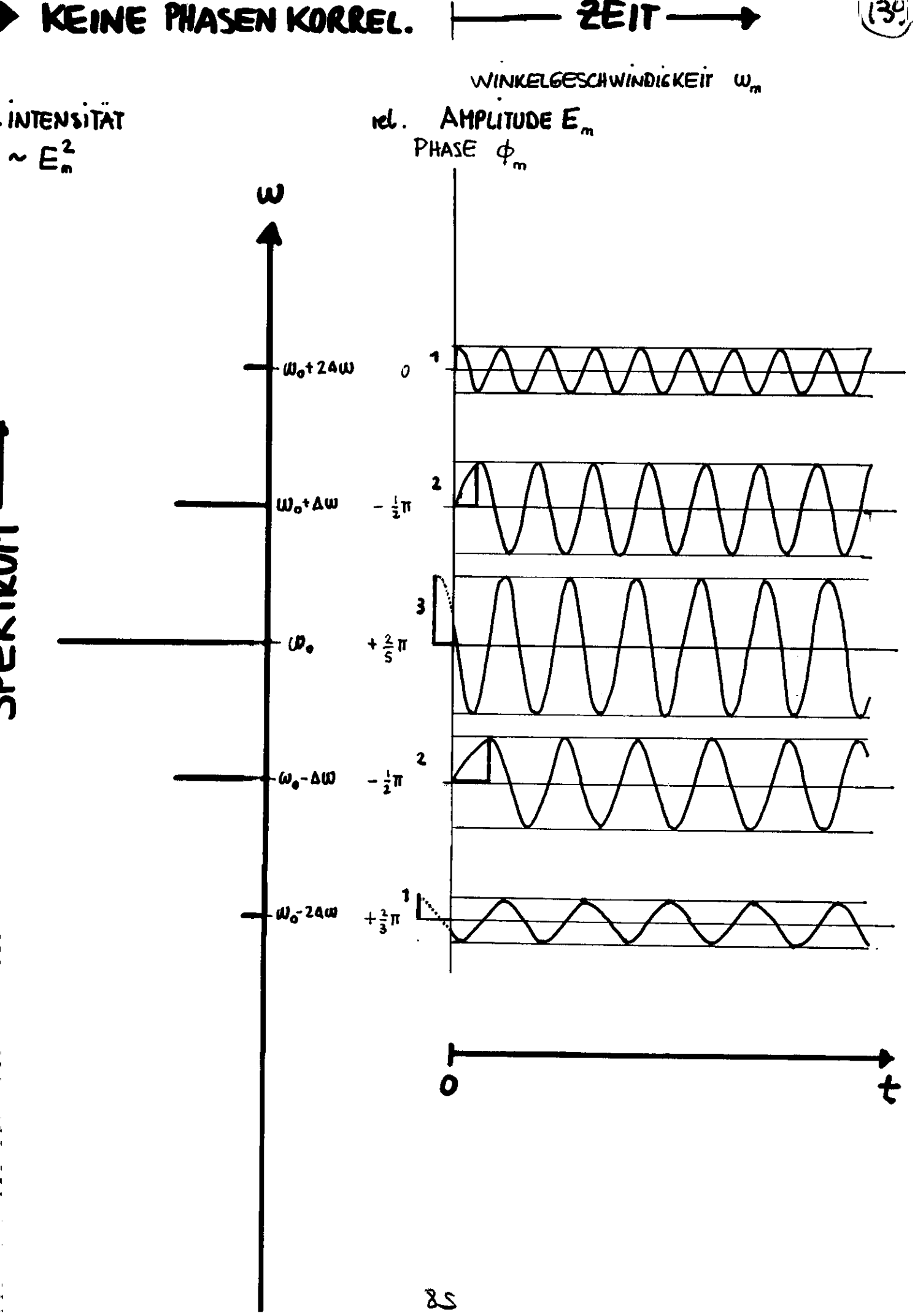

▶ PHASEN-KORRELATION

rel.
INTENSITÄT
$\sim E_m^2$

rel. AMPLITUDE E_m
PHASE ϕ_m

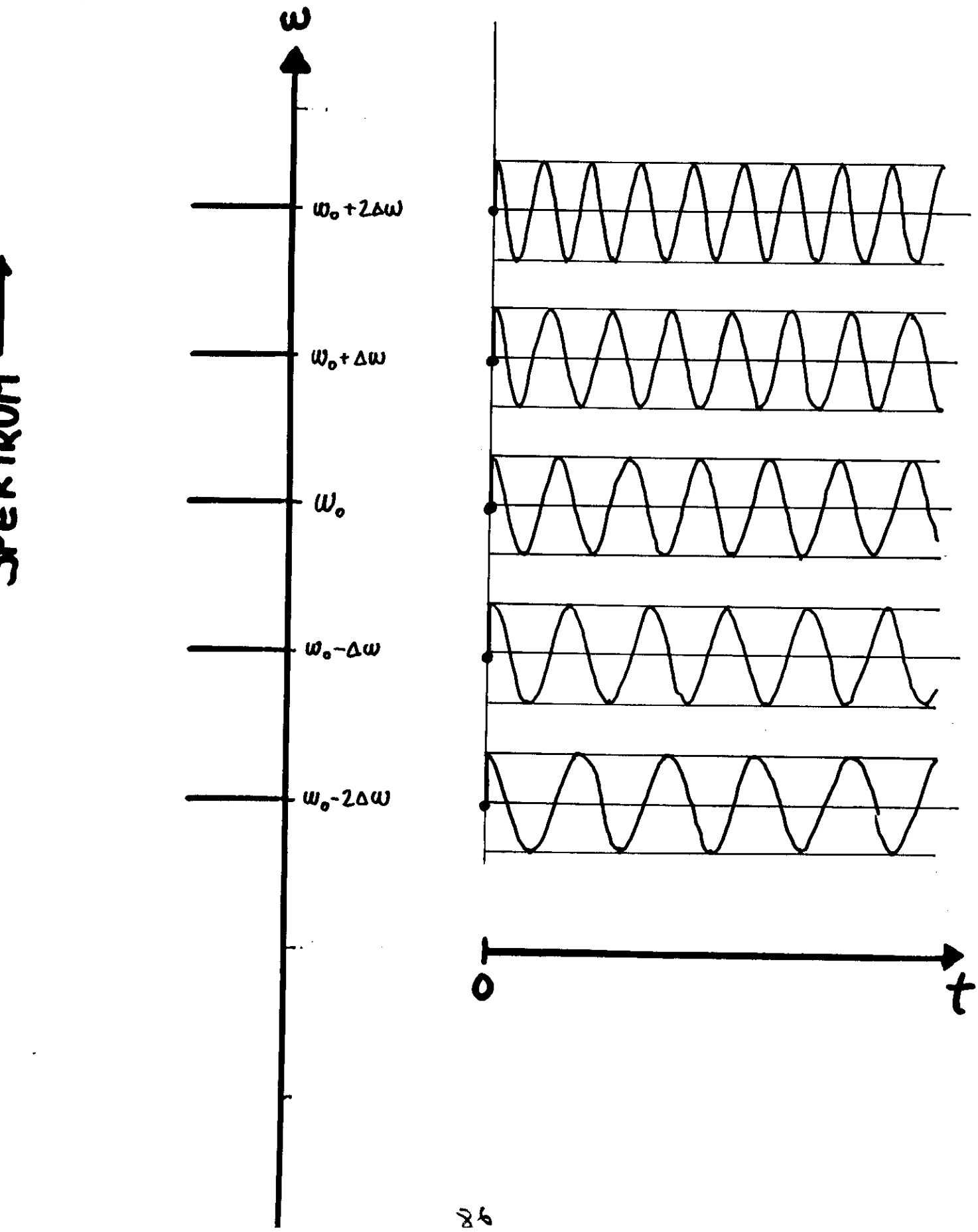

C2 SYNCHRONES PUMPEN

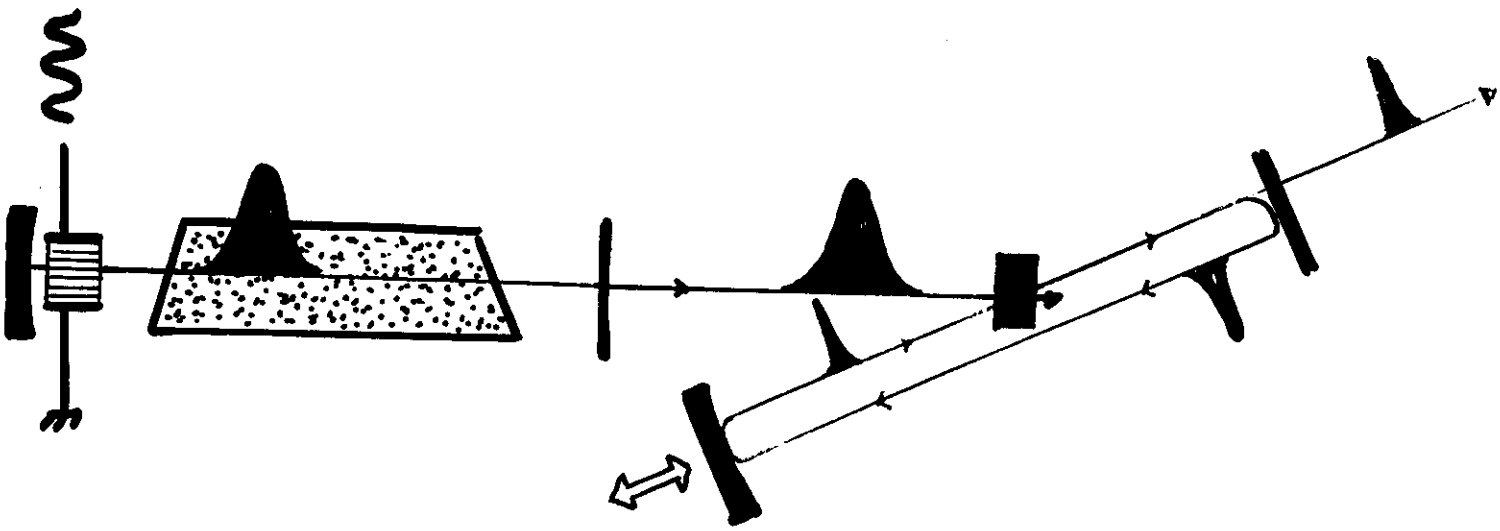

RUBIN ——— 694.3 nm ———→ IR - FARBSTOFFE

Nd: GLASS ——→ 2ν ——— 503.2 nm ———→ Rh6G

Ar^+ ——— 488 nm ———→ Rh6G usw .... ——→ 2ν ——→

CW-GEPUMPTE, PASSIV ML FARBSTOFF-LASER

(146)

ZUERST: E. IPPEN, C.V. SHANK, A. DIENES
APPL. PHYS. LETT. 21 (1972) 348

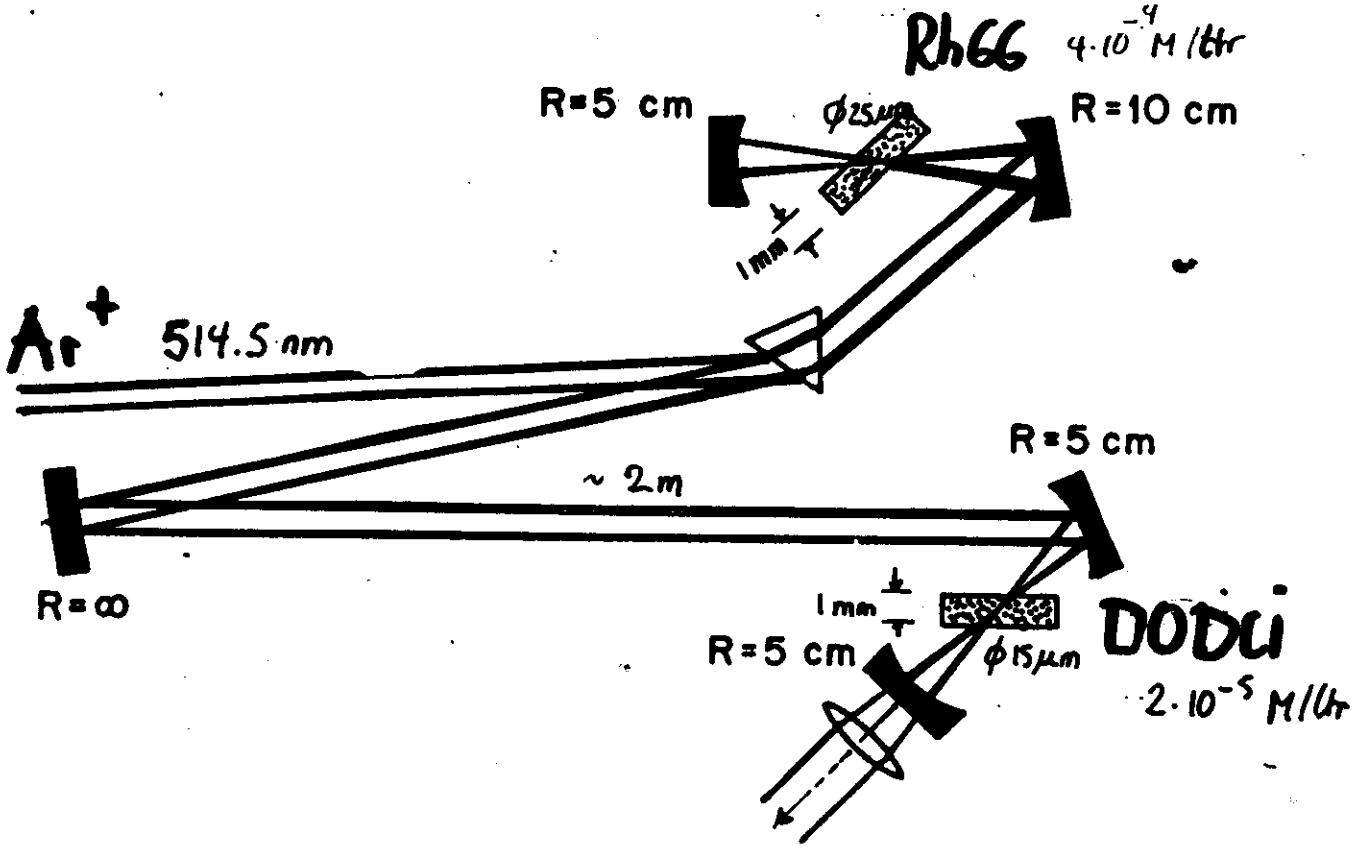

5-6.5 Å FWHM, ABSTIMMBAR 590-610 nm
1.1 ps
50-100 W PEAK POWER

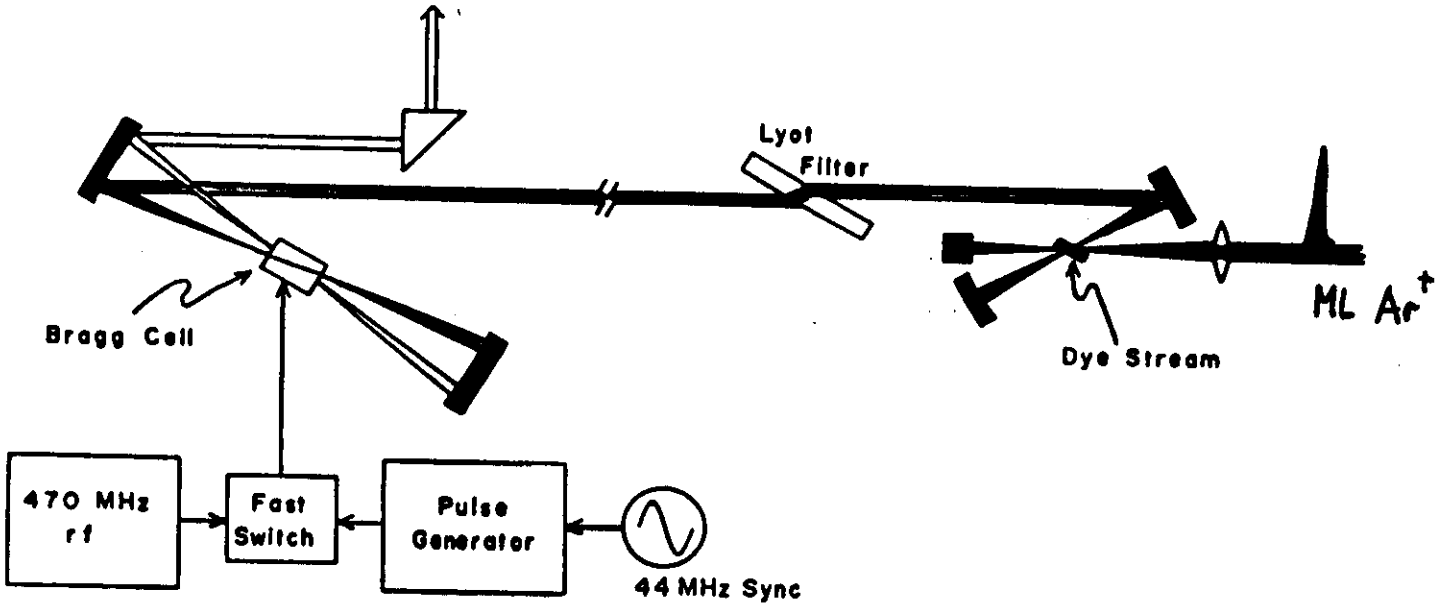

→ LÄNGEN-VERSTIMMUNG

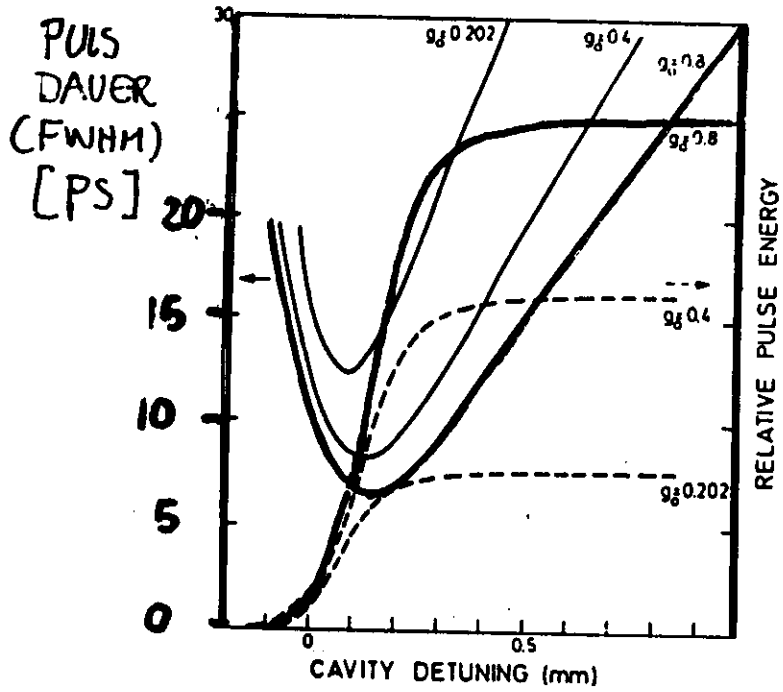

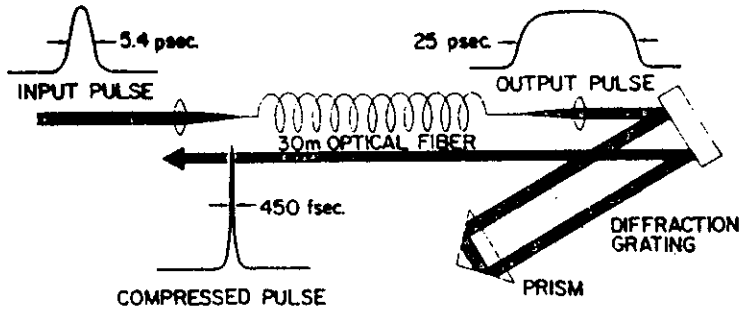

Figure 1 The optical pulse compressor.

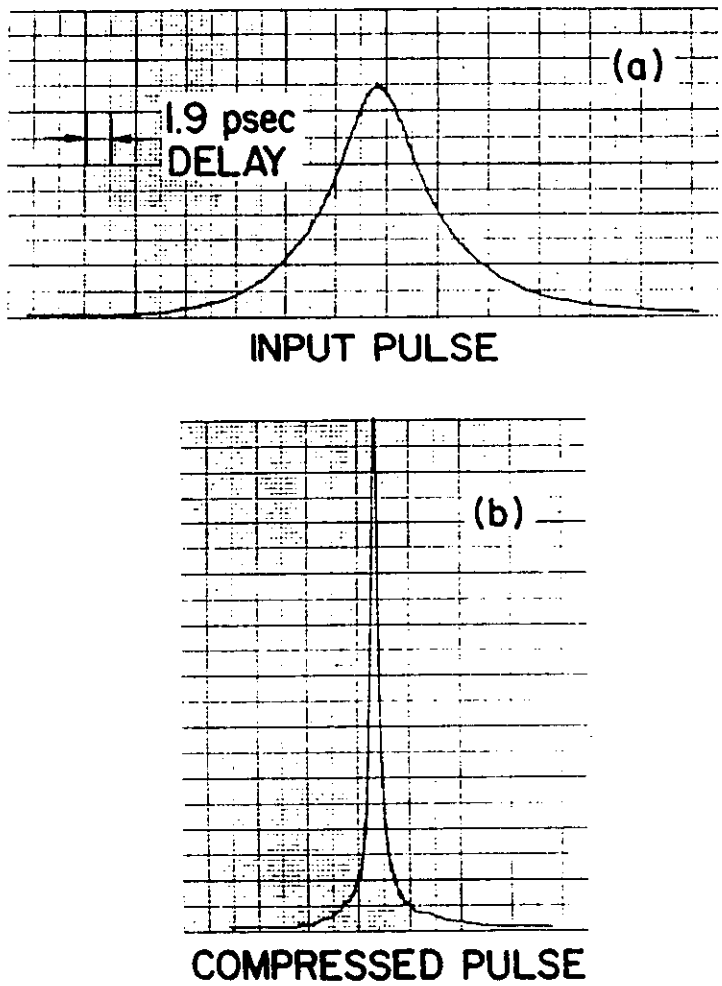

Figure 2 (a) Input pulse to the optical pulse compressor.

(b) Compressed pulse from the optical pulse compressor. For both pulses each large division corresponds to the indicated delay of 1.9psec.

B. Nikolaus, D. Grischkowsky
Appl. Phys. Lett. 1 (1983)

ULTRASHORT-PULSE (MODE-LOCKED) DYE LASERS

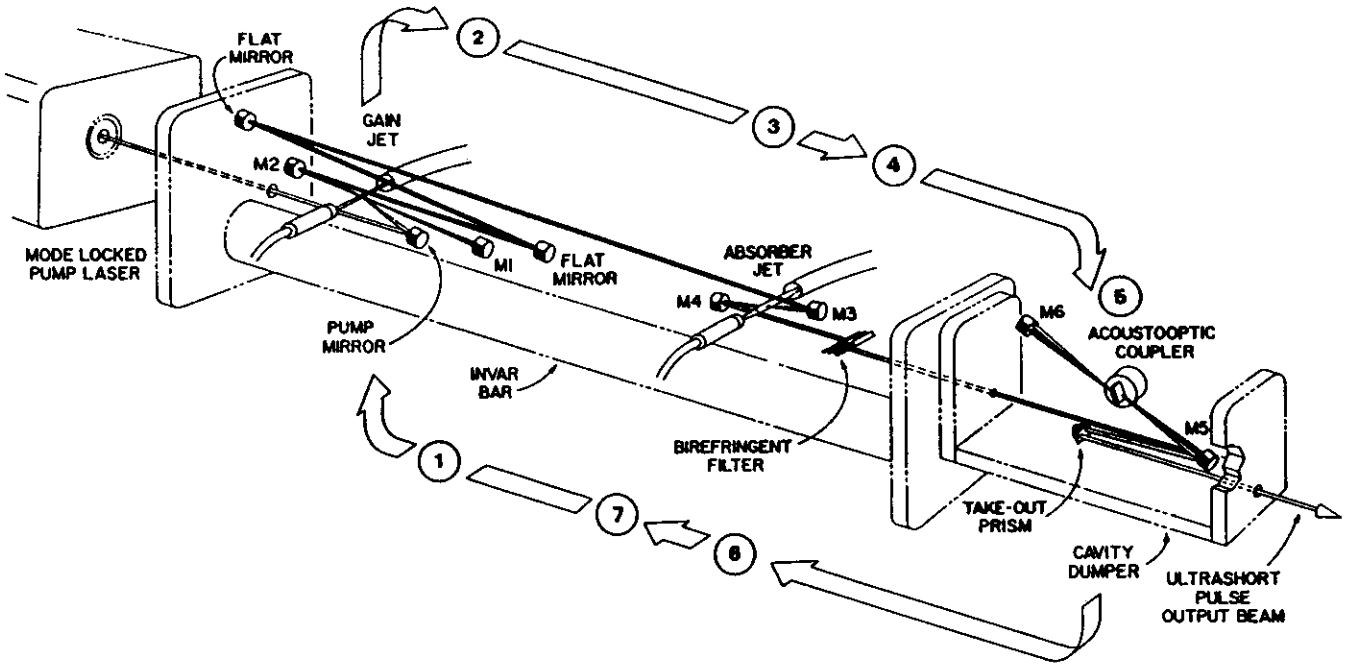

Ultrashort pulse dye laser of current design for "hybrid" mode-locking (employing both synchronous pumping and a saturable absorber). Shown in place of an output mirror is a cavity dumper assembly, which is driven in synchronism with the circulating pulse to couple out a reduced number of pulses, at higher energy per pulse. (Courtesy of Coherent, Inc., Palo Alto, Calif.)

AKTIV

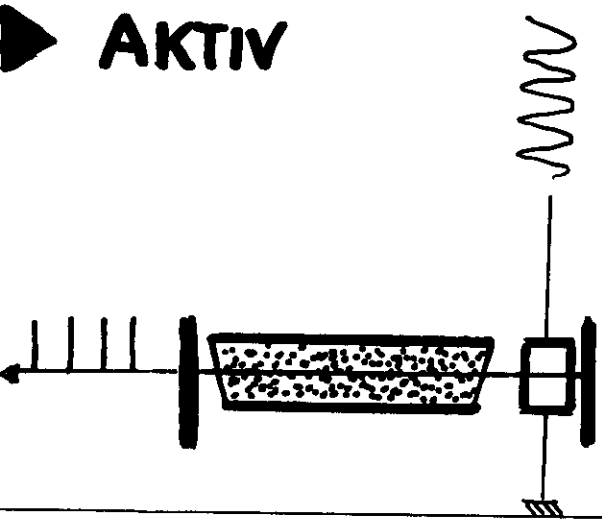

Ar^+

Nd:YAG

L.E. HARGROVE, R.L. FORK, M.A. POLLACK

APPL. PHYS. LETT. 5 (1964) 4

He-Ne-LASER MIT AKUSTO-OPTISCHEM MODULATOR

SYNCHRON GEPUMPT

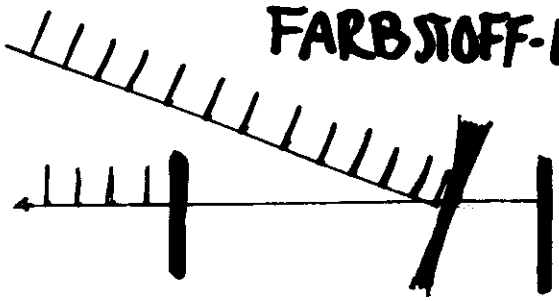

FARBSTOFF-L.

D.J. BRADLEY, A.J.F. DURRANI
PHYS. LETT. 27A (1968) 73
RUBIN PUMP-LASER:

W.H. GLENN ....
APPL. PHYS. LETT. 12 (1968) 54
Nd:YAG LASER, x 2.
R66, RhB

PASSIV

Nd:GLASS

FARBSTOFF-L

W. SCHMIDT, F.P. SCHÄFER
PHYS. LETT 26A (1968) 558
BLITZLAMPEN-GEPUMPTER RhGG-LASER, + DODCI

D.J. BRADLEY, F.O'NEILL
OPTO-ELECTRONICS 1 (1969) 69

"

ZOEKST:

R. FORK, B.I. GREENE. C.V. SHANK
APPL. PHYS. LETT. 38 (1981) 671

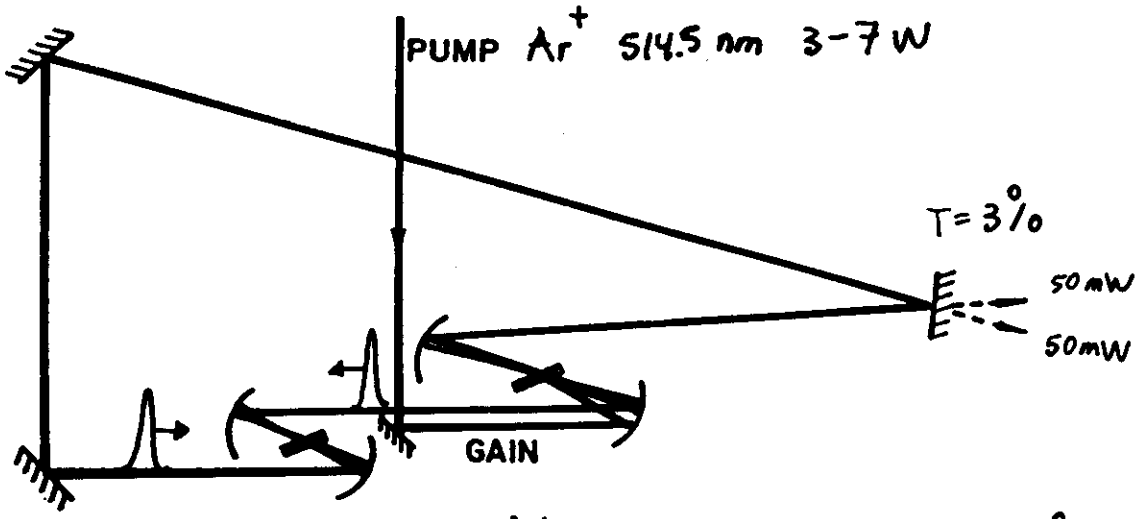

ABSORBER DODCI / ET.6CYCOC ; 10μm ; T_o = 80%

. **Colliding pulse mode-locked laser resonator configuration**

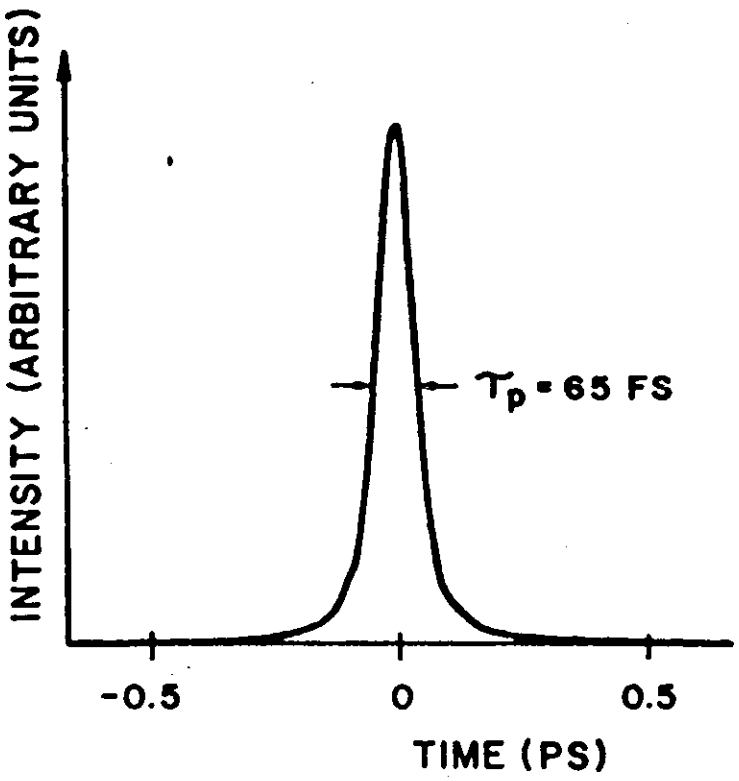

PRODUKT

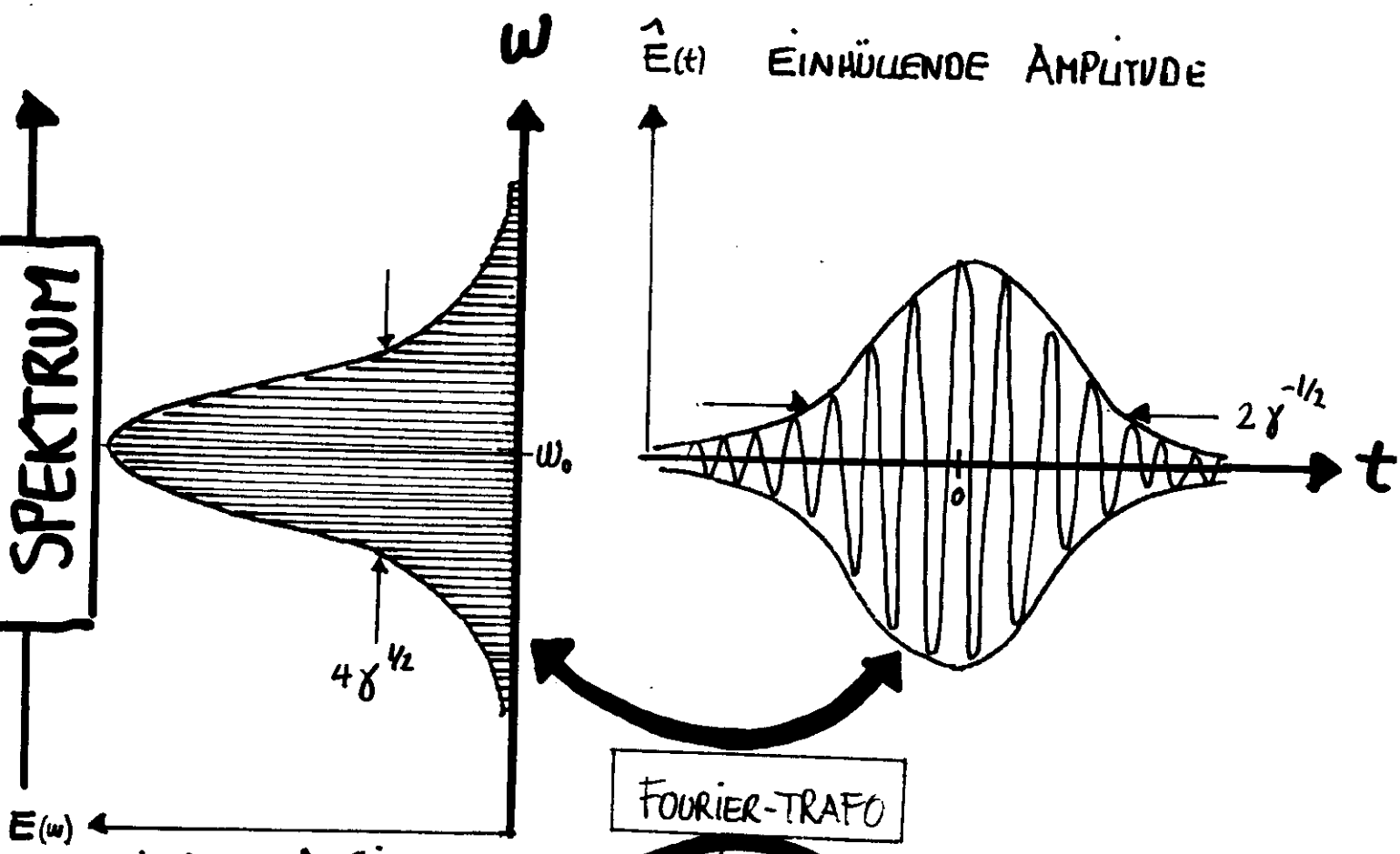

FOURIER-TRAFO

$$E(\omega) = E(\omega_0)\exp\left(-\frac{1}{4\gamma}(\Delta\omega)^2\right) \qquad \hat{E}(t) = \hat{E}_0\exp(-\gamma t^2)$$

$I(\omega) \sim E^2(\omega)$ $\qquad$ $I(t) \sim \hat{E}^2(t)$

$$\Delta\omega_{FWHM} = 2(\gamma 2\ln 2)^{1/2} \qquad \Delta t_{FWHM} = \left(\frac{2\ln 2}{\gamma}\right)^{1/2}$$

$$\Delta\nu_{FWHM} \times \Delta t_{FWHM} = \frac{2\ln 2}{\pi} = \underline{0.441}$$

THE γ VALUES AND THE p VALUES CALCULATED FOR SEVERAL WAVE PACKETS OF ENVELOPE $A(t)$

ZEIT- BANDBREITE-PRODUKT

$I(t)$	$A(t)$	$\frac{t_{FWHM}(\text{AUTOCORREL.})}{t_p}$	$p = \Delta\nu \times t_p$
GAUSS	$\exp[-\frac{1}{2}(t/t_0)^2]$	1.414	0.441
	$\exp[-\frac{1}{2}\lvert t/t_0\rvert]$	2.442	0.142
	$\exp[-\frac{1}{2}t/t_0]\theta(t)$	2.000	0.11
sech^2	$1/\cosh(t/t_0)$	1.53	0.315
	$\sin(t/t_0)/(t/t_0)$	1.29	0.892
	$\sin^2(t/t_0)/(t/t_0)^2$	1.41	0.366
	rect (t/t_0)	1.000	0.892
	$[1 + (t/t_0)^2]^{-1}$	1.66	0.142

* Rect (t/t_0)—Rectangular pulse of width $t_p = t_0$. $\theta(t)$—Unit step function.

A5 RELAXATIONS-OSZILLATIONEN

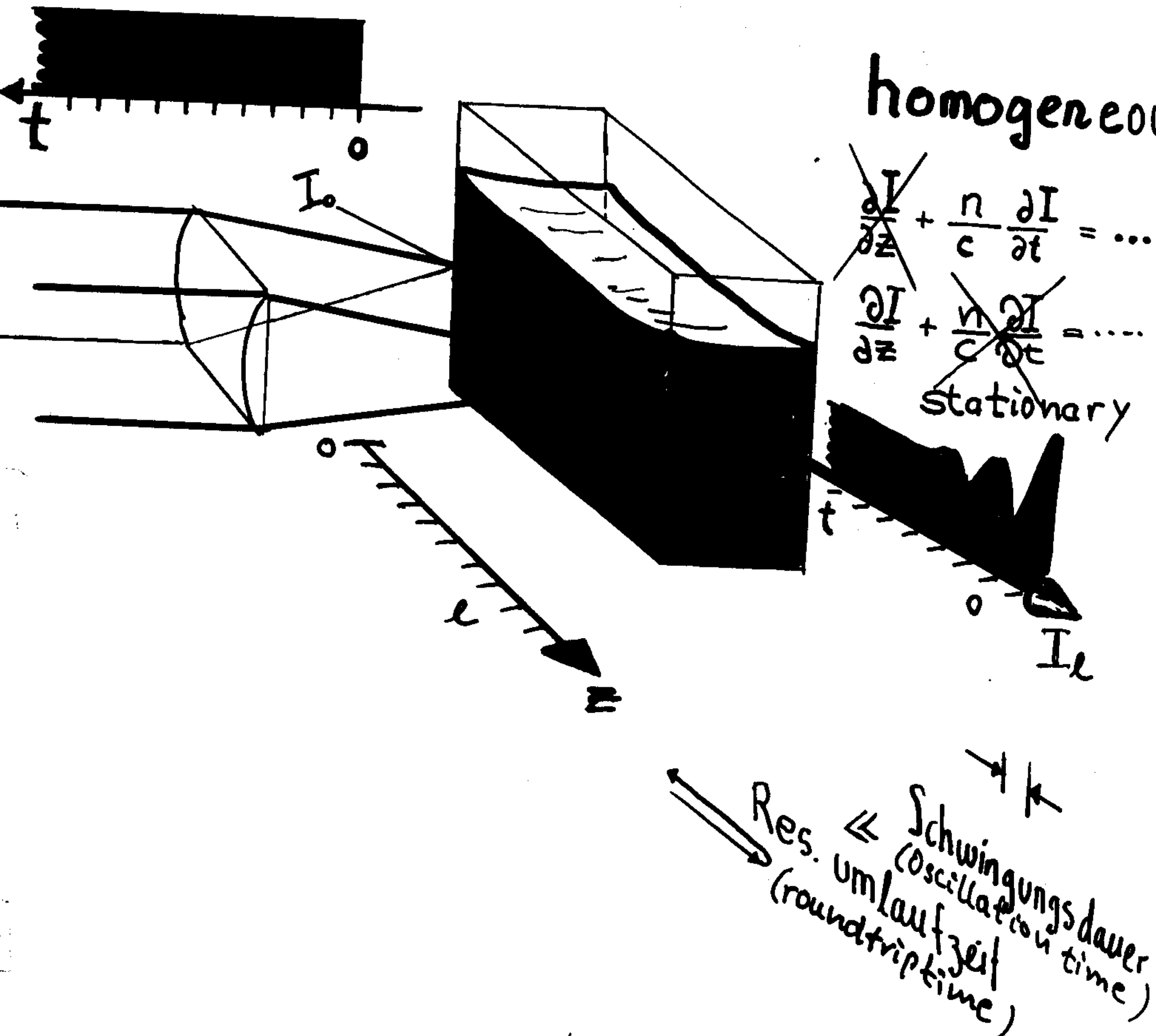

$$\frac{\partial I}{\partial z} + \frac{n}{c}\frac{\partial I}{\partial t} = \ldots$$

$$\frac{\partial I}{\partial z} + \frac{n}{c}\frac{\partial I}{\partial t} = \ldots$$

KINETIK

no Cavity

	Pumpe	stim. Em.	spont. Em. usw

$$\frac{\partial N_1}{\partial t} = +\sigma_p I_p N_0 - \sigma_e I N_1 - \frac{1}{\tau} N_1$$

$$\frac{n}{c}\frac{\partial I}{\partial t} = +\sigma_e I N_1$$

With cavity:

$\frac{n}{c} \cdot I = Q$ Photonendichte (Photon density) $\left[\frac{\text{Photonen}}{cm^3}\right]$

$$\frac{\partial Q}{\partial t} = +\underbrace{\sigma_e \frac{c}{n}}_{B\,[cm^3 s^{-1}]} Q N_1 - \frac{1}{\tau_c} Q$$

$$\frac{\partial N_1}{\partial t} = +\overbrace{W}^{R\,[s^{-1}cm^{-3}]} N_0 - \underbrace{\sigma_e \frac{c}{n}}_{B\,[cm^3 s^{-1}]} Q N_1 - \frac{1}{\tau} N_1$$

N_0 (10^{-3} molar)

$$\frac{0.132 \cdot 10^9 s^{-1} \cdot 6.02 \cdot 10^{17} cm^3}{0.8 \cdot 10^{26} s^{-1} cm^{-3}} \qquad \frac{1.7 \cdot 10^{-16} cm^2 \cdot 3 \cdot 10^{10} cm\, s^{-1} / 1.33}{3.84 \cdot 10^{-6} cm^3 s^{-1}}$$

(Resonator-Lebensdauer (resonator lifetime) $\tau_c = -\frac{t_c}{\ln \sqrt{R_1 \cdot R_2}}$)

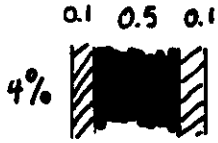

$t_c = 32\,ps$ $\quad \tau_c = \frac{32\,ps}{3.2} = \underline{10\,ps}$

● STATIONÄRE LÖSUNG

$$N_1^{\infty} = \frac{1}{B\tau_c}$$

$$Q^{\infty} = \frac{R - \frac{N_1^{\infty}}{\tau}}{BN_1^{\infty}}$$

$N_1^{\infty} = 0.26 \cdot 10^{17}\ cm^{-3}$

$Q^{\infty} = 0.75 \cdot 10^{15}\ cm^{-3}$

● OSZILLATION :

"RELAXATION OSZILLATION"
"SPIKING"

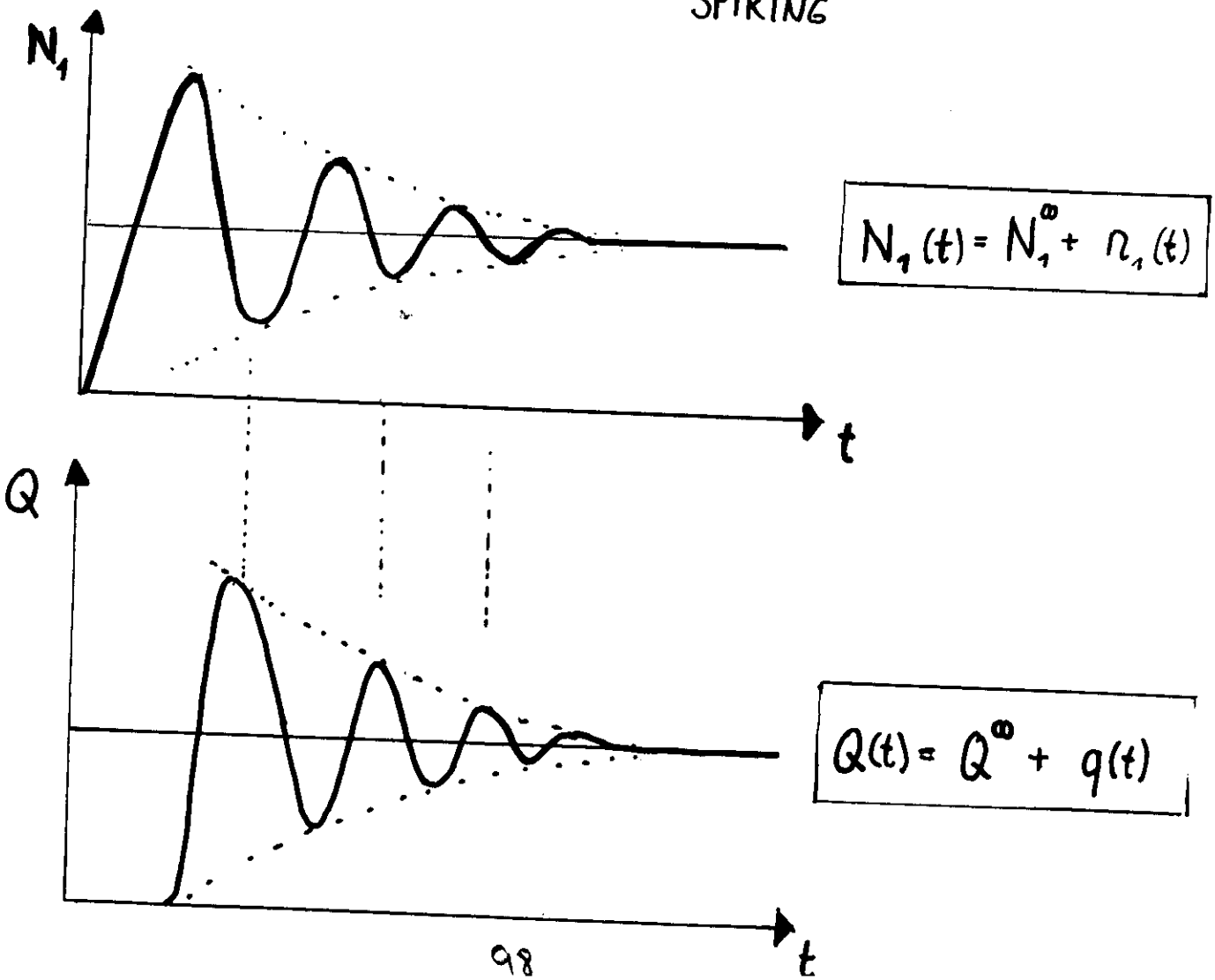

$N_1(t) = N_1^{\infty} + n_1(t)$

$Q(t) = Q^{\infty} + q(t)$

● ANALYTISCHE LÖSUNG FÜR DIE RELAXATIONS-OSZILLATION

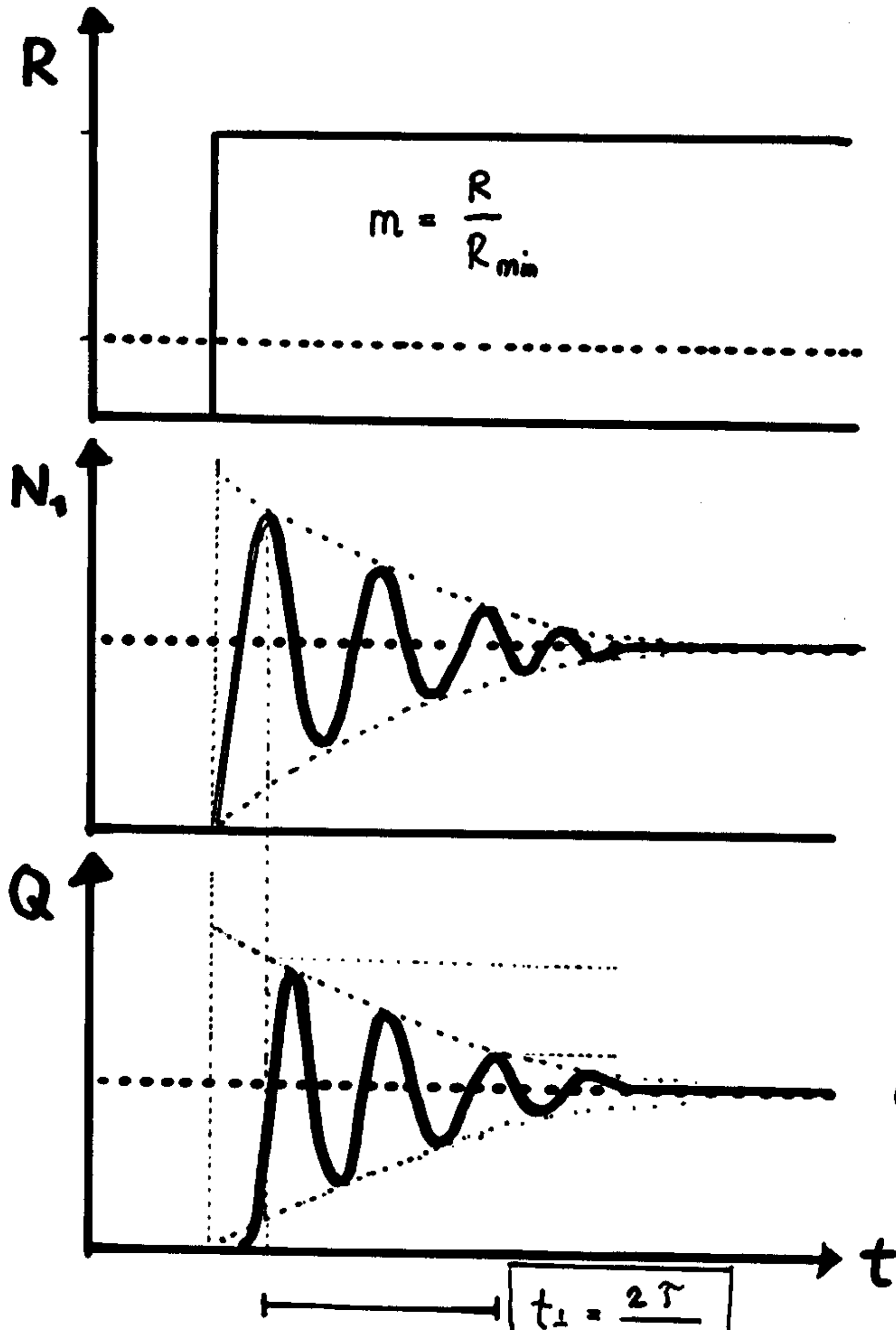

$$m = \frac{R}{R_{min}}$$

$$R_{min} = \frac{N_1^\infty}{\tau}$$

$$N_1^\infty = \frac{1}{B \cdot \tau_c} = \frac{1}{\sigma_e \frac{c}{n} \cdot \tau_c}$$

$$Q^\infty = \frac{R - \frac{N_1^\infty}{\tau}}{B \cdot N_1^\infty}$$

$$t_{\frac{1}{e}} = \frac{2\tau}{m}$$

$$\frac{T}{2} = 2\pi \sqrt{\tau_c \cdot \tau} \, \frac{1}{\sqrt{4(m-1) - m^2 \frac{\tau_c}{\tau}}}$$

RELAX.-OSZILLATIONEN FÜR m … $\frac{4(m-1)}{\dots} > \frac{\tau_c}{\dots}$

Numerical Solution

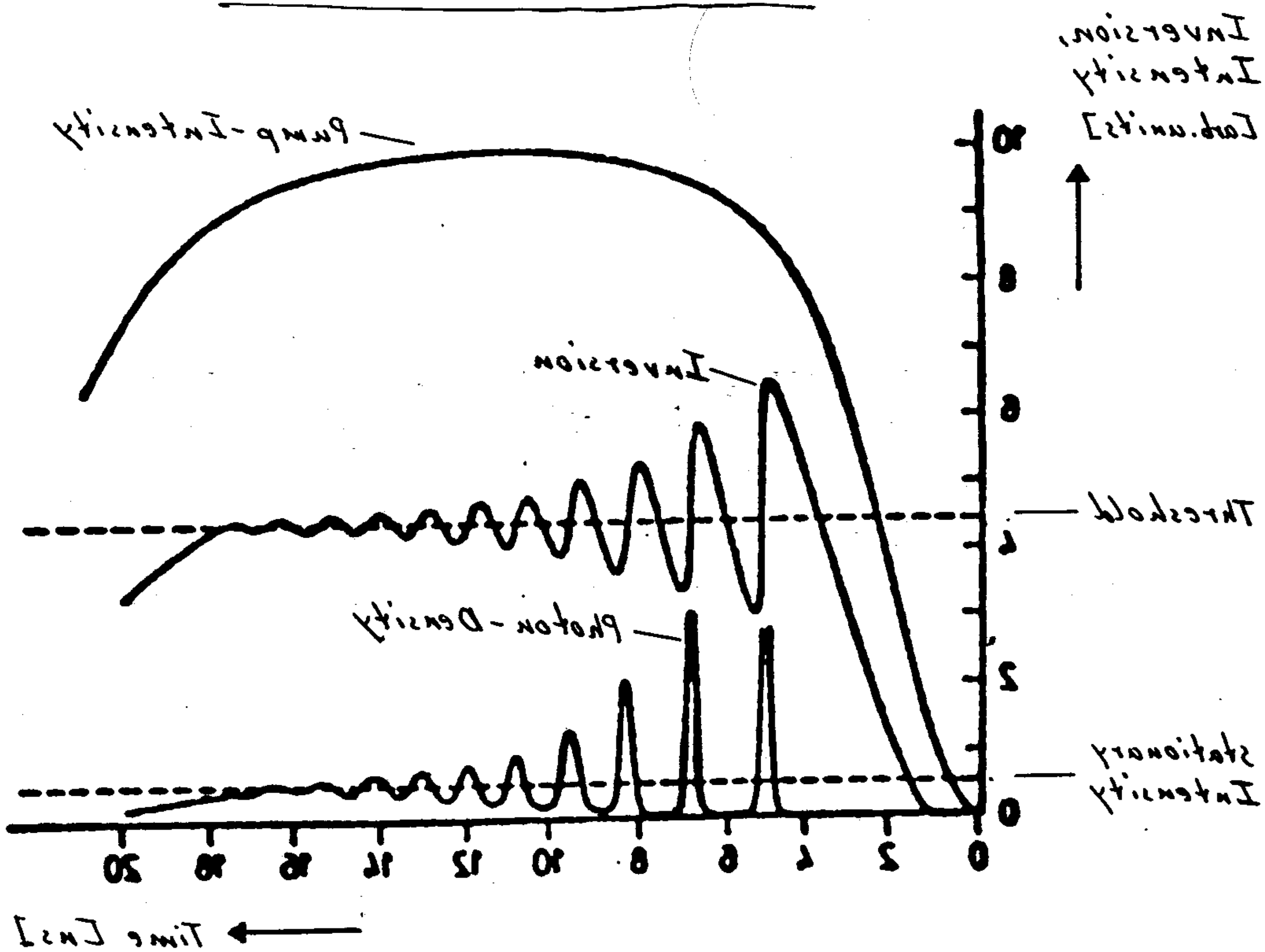

BERÜCKSICHTIGUNG DES PUMP-VERLAUFS

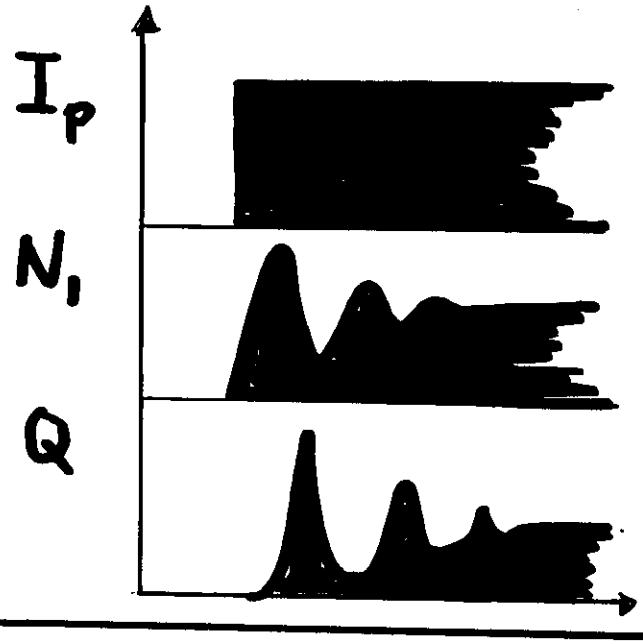

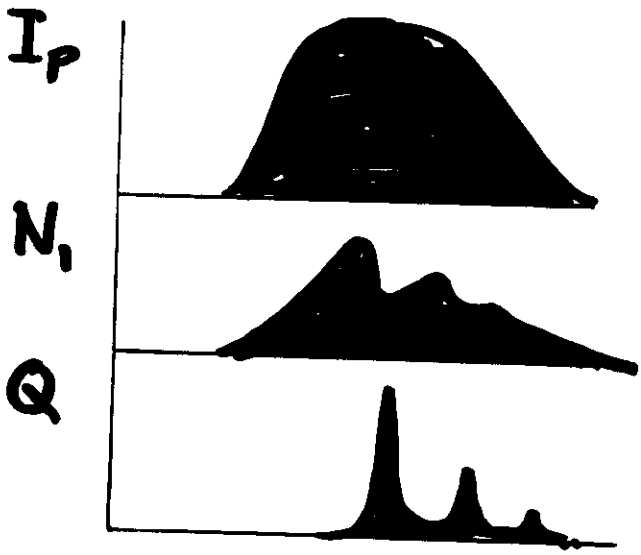

P. SIMON, J. KLEBNICZKI, G. SZABO, OPT. COMMUN. 56 (1986) 359

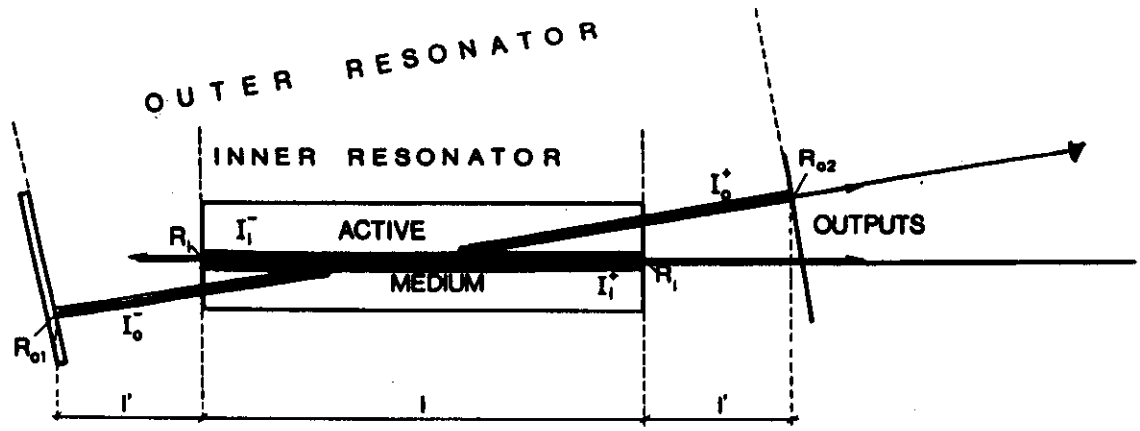

Quantity	Numerical value	Quantity	Numerical value
N	4.5×10^{18} cm^{-3}	S	0.3
σ_p	2.8×10^{-17} cm^2	Ω	2×10^{-5}
σ_e	2.4×10^{-16} cm^2	η	1.329
τ	3×10^{-9} s	η'	1.467
	1.1×10^{25} cm^{-2} s^{-1} (l = 2 mm)	R_i	0.024
W_o	4.4×10^{24} cm^{-2} s^{-1} (l = 5 mm)	R_{o1}	1
	2.2×10^{24} cm^{-2} s^{-1} (l = 10 mm)	R_{o2}	0.5

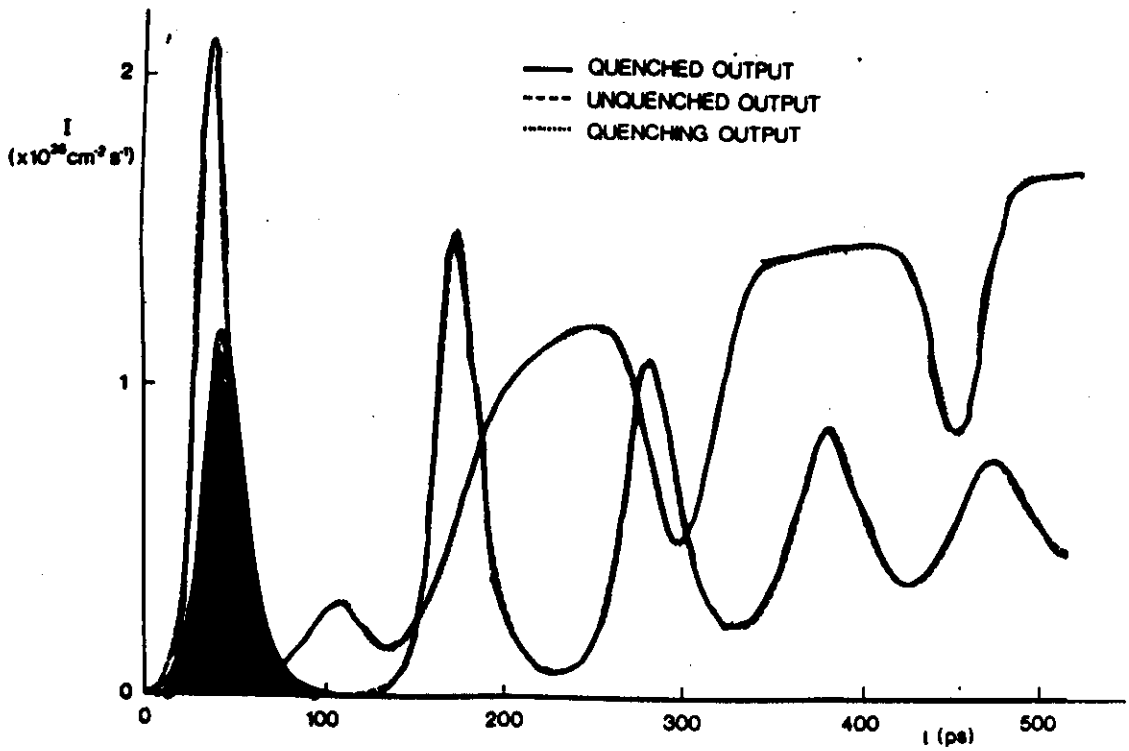

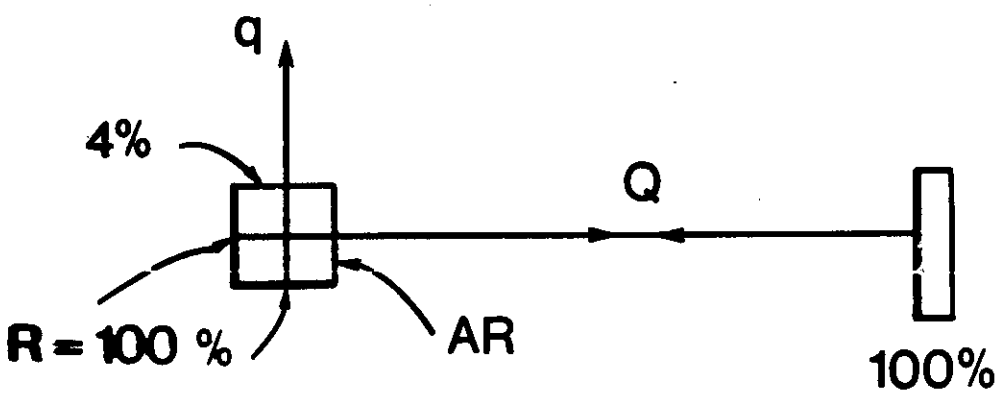
q
4%
Q
R = 100 %
AR
100%

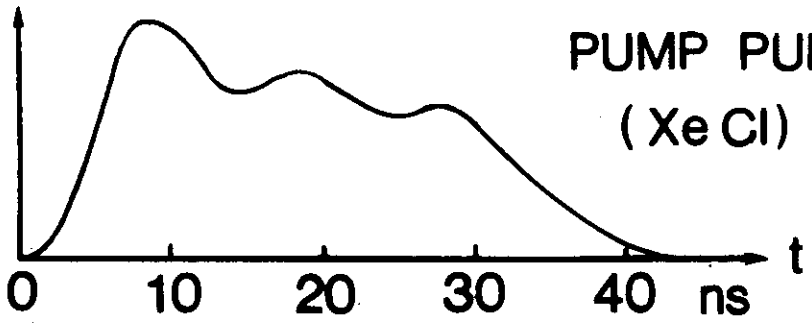
PUMP PULSE
(Xe Cl)
t
0
10
20
30
40
ns

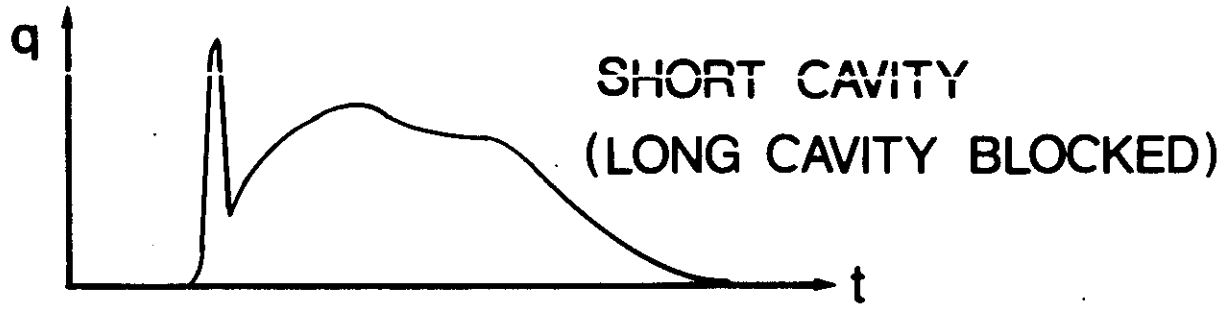
q
SHORT CAVITY
(LONG CAVITY BLOCKED)
t

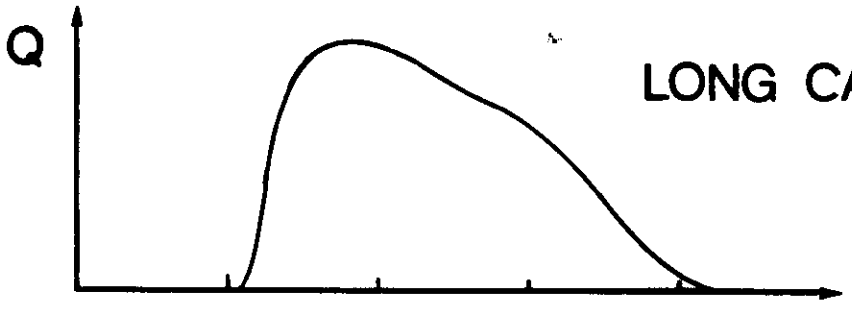
Q
LONG CAVITY
t

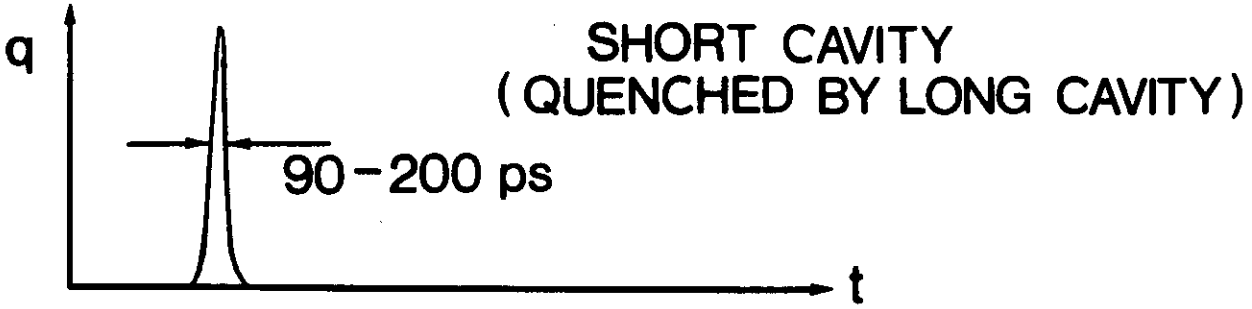
q
SHORT CAVITY
(QUENCHED BY LONG CAVITY)
90 - 200 ps
t

ABSTIMMUNG DER WELLENLÄNGE

A.J. COX, G.W. SCOTT, APPL. OPT. 18 (1979) 532

Bis - MSB

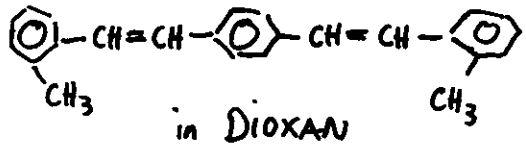

in DIOXAN

$d = 80\ \mu m$

$n = 1.4224$

FSR = 0.78 nm

Schematic cross section of the short-cavity dye laser.

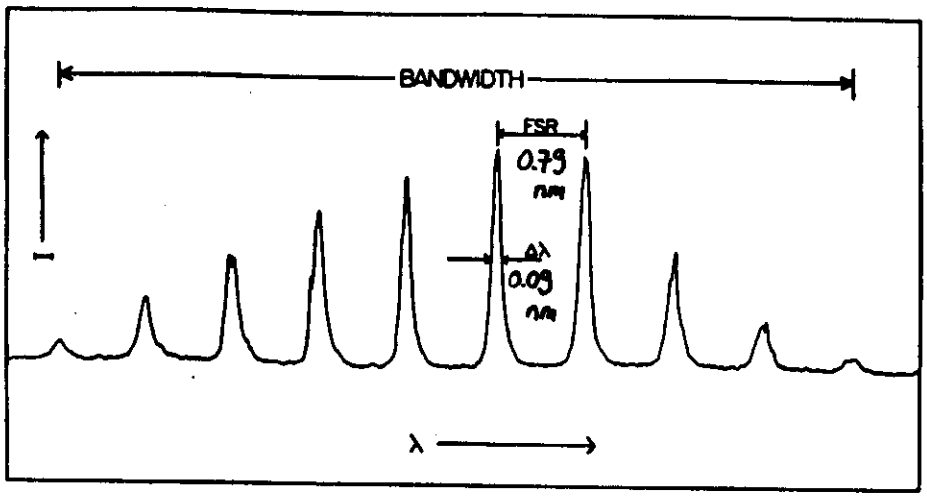

Spectral output of the short-cavity dye laser.

Sz. BOR, B. RACZ

APPL. OPTICS 24 (1985) 1910

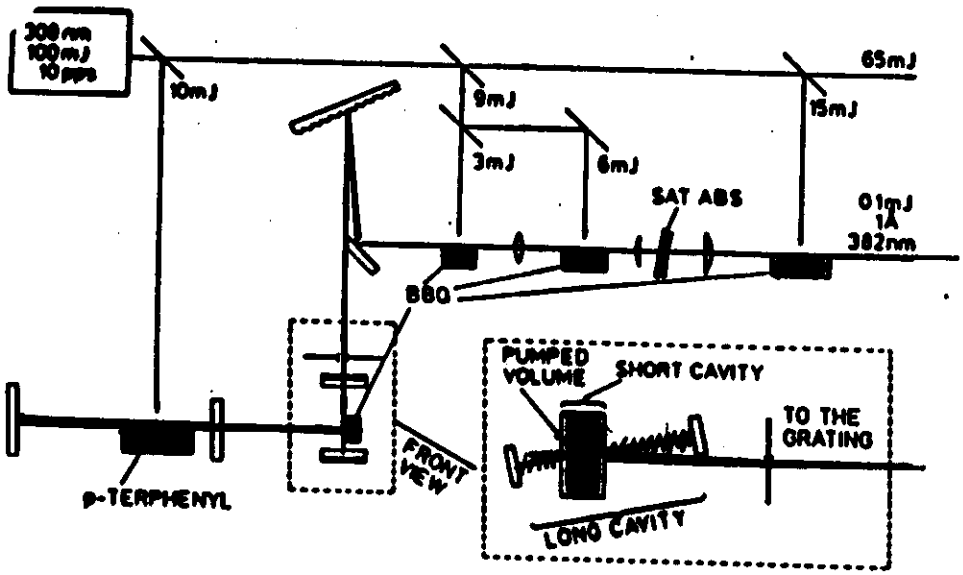

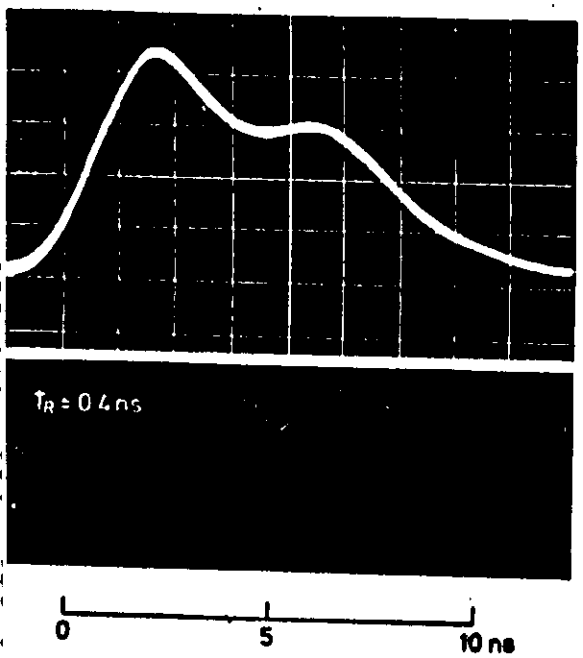

308 nm

340 nm

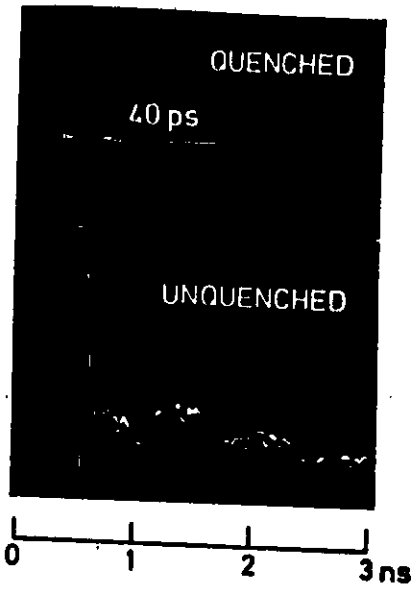

382 nm

Gesamt-Verkürzungsfaktor ≈300

Ultrashort UV-pulses

PSL 4000
Picosecond Excimer Laser

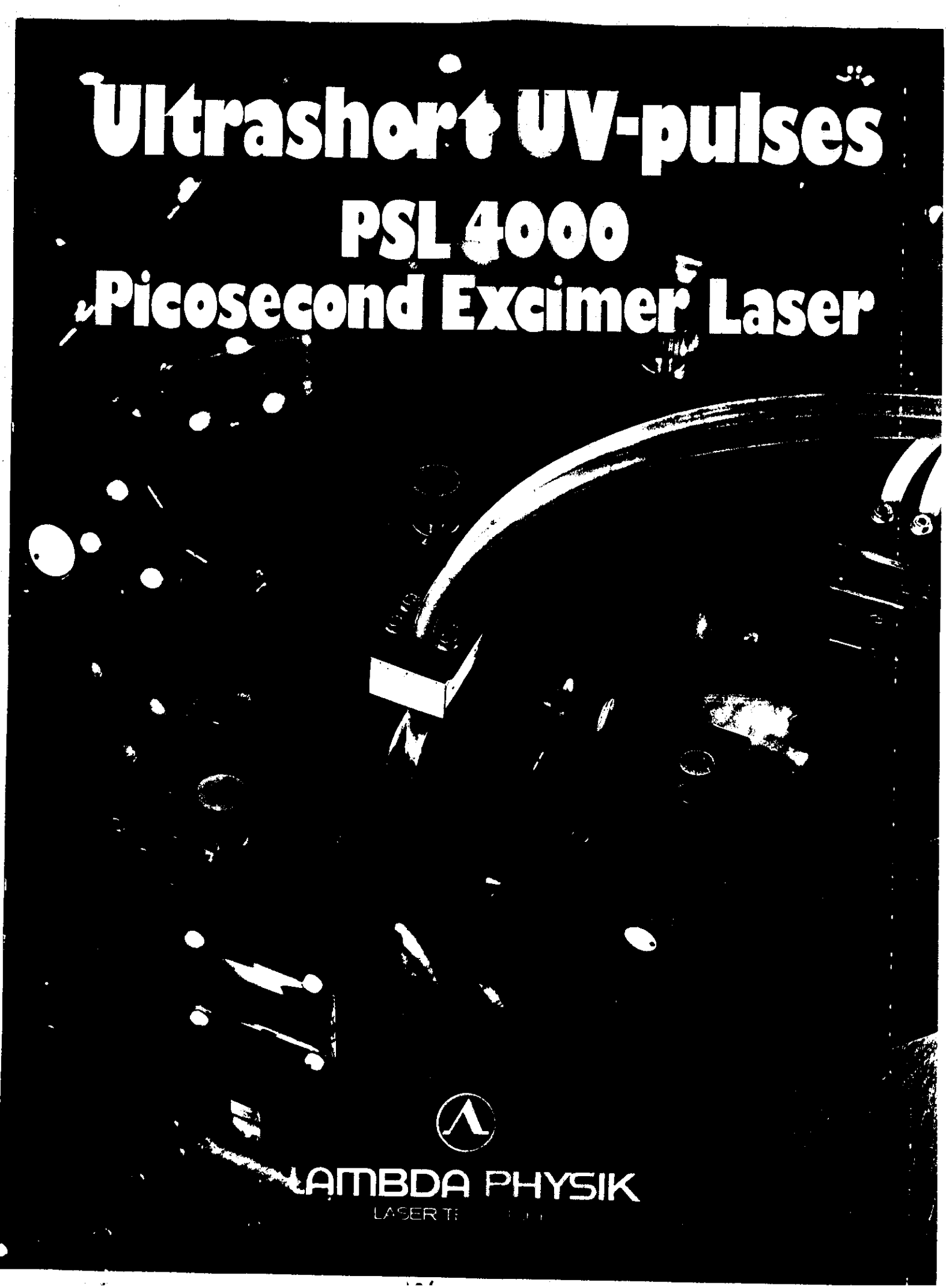

LAMBDA PHYSIK

LASER T[illegible]

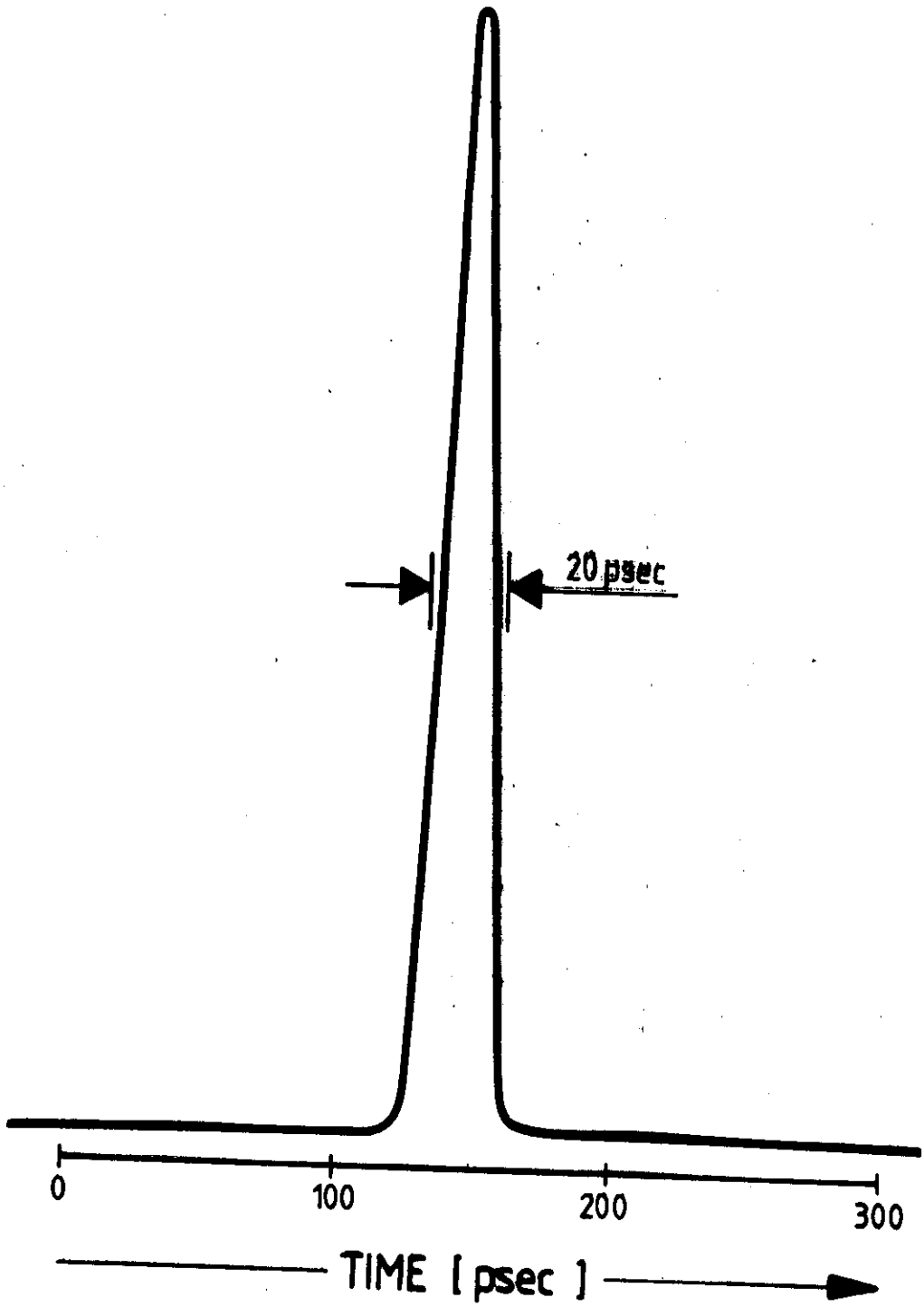
20 psec
0
100
200
300
TIME [psec]

Distributed Feedback Dye Laser

(DFDL)

a) How to Create a volume grating in a dye solution

b) Consequences on temporal behaviour

c) recent achievements of this technique

ERZEUGUNG DER MODULATION

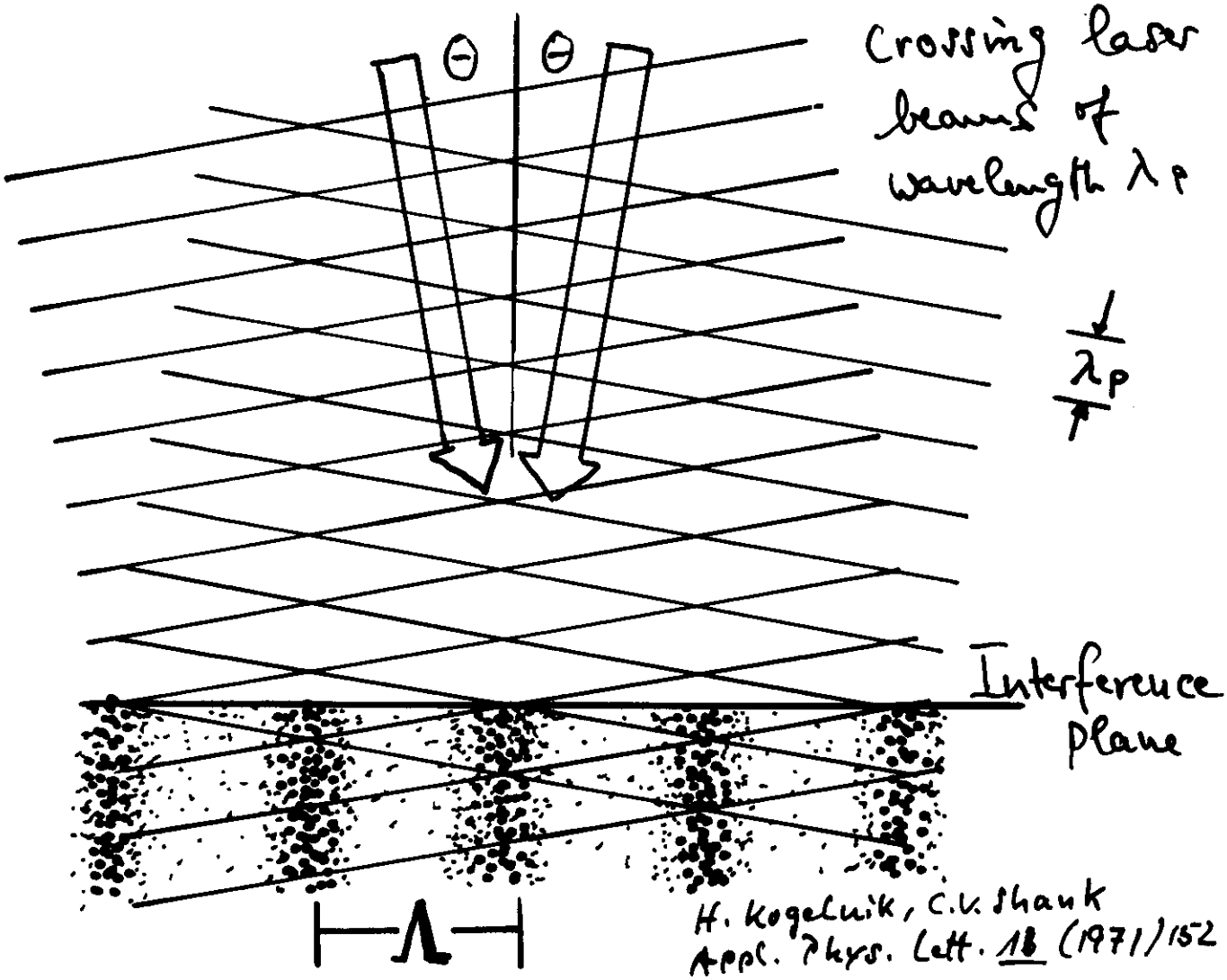

H. Kogelnik, C.V. Shank
Appl. Phys. Lett. 18 (1971) 152

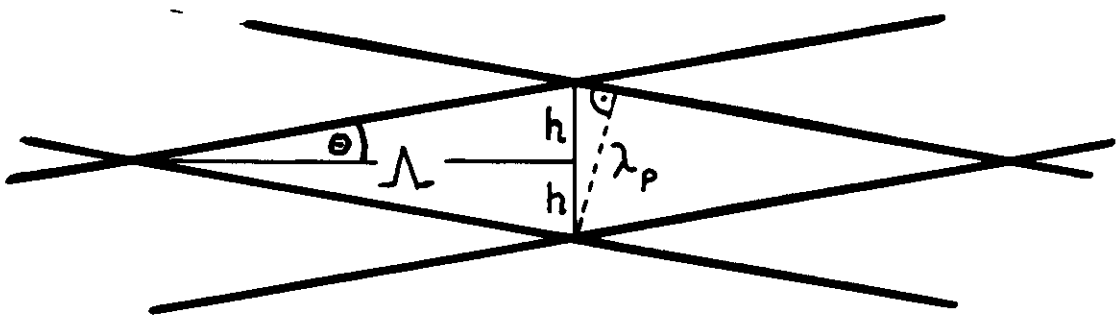

$$2 \cdot h \cdot \cos\theta = \lambda_p$$

$$\frac{h}{\Lambda} = \tan\theta \qquad h = \lambda_p / 2 \cdot \cos\theta$$

$$\boxed{\Lambda = \frac{h}{\tan\theta} = \frac{\lambda_p}{2 \cdot \cos\theta \cdot \tan\theta}} \boxed{= \frac{\lambda_p}{2 \cdot \sin\theta}}$$

MODULATION DER DICKE VON OPTISCHEN WELLENLEITERN

DFB - Semiconductor Laser

modulation of thickness in optical waveguides

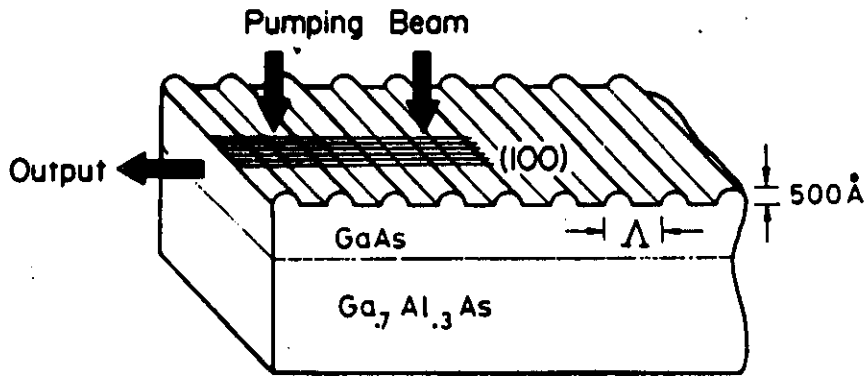

Schematic structure of a GaAs DFB laser.

WACHSTUM DER FELD-AMPLITUDEN DURCH VERSTÄRKUNG UND RÜCK-KOPPLUNG

Growth of field amplitudes with periodic gain modulation

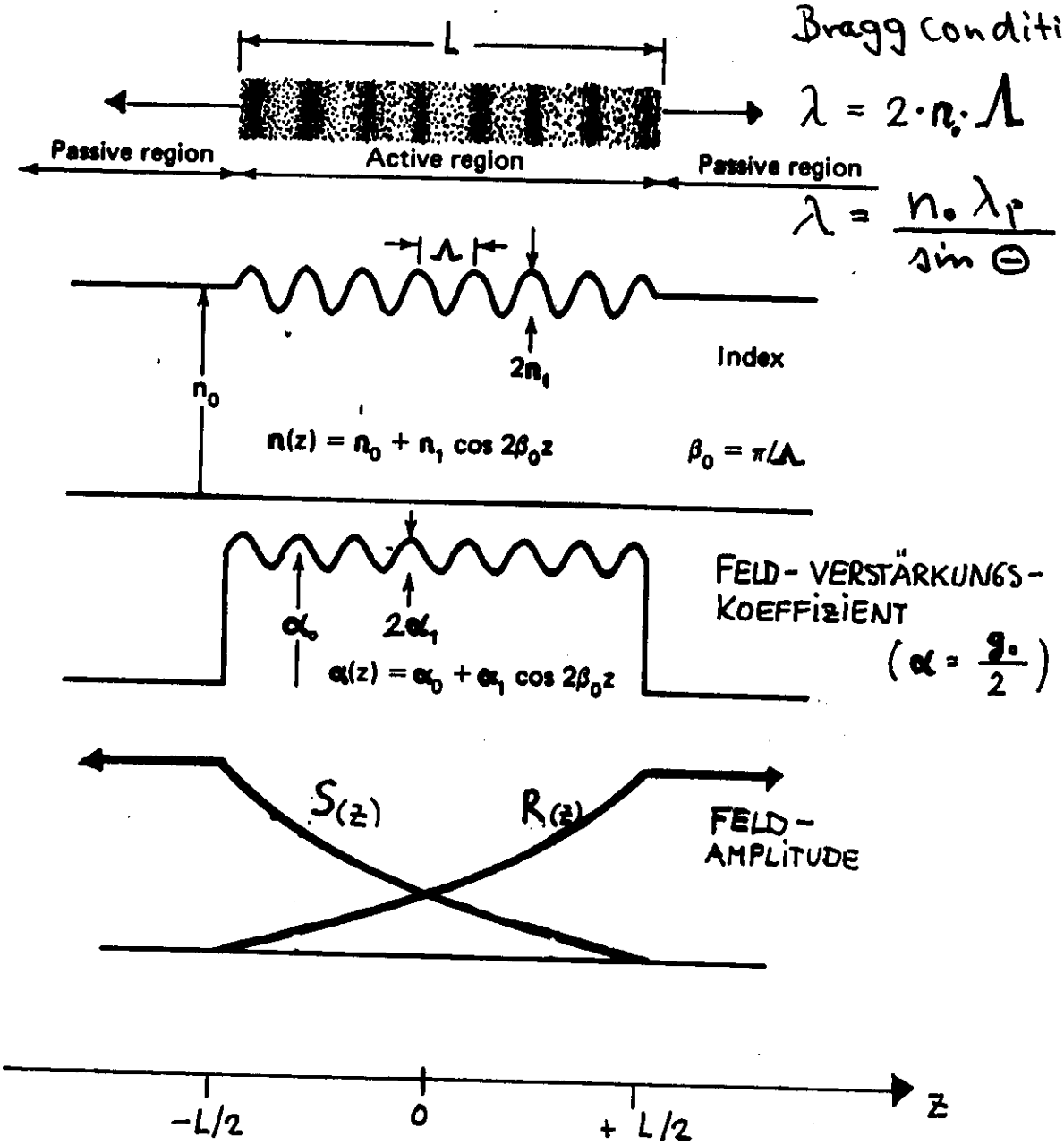

ZEIT-VERHALTEN DES FARBSTOFF-LASERS MIT VERTEILTER RÜCK-KOPPLUNG

▶ KINETIK (Kinetics of DFDL)

	opt. Pumpen	Stim. Emission	spont.
Molekule (molecules)	$\frac{\partial N_1}{\partial t} = I_p \sigma_p N_0 - \frac{\sigma_e c}{n} Q N_1 - \frac{N_1}{\tau}$		
Photonen (photons)	$\frac{\partial Q}{\partial t} =$	$+ \frac{\sigma_e c}{n} Q N_1 -$	$\frac{Q}{\tau_c}$

RESONATOR-LEBENSDAUER

resonator decay time:

$$\tau_c = \frac{n \cdot L^3}{8 \pi^2 c} \left(\sigma_e N_1\right)^2$$

S. R. CHINN, OPT. COMMUN. 19 (1976) 208

NUMERISCHE LÖSUNG

Zs. Bor, IEEE J. QE-16 (1980) 517

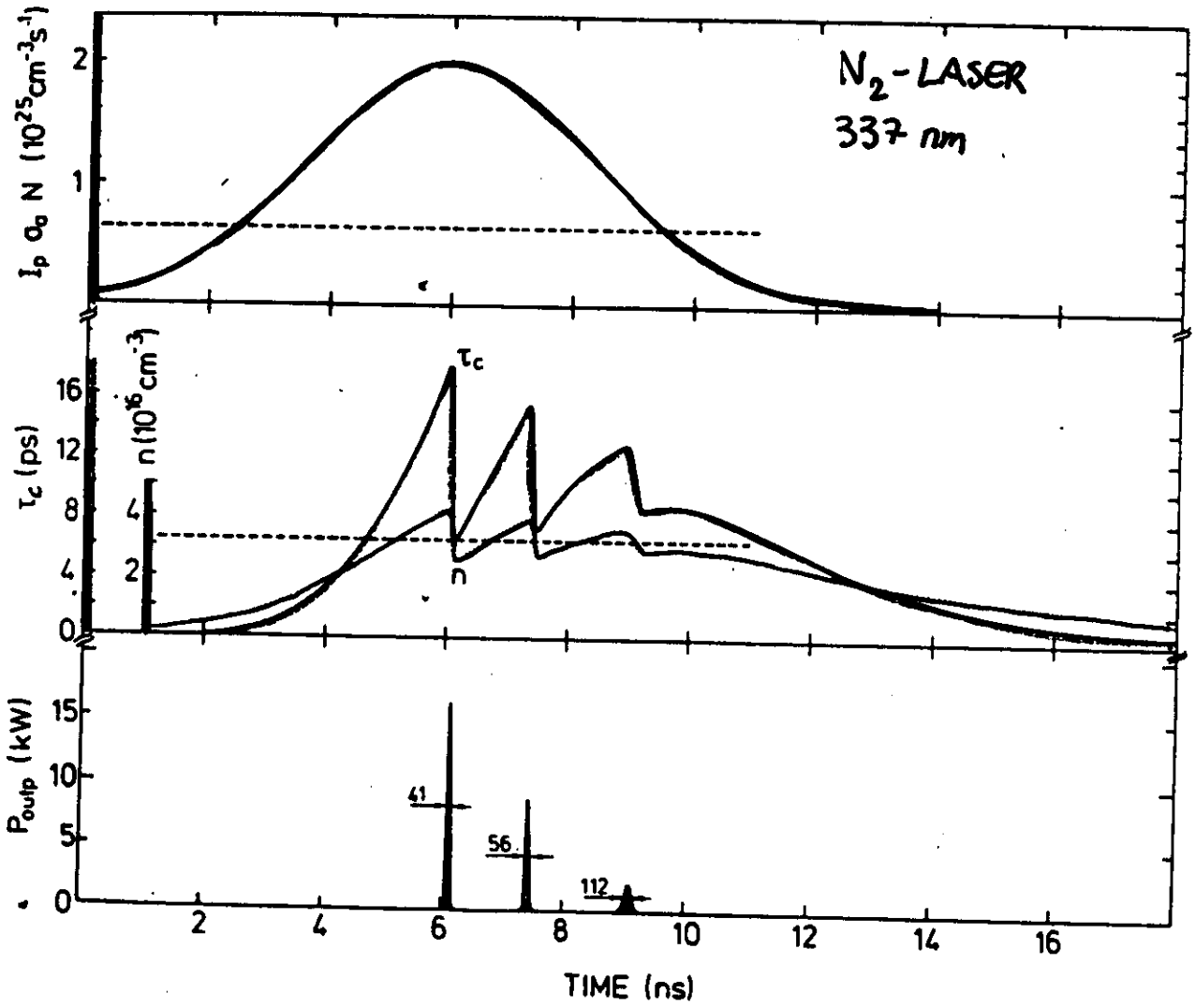

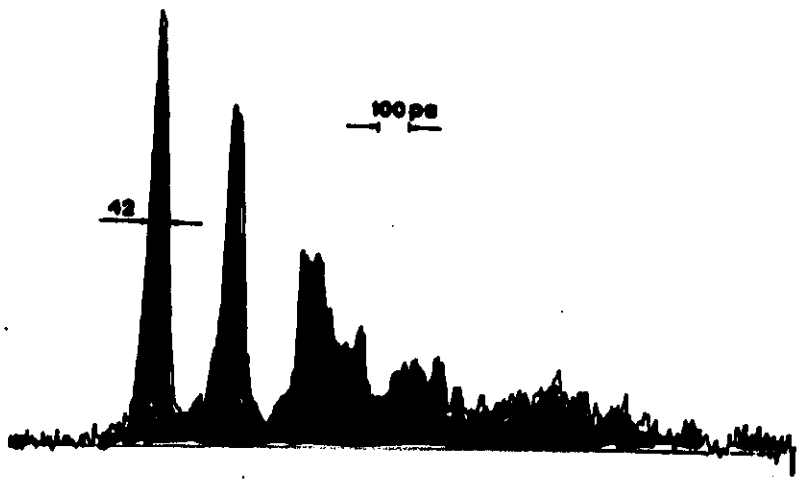

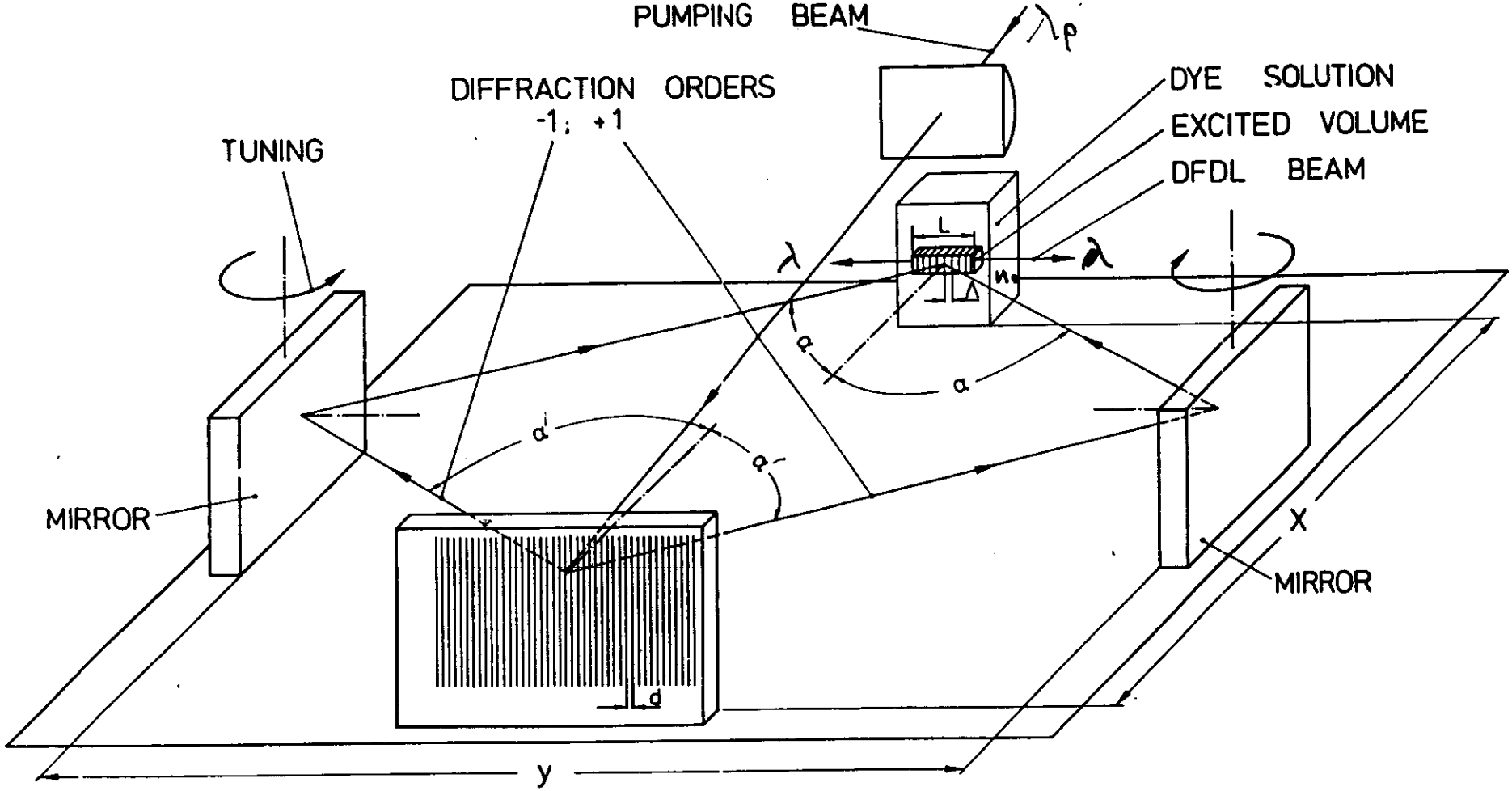

HOLOGRAPHIC GRATING
2442 l/mm

Achromatic arrangement: $\lambda = \frac{n_0 \lambda_p}{\sin\alpha}$; $\lambda_p = n d \sin\alpha$ $(n = \pm 1)$

λ independent of λ_p for $\alpha' = \alpha$

n_0 refractive index

● INTENSIVE, KURZE LASER-IMPULSE

S. SZATMÁRI, F.P. SCHÄFER,
OPT. COMMUN. 48 (1983) 279

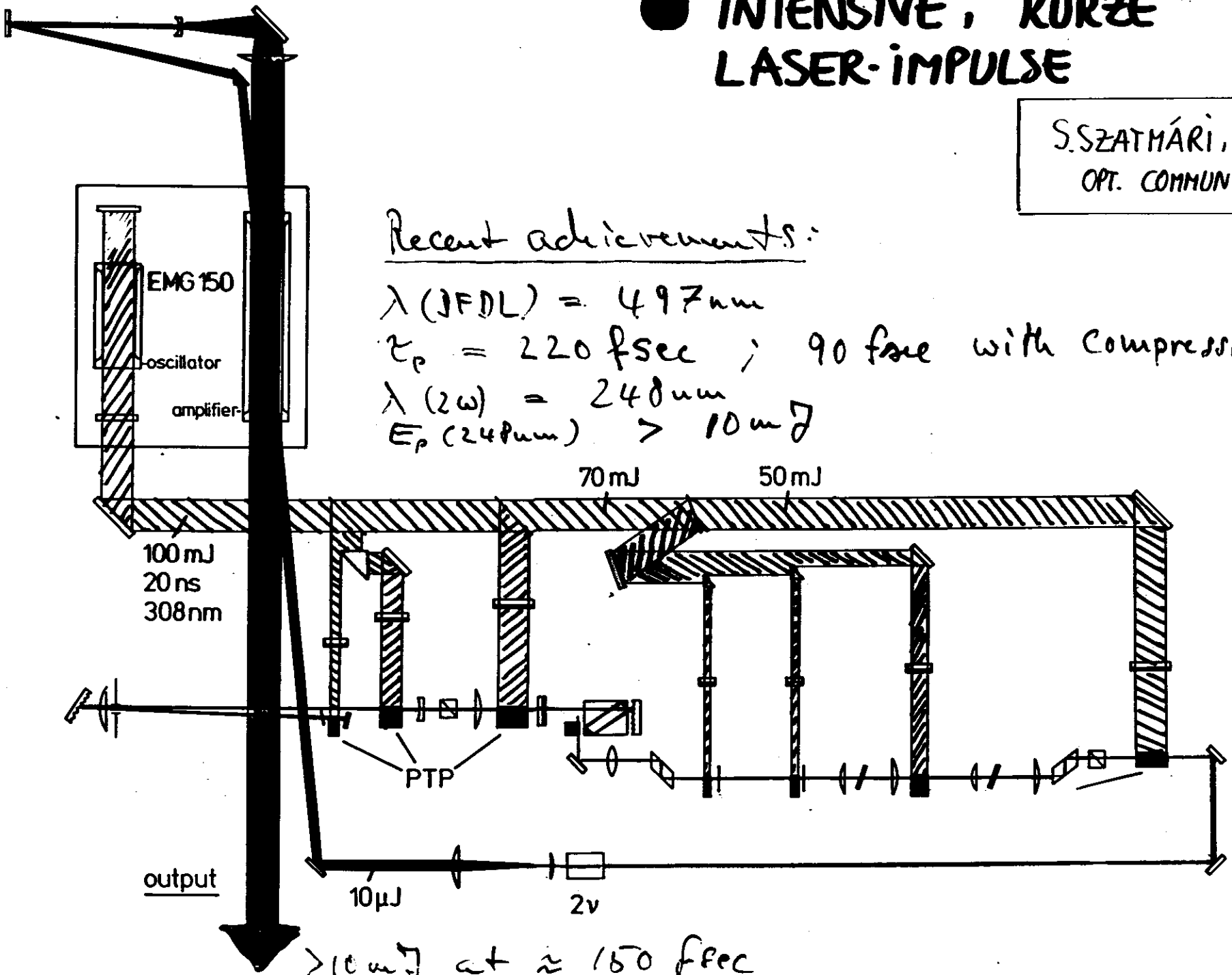

Recent achievements:

λ (JFDL) = 497 nm

τ_p = 220 fsec ; 90 fsec with Compression

λ (2ω) = 248 nm

E_p (248 nm) > 10 mJ

> 10 mJ at ≈ 150 ffec

PHOTOCHEMISCHE METHODEN:

IMPULS-VERKÜRZUNG MITHILFE PHOTOCHROMER FARBSTOFFE

Tautomer

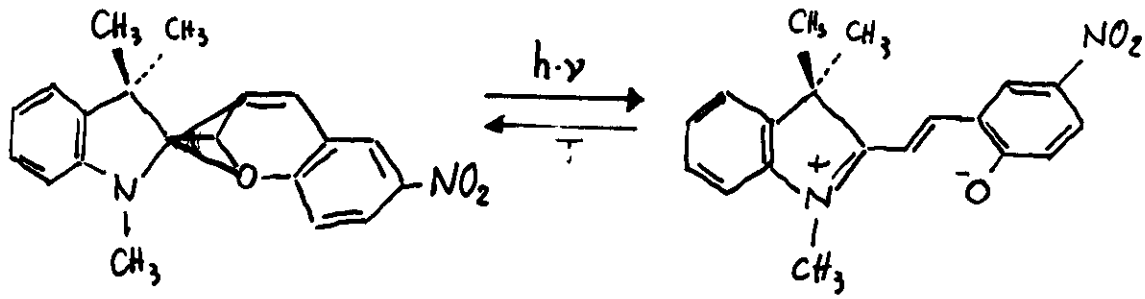

absorbs at: **UV** ($\lambda \approx 375$ nm)

FARBIG

absorbs at: ($\lambda_{max} \approx 575$ nm)

Tautomer

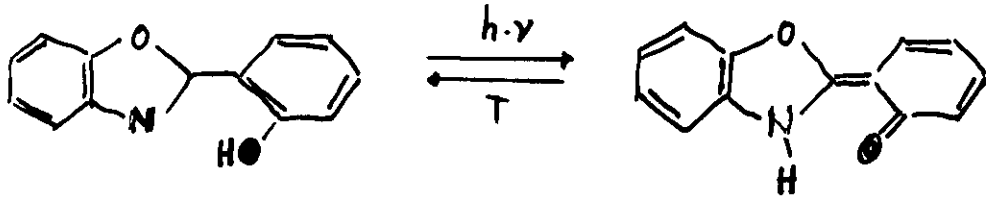

(proton transfer)

Pulse shortening assisted by photochemical reactions in photochromic dyes

PBX-OH

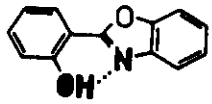

PBX-OH TAUTOMER

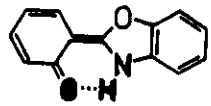

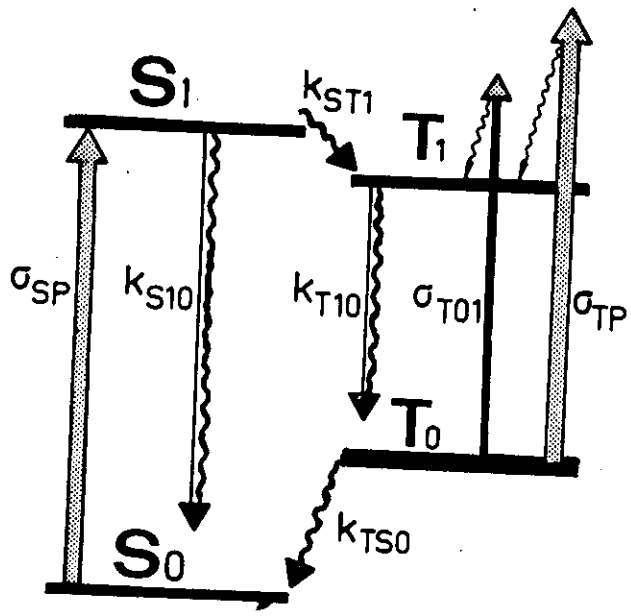

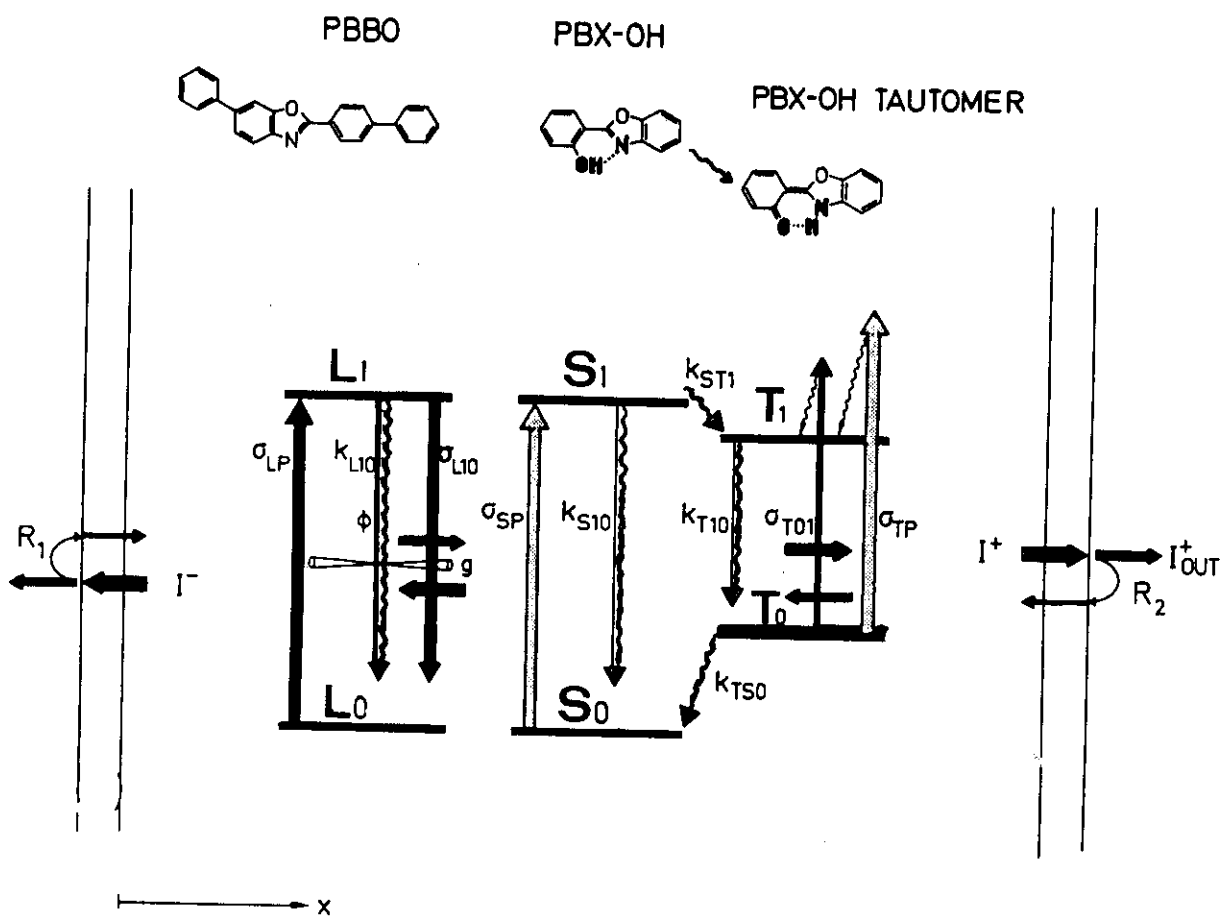
PBBO
PBX-OH
PBX-OH TAUTOMER
L1
L0
S1
S0
T1
T0
σ_{LP}
k_{L10}
σ_{L10}
ϕ
g
σ_{SP}
k_{S10}
k_{ST1}
k_{T10}
σ_{T01}
σ_{TP}
k_{TS0}
R_1
I^-
I^+
I^+_{OUT}
R_2
x

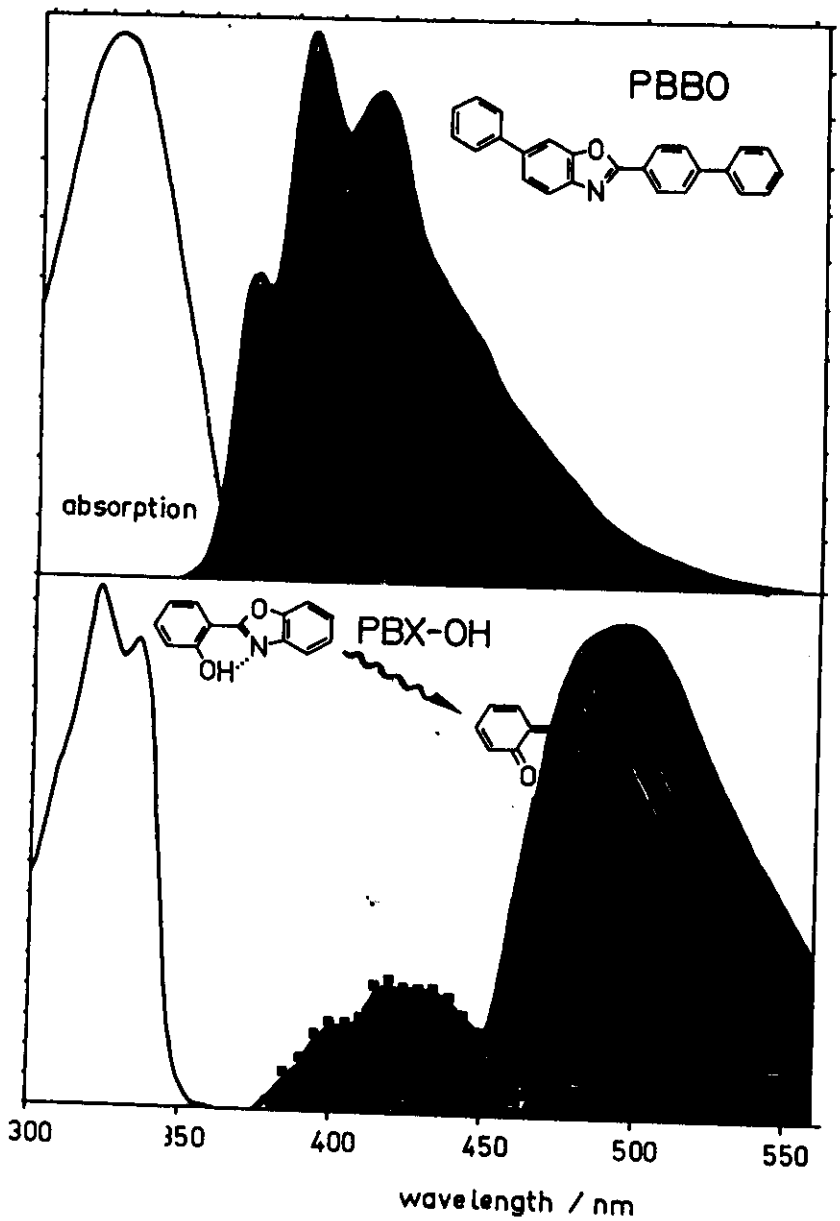
PBBO
absorption
PBX-OH
OH
300
350
400
450
500
550
wavelength / nm

N. ERNSTING, B. NIKOLAUS
APPL. PHYS. B 39 (1986) 155

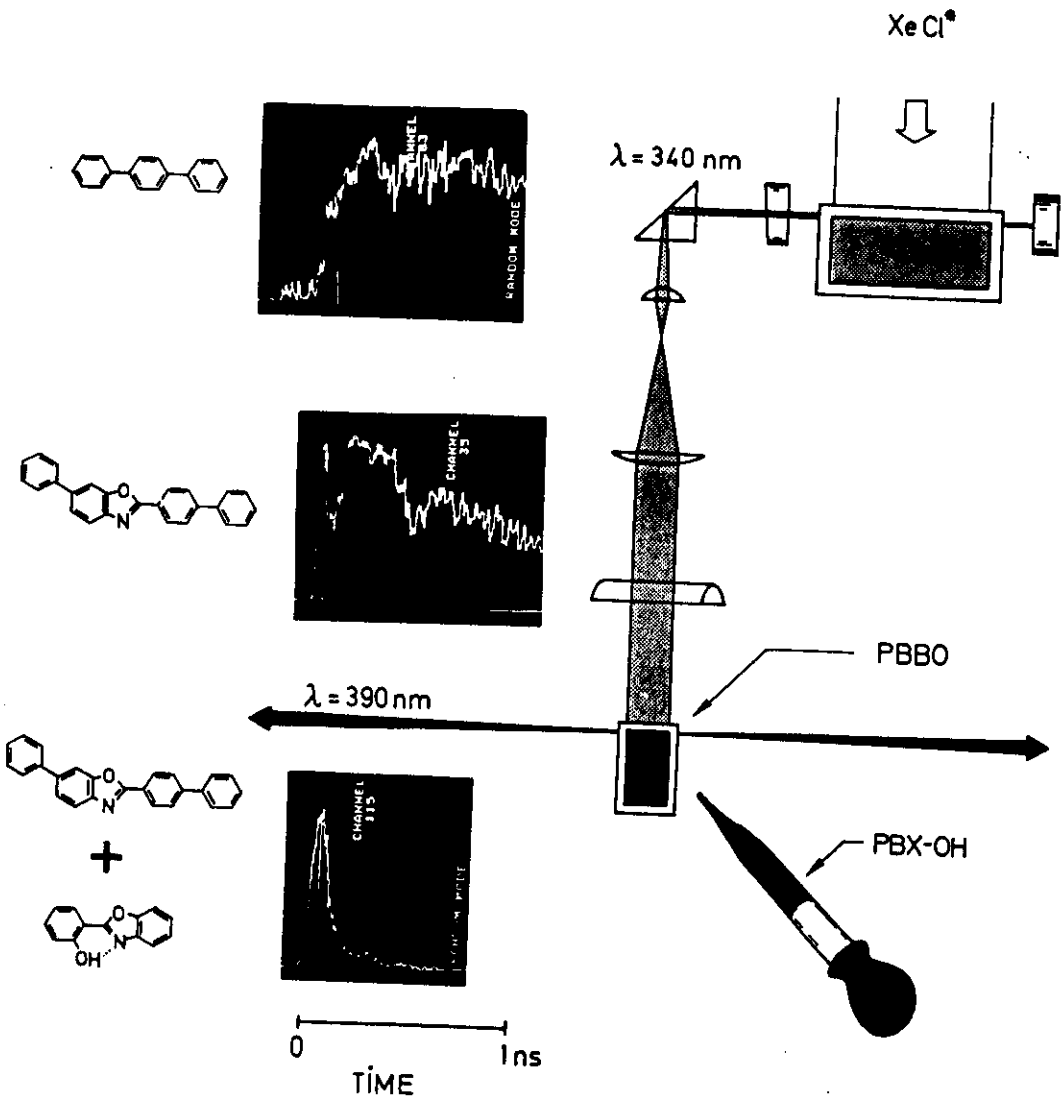

Nächste Entwicklungsstufe eines Modells

(immer noch primitiv)

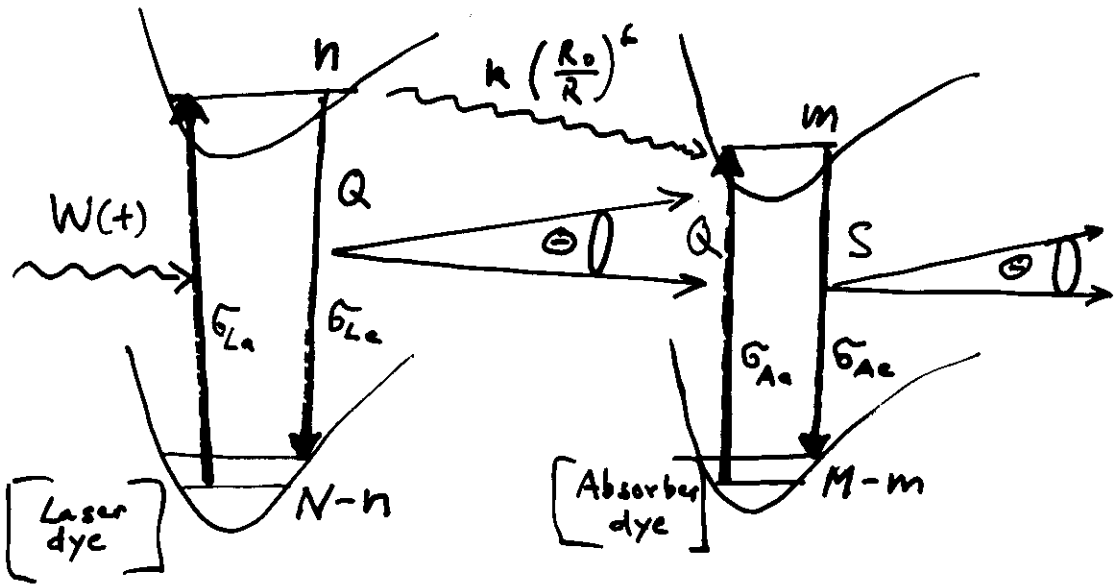

ortsunabhängige Ratengleichungen:

a) $\dot{n} = \sigma_{La} P (N-n) - \sigma_{Le} c Q n - n/\tau_L$

b) $\dot{m} = \sigma_{Aa} c Q (M-m) - \sigma_{Ae} c S m - m/\tau_A$

c) $\dot{Q} = \sigma_{Le} c Q n + \Phi_L \Theta n/\tau_L - \sigma_{Aa} c Q (M-m) - Q/\tau_c$

d) $\dot{S} = \sigma_{Ae} c S m + \Phi_A \Theta m/\tau_A - S/\tau_c$

P : 10^{25} cm^{-2} sec^{-1} ;

$\sigma_{L,A}$: $1.5 \cdot 10^{-16}$ cm^2 ;

τ_c : 40 ps ;

$\phi_{L,A}$: 0.05 ;

Θ : 1 mrad ;

$\tau_{L,A}$: 5 ns ;

N : $8 \cdot 10^{17}$ cm^{-3}

M : variabel ($10^{16} - 2 \cdot 10^{16}$)

$P(t) \sim a x^2 e^{-bx^2}$

(150 ml) DCM + (5 ml, 10^{-3} mol/l) DTDC

↓ Pumprate schrittweise reduziert

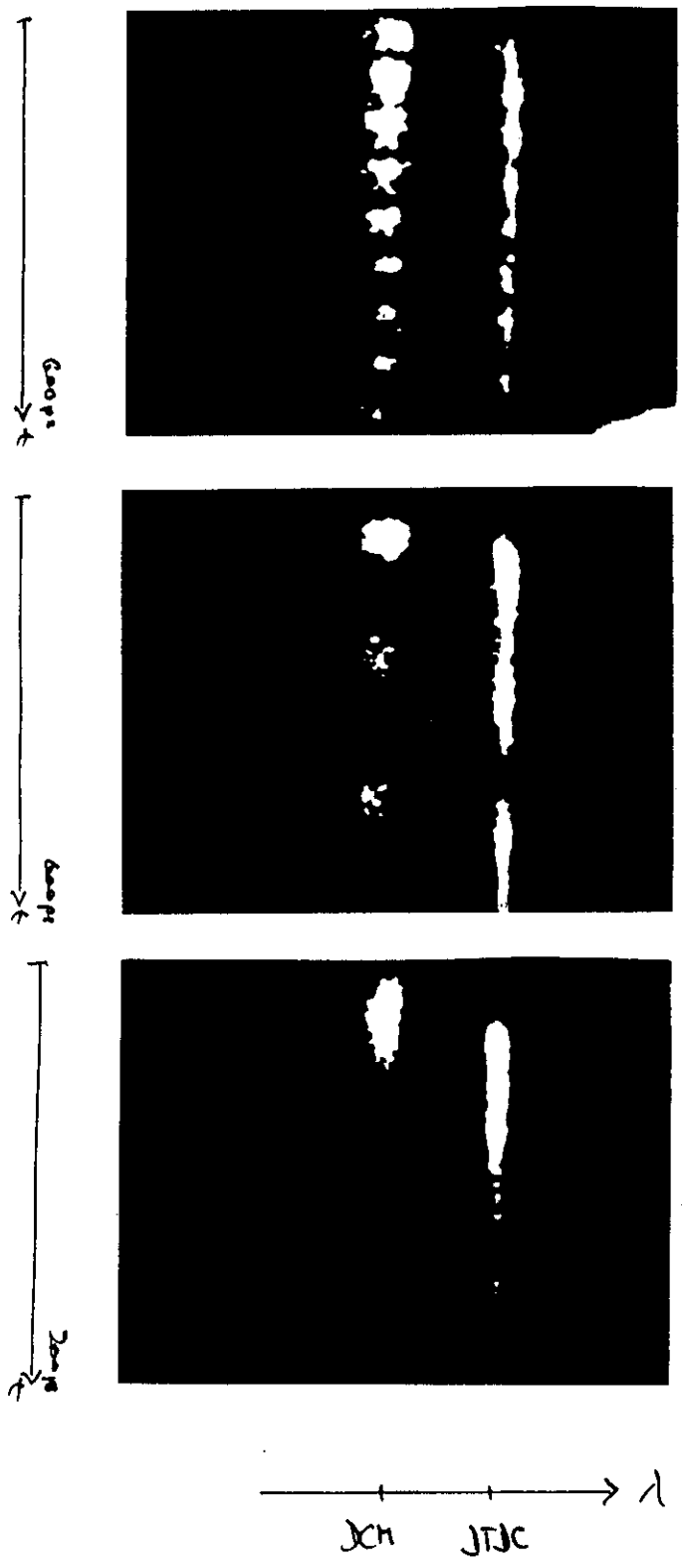

(150ml) DCM + (n · 5ml) TT-Furan (10^{-3} mol/l)

n = 0, 1, 2, 3, 4, 5

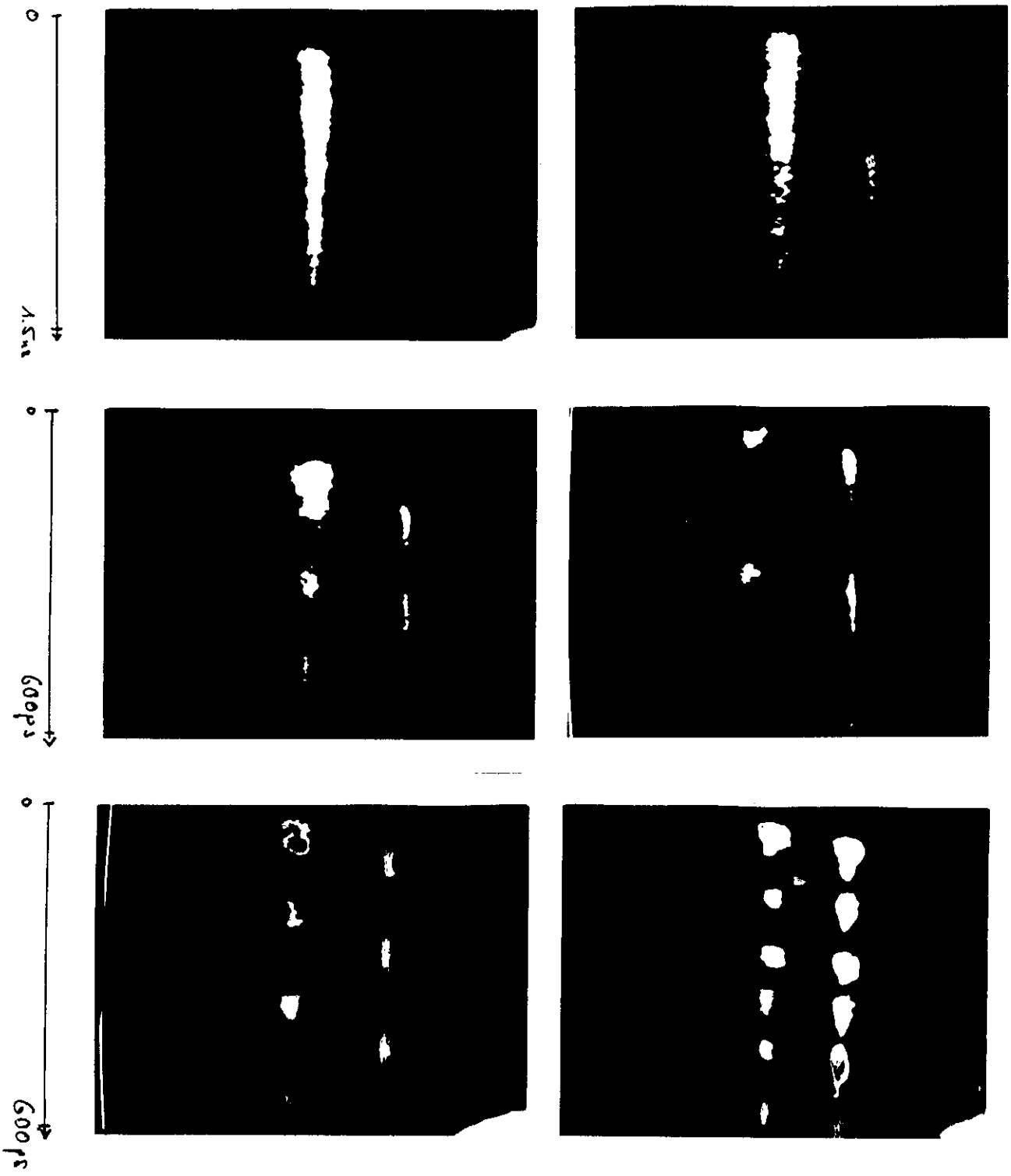

→ λ

Links: DCM
rechts: TT Furan

Stilben + C VO_3

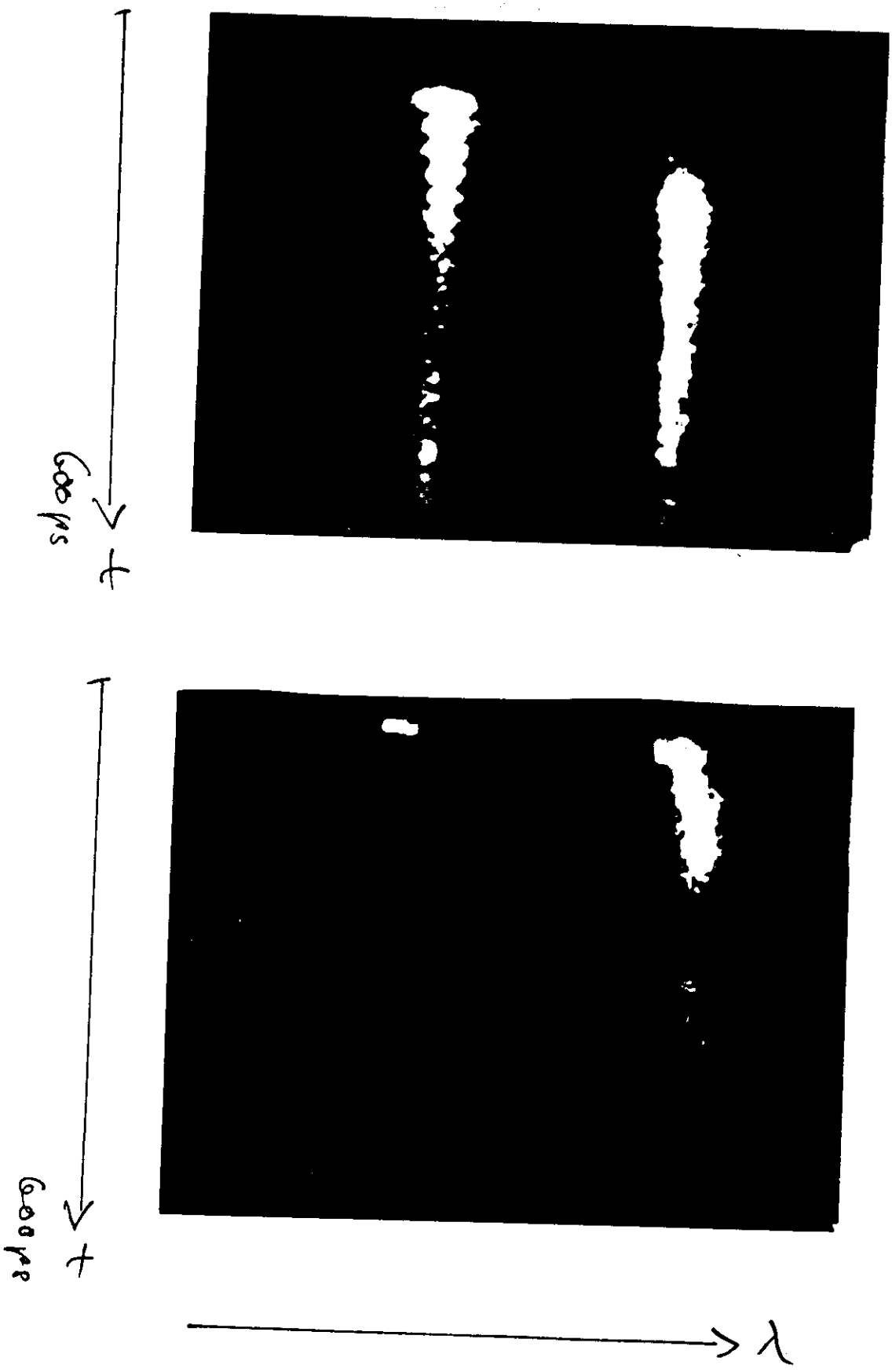

MPC94E E 06.06.85 16.24

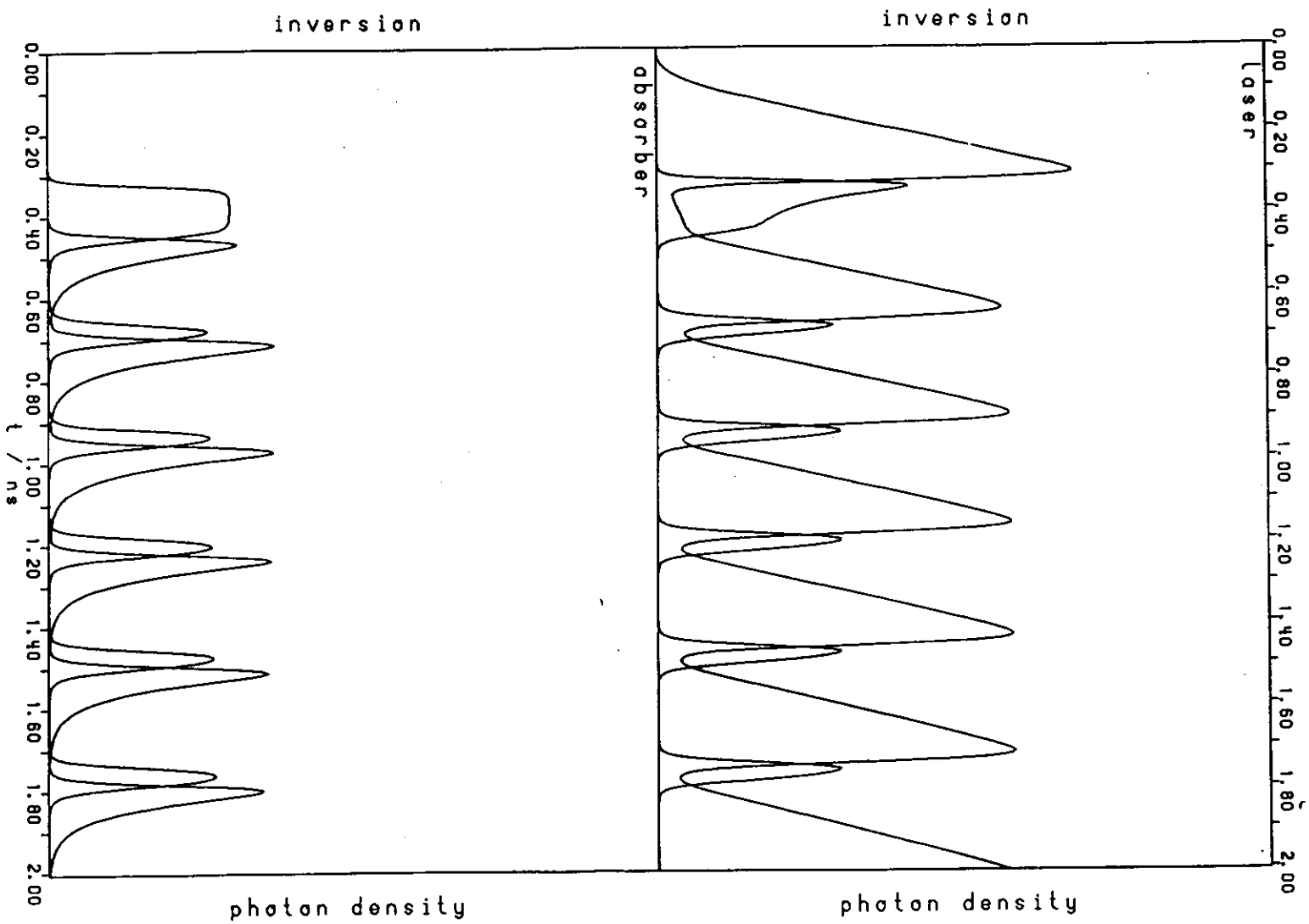

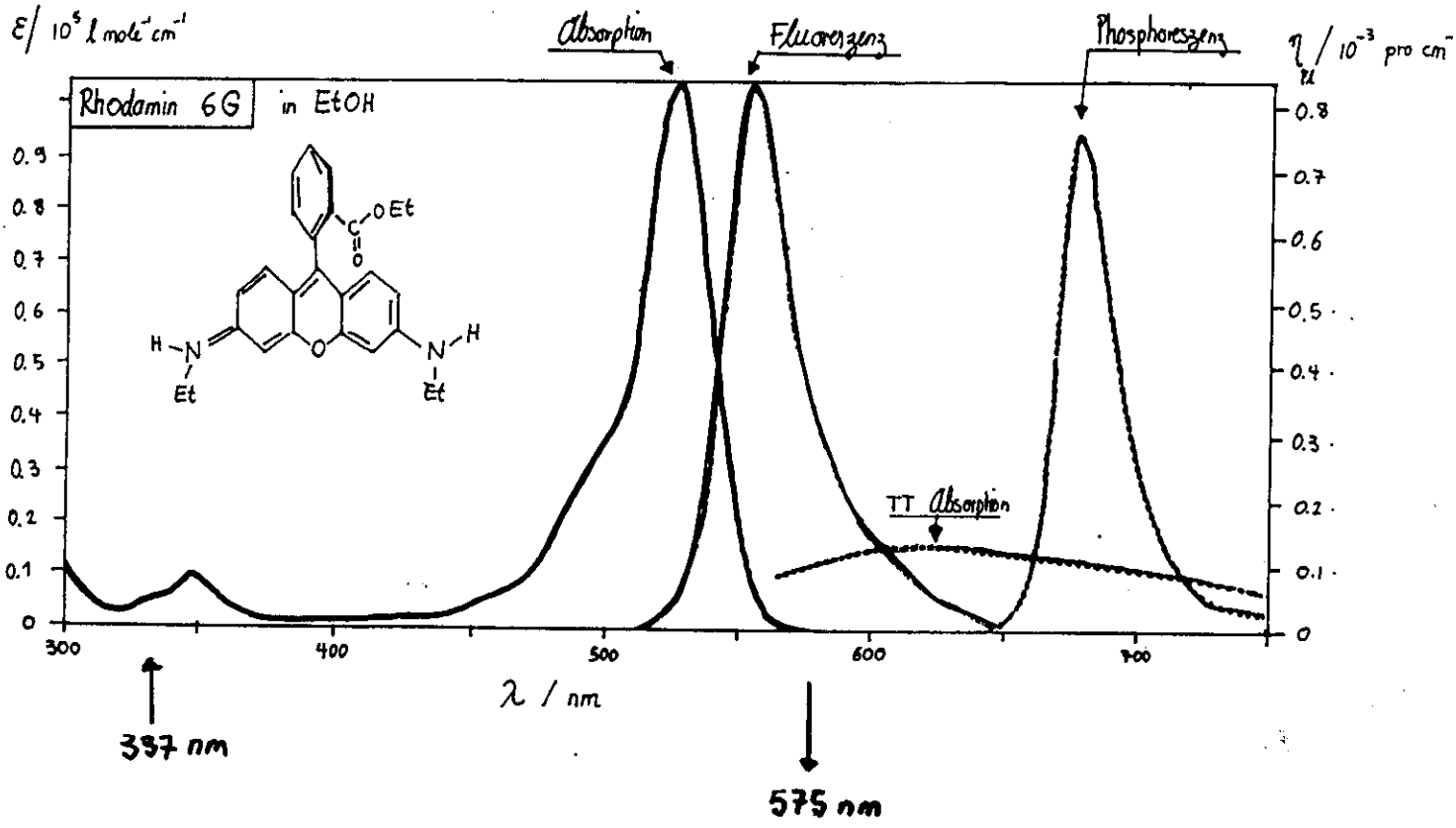
ε / 10⁵ l mol⁻¹ cm⁻¹
Absorption
Fluoreszenz
Phosphoreszenz
η / 10⁻³ pro cm⁻¹
Rhodamin 6G
in EtOH
TT Absorption
λ / nm
337 nm
575 nm

P. JURAMY, P. FLAMANT,
Y.H. MEYER
IEEE J. QE-13 (1977) 855

10 µs PUMP-PULS

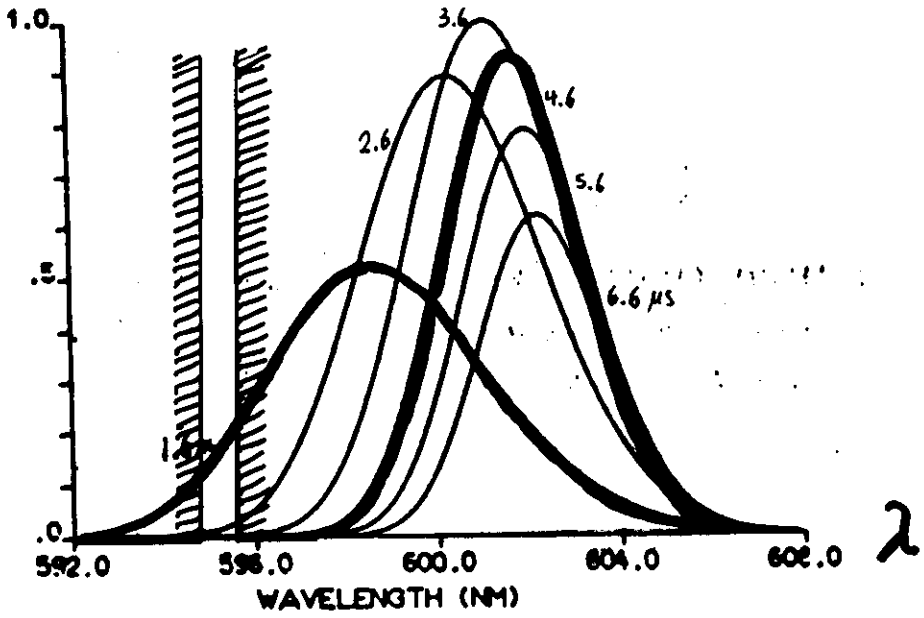

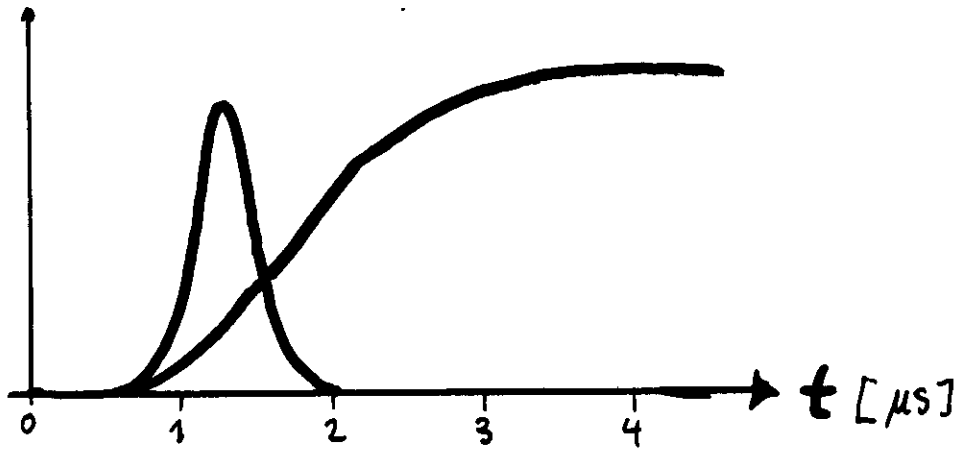

Spektrale Entwicklung eines Laserstrahls

Y. H. Meyer
P. Flamant

Opt. Commun. 1976

Änderung d. Photonenfluß:

$$\frac{d\Phi_{\nu,t}}{dt} = \frac{\Phi_{\nu,t}}{T}\left\{2l\left[\sigma_e N_1(t) - \sigma_a N_0(t)\right] - \alpha_\nu\right\}$$

$$N_1 + N_0 = N$$

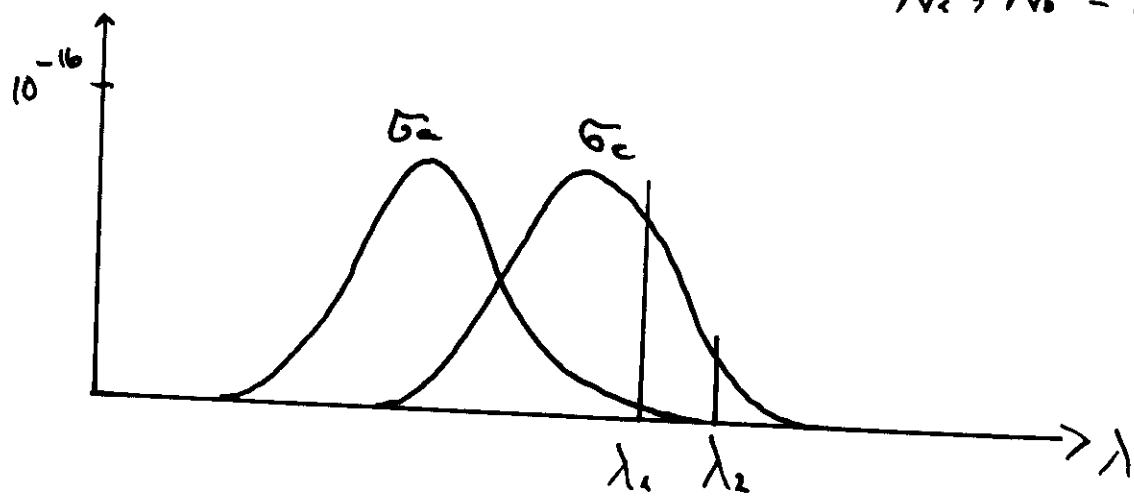

Entwicklung für 2 Wellen unterschiedlicher Frequenz:

$$I(\nu_1,t) = I(\nu_2,t)^{\delta_{12}} \exp\left(t/\tilde{\tau}_{12}\right)$$

$$\delta_{12} = (\sigma_{e1} + \sigma_{a1}) / (\sigma_{e2} + \sigma_{a2})$$

$$\tilde{\tau}_{12} = T / \left[2lN(\delta_{12}\sigma_{a2} - \sigma_{e1}) + \delta_{12}\cdot\alpha_2 - \alpha_1\right]$$

allgemein gilt: $\sigma_1 > \sigma_2$ und $\tilde{\tau}_{12} < 0$

das bedeutet: Rot-Verschiebung

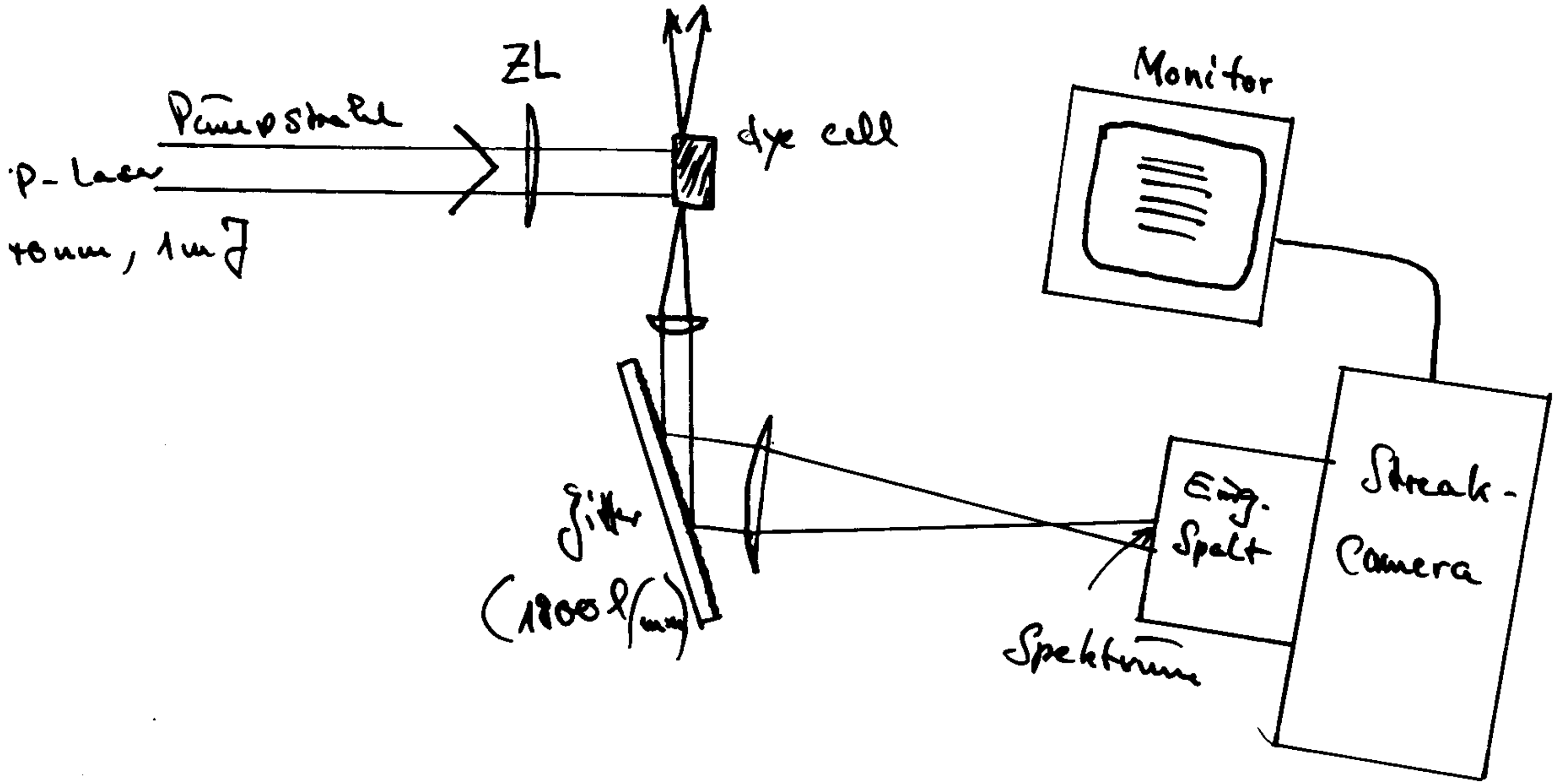

ZL
Pumpstrahl
P-Laser
10 mm, 1 mJ
dye cell
Monitor
Gitter
(1800 l/mm)
Eing.
Spalt
Streak-
Camera
Spektrum

Draft of Streak camera picture

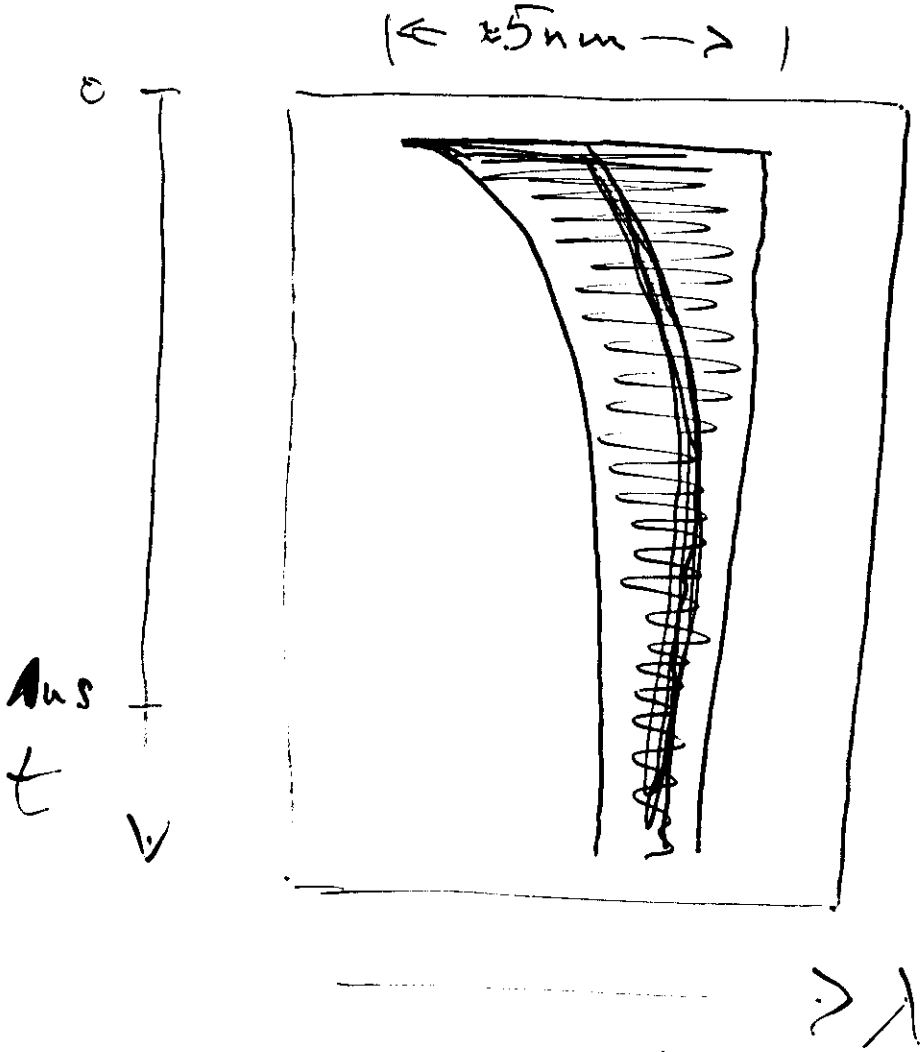

Y.H. MEYER, P. FLAMANT

OPT. COMMUN. (19 (1976) 20)

56 (1985) 61